MODELING AND ACTIVE STEERING CONTROL OF ARTICULATED VEHICLES WITH MULTI-AXLE SEMI-TRAILERS

A THESIS SUBMITTED TO
THE GRADUATE SCHOOL OF NATURAL AND APPLIED SCIENCES
OF
MIDDLE EAST TECHNICAL UNIVERSITY

BY

MECİD UĞUR DİLBEROĞLU

IN PARTIAL FULFILLMENT OF THE REQUIREMENTS
FOR
THE DEGREE OF MASTER OF SCIENCE
IN
MECHANICAL ENGINEERING

SEPTEMBER 2015

MODELING AND ACTIVE STEERING CONTROL OF ARTICULATED VEHICLES WITH MULTI-AXLE SEMI-TRAILERS

submitted by **MECİD UĞUR DİLBEROĞLU** in partial fulfillment of the requirements for the degree of **Master of Science in Mechanical Engineering Department, Middle East Technical University** by,

Prof. Dr. Gülbin Dural Ünver _____
Dean, Graduate School of **Natural and Applied Sciences**

Prof. Dr. R.Tuna Balkan _____
Head of Department, **Mechanical Engineering**

Prof. Dr. Y. Samim Ünlüsoy _____
Supervisor, **Mechanical Engineering Dept., METU**

Examining Committee Members:

Prof. Dr. Metin Akkök _____
Mechanical Engineering Dept., METU

Prof. Dr. Y. Samim Ünlüsoy _____
Mechanical Engineering Dept., METU

Prof. Dr. Mehmet Çalışkan _____
Mechanical Engineering Dept., METU

Prof. Dr. R. Tuna Balkan _____
Mechanical Engineering Dept., METU

Asst. Prof. Dr. Kutluk Bilge Arıkan _____
Mechatronics Engineering Dept., Atılım University

Date:

11.09.2015

I hereby declare that all information in this document has been obtained and presented in accordance with academic rules and ethical conduct. I also declare that, as required by these rules and conduct, I have fully cited and referenced all material and results that are not original to this work.

Name, Last name: M.Uğur DİLBEROĞLU

Signature :

ABSTRACT

MODELING AND ACTIVE STEERING CONTROL OF ARTICULATED VEHICLES WITH MULTI-AXLE SEMI-TRAILERS

Dilberoğlu, Mecid Uğur
M.S, Department of Mechanical Engineering
Supervisor: Prof. Dr. Y. Samim Ünlüsoy

September 2015, 112 pages

The main goal of this study is the design of an active trailer steering (ATS) control strategy for articulated heavy vehicles (AHV). The control strategy should be effective both at low and high forward speeds. A 5 DOF yaw/roll dynamic model of a tractor and multi-axle semi-trailer combination is developed. The nonlinear vehicle model is implemented on MATLAB® platform.

A linearized version of the AHV model is used in the design of active trailer steering controller. A new control strategy, Lateral Acceleration Characteristic Following (LACF) Controller, in which the trailing unit tries to follow the lateral acceleration characteristics of the towing unit is proposed. The performance of a number of existing classical and more recent control strategies are obtained for standardized test conditions. The results from the proposed control strategy are compared with those of the existing active steering control strategies. Linear Quadratic Regulator (LQR) technique is used throughout the thesis. Simulation results obtained via MATLAB®

show that the proposed control strategy is more successful than the existing strategies when evaluated on the basis of combined low and high speed performance.

Keywords: Articulated Heavy Vehicles, Dynamic Modeling and Simulation, Vehicle Lateral Dynamics, Linear Quadratic Regulator

ÖZ

ÇEKİCİ VE ÇOK AKSLI YARI TREYLER KOMBİNASYONLARININ MODELLENMESİ VE AKTİF YÖNLENDİRME KONTROLÜ

Dilberoğlu, Mecid Uğur
Yüksek Lisans, Makina Mühendisliği Bölümü
Tez Yöneticisi: Prof. Dr. Y. Samim Ünlüsoy

Eylül 2015, 112 sayfa

Bu çalışmanın temel amacı çekici ve çok akslı yarı treyler kombinasyonlarında kullanılmak üzere bir aktif yönlendirme kontrol yönteminin geliştirilmesidir. Aktif kontrol stratejisinin hem düşük hem de yüksek hızlarda etkin olması öngörülmüştür. Bu amaçla çekici ve çok akslı yarı treyler kombinasyonları için beş serbestlik dereceli dinamik bir dönme/yalpa modeli geliştirilmiştir. Doğrusal olmayan dinamik model, çekici ve yarı treylerin performansını test etmek amacıyla, MATLAB ortamında oluşturulmuştur.

Aktif yönlendirme kontrol sisteminin tasarımında ise doğrusallaştırılmış dinamik model kullanılmıştır. Yeni bir kontrol stratejisi olarak Yanal İvme Karakteristiği İzleme (YİKİ) kontrolcüsü geliştirilmiştir. Bu yöntemdeki temel fikir, treylerin yanal ivmesinin çekicinin yanal ivme karakteristiğini takip etmeye çalışmasıdır. Literatürde bulunan klasik ve göreceli olarak yeni kontrol stratejileri uygulanarak standartlaştırılmış test sonuçları elde edilmiştir. Önerilen kontrol stratejisi kullanılarak

elde edilen sonuçlar, literatürdeki diğer belli başlı aktif yönlendirme kontrol yöntemleriyle kıyaslanmıştır. Kontrolcü tasarımında Doğrusal Kuadratik Regülatör (DKR) yöntemi uygulanmıştır. Elde edilen simülasyon sonuçları, düşük ve yüksek hız performansları beraberce değerlendirildiğinde, önerilen kontrol stratejisinin mevcut stratejilerden daha başarılı olduğunu göstermektedir.

Anahtar Kelimeler: Çekici Yarı Treyler Kombinasyonları, Araç Modellemesi, Araç Yanal Dinamiği, Doğrusal Kuadratik Regülatör

To my lovely wife and parents

ACKNOWLEDGEMENTS

My supervisor Prof. Dr. Y. Samim Ünlüsoy, I would like to take this opportunity to express my deepest appreciation to you. This work would not be possible without your wisdom and guidance. Thank you sincerely.

Dear committee members Prof. Dr. Metin Akkök , Prof. Dr. Mehmet Çalışkan, Prof. Dr. R. Tuna Balkan, and Asst. Prof. Dr. Kutluk Bilge Arıkan, I am greatful to you for your genuine interest in increasing the quality of this work. Your valuable feedback served this purpose to a great extent. Thank you sincerely.

I would like to state my appreciation to my dear friend and colleague Sina M. Alemdari for his contributions and support.

My family, friends and wife, you have always encouraged me throughout this study. I am so lucky to have you.

TABLE OF CONTENTS

LIST OF TABLES

TABLES

LIST OF FIGURES

FIGURES

LIST OF ABBREVIATIONS

AHV	Articulated Heavy Vehicles
PTS	Passive Trailer Steering
ATS	Active Trailer Steering
LQR	Linear Quadratic Regulator
PFOT	Path-following Off-tracking
RWA	Rearward Amplification Ratio
TOT	Transient Off-tracking
HSOT	High Speed Steady State Off-tracking
LSOT	Low Speed Steady State Off-tracking
COG	Center of Gravity
SR	Steer Ratio
ACS	Active Command Steering
VD	Virtual Driver Steering Controller
LPDP	Lateral Position Deviation Preview Controller
LUF	Lead-Unit Following Controller
LACF	Lateral Acceleration Characteristics Controller

NOMENCLATURE

g	Gravitational acceleration constant
h_f	Height of the fifth wheel measured from the ground
h_{fr}	Difference in height of roll center of sprung mass of the tractor unit and the height of fifth wheel
h_{frt}	Difference in height of roll center of sprung mass of the semi-trailer unit and the height of fifth wheel
h_s	Height of the sprung mass center of gravity of the tractor unit measured from the ground
h_{st}	Height of the sprung mass center of gravity of the semi-trailer unit measured from the ground
h_r	Height of the roll center of sprung mass of the tractor measured from the ground
h_{rt}	Height of the roll center of sprung mass of the semi-trailer measured from the ground
h^*	Difference in height of roll center of sprung mass of the tractor unit and its sprung mass COG
${h_t}^*$	Difference in height of roll center of sprung mass of the semi-trailer unit and its sprung mass COG
l_1	Distance between the total mass COG of tractor unit and 1st axle center
l_2	Distance between the total mass COG of tractor unit and 2nd axle center
l_3	Distance between the total mass COG of the semi-trailer unit and 3rd axle center
l_4	Distance between the total mass COG of the semi-trailer unit and 4th axle center
l_5	Distance between the total mass COG of the semi-trailer unit and 5th axle center

l_f	Distance between the COG of the tractor unit and the articulation point
l_{ft}	Distance between the COG of the semi-trailer unit and the articulation point
m	Total mass of the tractor unit
m_s	Sprung mass of the tractor unit
m_{st}	Sprung mass of the semi-trailer unit
m_t	Total mass of the semi-trailer unit
p	Roll velocity of the tractor unit
p_t	Roll velocity of the semi-trailer unit
r	Yaw velocity at the COG of the tractor unit
r_t	Yaw velocity at the COG of the semi-trailer unit
r_Δ	Yaw velocity at the COG of the tractor unit obtained via the time delay
v	Side slip velocity at the COG of the tractor unit
v_t	Side slip velocity at the COG of the semi-trailer unit
y_e	Lateral position of the center of rear end of the semi-trailer unit
y_r	Lateral position of the center of active rear axle of the semi-trailer unit
y_{5th}	Lateral position of the fifth wheel
$y_{5th\Delta}$	Lateral position of the fifth wheel obtained via the time delay
$\ddot{y}_t$	Lateral acceleration at the COG of the tractor unit
$\ddot{y}_s$	Lateral acceleration at the COG of the semi-trailer unit

C_1	Total cornering stiffness of the tires on the front axle of the tractor
C_2	Total cornering stiffness of the tires on the rear axle of the tractor
C_3	Total cornering stiffness of the tires on the front axle of the semi-trailer
C_4	Total cornering stiffness of the tires on the middle axle of the semi-trailer
C_5	Total cornering stiffness of the tires on the rear axle of the semi-trailer
F_{xf}	Reaction force at the fifth wheel in the x-direction
F_{xi}	Total force generated by the i^{th} axle tires in the x-direction
F_{yf}	Reaction force at the fifth wheel in the y-direction
F_{yi}	Total force generated by the i^{th} axle tires in the y-direction
I_{sxx}	Roll moment of inertia of sprung mass of tractor unit about the COG of its sprung mass center
I_{sxxt}	Roll moment of inertia of sprung mass of semi-trailer unit about the COG of its sprung mass center
I_{sxz}	Yaw/roll product of moment of inertia of sprung mass of tractor unit about the COG of its sprung mass center
I_{sxzt}	Yaw/roll product of moment of inertia of sprung mass of semi-trailer unit about the COG of its sprung mass center
I_{zz}	Yaw moment of inertia of whole mass of tractor unit about the COG of its whole mass center
I_{zzt}	Yaw moment of inertia of whole mass of semi-trailer unit about the COG of its whole mass center
K_s	Driver steering sensitivity coefficient for the driver model
K_{12}	Total roll stiffness of coupling point between tractor and semi-trailer units
R_t	The turning radius of tractor unit calculated from the path of its center of gravity
R_{tr}	The turning radius of tractor unit calculated from the path of its right endpoint

R_s	The turning radius of semi-trailer unit calculated from the path of its center of gravity
R_{sl}	The turning radius of semi-trailer unit calculated from the path of its left endpoint
U	Longitudinal velocity of the tractor unit
U_t	Longitudinal velocity of the semi-trailer unit
α_1	Slip angle at the front axle tires of the tractor unit
α_2	Slip angle at the rear axle tires of the tractor unit
α_3	Slip angle at the front axle tires of the semi-trailer unit
α_4	Slip angle at the middle axle tires of the semi-trailer unit
α_5	Slip angle at the rear axle tires of the semi-trailer unit
β	The constant associated with the articulation angle in active command steering
δ_1	Steering angle at front axle of the tractor unit
δ_3	Steering angle at front axle of the semi-trailer unit
δ_4	Steering angle at middle axle of the semi-trailer unit
δ_5	Steering angle at rear axle of the semi-trailer unit
δ_s	Active steering angle of the combined axles of the semi-trailer unit
τ	Direction angle of the tractor unit on global coordinates
θ	Direction angle of the semi-trailer unit on global coordinates
ϕ	Roll angle of the tractor unit
ϕ_t	Roll angle of the semi-trailer unit

ψ	Articulation angle between the tractor and semi-trailer units
ψ_{ps}	Pseudo look-ahead angle of the driver model
μ	Steer ratio identified for any forward speed of the vehicle
ρ_i	Weighting factor associated with the i^{th} term of the quadratic performance index
$\sum K_{\phi}$	Total roll stiffness of suspensions and tires of the tractor unit
$\sum K_{\phi t}$	Total roll stiffness of suspensions and tires of the semi-trailer unit
$\sum C_{\phi}$	Total roll damping of suspensions and tires of the tractor unit
$\sum C_{\phi t}$	Total roll damping of suspensions and tires of the semi-trailer unit

CHAPTER 1

INTRODUCTION

1.1. ARTICULATED HEAVY VEHICLES (AHVs)

The transportation of the goods is an essential requirement for almost all kinds of production and trade. Freight transportation issues require the use of roads and highways for the operation of suitable land vehicles. Being one of the widely used ground vehicles, articulated heavy vehicles has a pivotal role in transportation of goods and materials. Cost effectiveness of the AHV makes them superior in the freight technology.

An AHV is generally known as a heavy commercial vehicle consisting of two or more parts, involving the towing and trailing vehicle units. In general, the towing unit supplies the required traction power to the connected vehicle units via its engine. On the other hand, the trailing vehicle units are used for the storage of the freight and goods. The following section provides a brief explanation of vehicle types and presents various combinations of AHV.

1.2. TYPES OF ARTICULATED HEAVY VEHICLES

Among the ground vehicles, articulated heavy vehicles (AHV) are generally designed by combining different vehicle units. Towing unit of the AHV, which usually has the powered engine and steerable axles for the use of the driver to carry the following vehicle units, is often called as the tractor or truck. On the other hand, the trailing units are divided into two broad sub-groups; semi-trailers and full-trailers. Trailing units are classified on the basis of the vertical load at their front side. Semi-trailers are directly

supported by their towing units at the connection points, whereas full-trailers have their own front axles to carry the load of the unit.

AHV combinations are characterized by their connections at the hitch points. In other words, articulated vehicles can be named with regard to the coupling types. Table 1-1 illustrates the well-known types of articulated heavy vehicles.

Regarding the necessary load carrying capacities and various road conditions, several arrangements of AHV's have been on the highways of different countries. The AHV combinations given in the Table 1-1 just demonstrate the basic configurations and their identification. A tractor and semi-trailer arrangement is selected for this study since it is one of the most commonly-used configuration.

Table 1-1: Typical combinations of AHVs [1]

Tractor & Semi-trailer	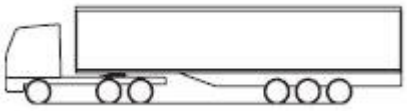
Truck-Trailer	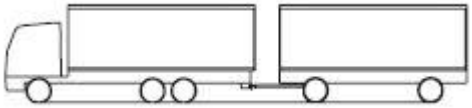
A-double	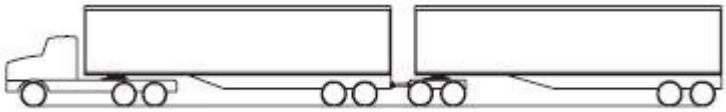
B-double	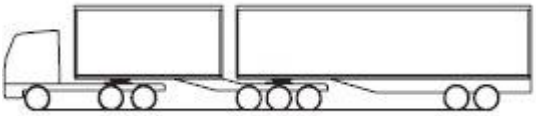
B-triple	
Tractor & Semi-trailer with Drawbar Trailer	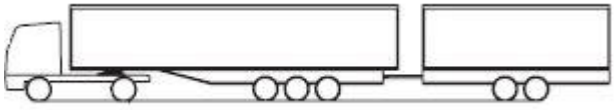

1.3. CHARACTERISTICS OF ARTICULATED HEAVY VEHICLES

The widespread use and increased popularity of heavy commercial vehicles are due to certain advantageous features they possess. Low fuel consumption and minimum labor force requirements are the most important factors that give rise to the increasing demand for heavy commercial vehicles. Only one driver is able to fulfill the labor requirement, controlling multiple units of vehicles. Compared to the other types of ground vehicles, the harmful exhaust gas emission rates of the AHV's are sufficiently low when scaled with their sizes [2].

Articulated heavy vehicles also have a number of serious drawbacks. As a consequence of their large sizes and heavy weights, it appears that the safety problems on highways have been the primary factor to be taken into account about AHVs [1]. It is evident that traffic accidents involving the AHVs exhibit higher risk of death than the other cases. As a result, a proper design of the heavy commercial vehicles plays a vital role in safety concerns about the highways.

1.4. DYNAMICS OF ARTICULATED HEAVY VEHICLES

Before examining the proper design of an AHV that satisfy the safety requirements, it is necessary to realize that there is another issue to be dealt with. Assembling multiple adjacent units together leads to complicated handling characteristics of articulated vehicles. The dynamic behavior of the AHVs is difficult to investigate due to the interaction between the towing and trailing units at their articulation points. Some unstable motion modes of the articulated vehicles are generally seen as a consequence strongly related to this complex dynamic behavior of AHV's.

1.4.1 Unstable Motion Modes

There are three main unstable motion modes of articulated vehicles currently being adopted in the literature. The first type of the instability is known as jack-knifing. Jack-knifing is a phenomenon that is described as the unstable yaw motion of the tractor. In case of a jack-knifing of an articulated vehicle, articulation angle between the tractor and the semi-trailer will be so high that leading unit cannot pull the trailing units anymore. Then, the trailing unit pushes the tractor from behind until they collide with each other. An illustration of a jackknifing situation is provided in the Figure 1-1.

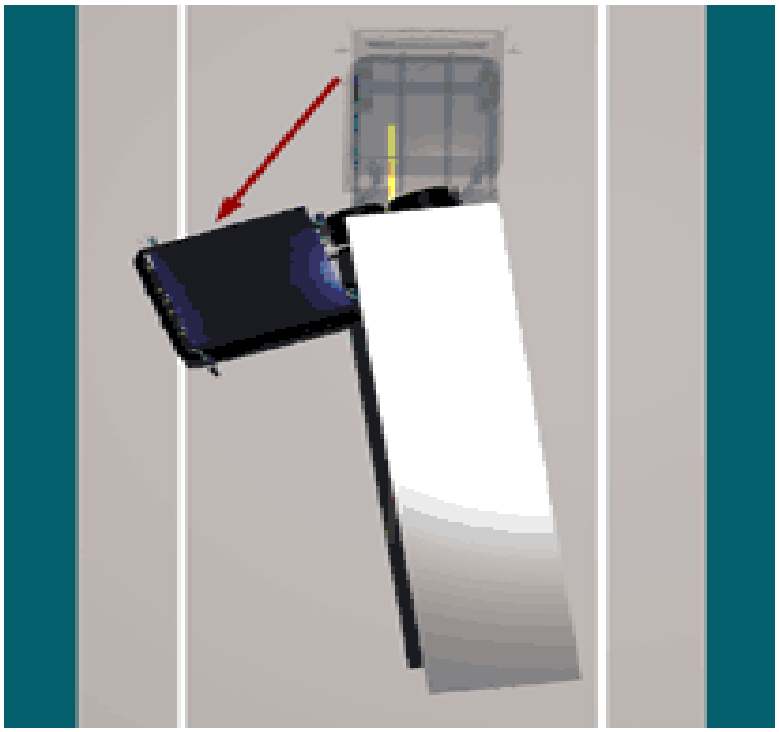

Figure 1-1: Jack-knifing of a tractor and semi-trailer combination

Second unstable motion mode of the articulated vehicles is called as trailer swing. As it is reflected in its name, uncontrolled lateral motion of the trailing unit take place in that case. Large motion of the trailing unit usually leads to sweeping of the other vehicles next to the AHV. Both unstable modes mentioned here may result from sudden excessive steering angles at high speeds as well as locked wheels of the rear axles of the tractor or trailer due to excessive braking. Figure 1-2 is an illustration of trailer swing case experienced by a car and trailer combination.

Rollover is the third type of the unstable motion modes of the AHVs. The most likely cause of rollover is high lateral acceleration of the trailing units. During the lane change maneuvers at high forward speeds, lateral acceleration of the trailing units is usually higher than that of the towing unit. Therefore, high roll angles of the trailing unit may result in the rollover of the vehicle. Center of gravity (COG) height, vehicle speed, steering actions etc. are the major factors that have influence on the rollover of the vehicle.

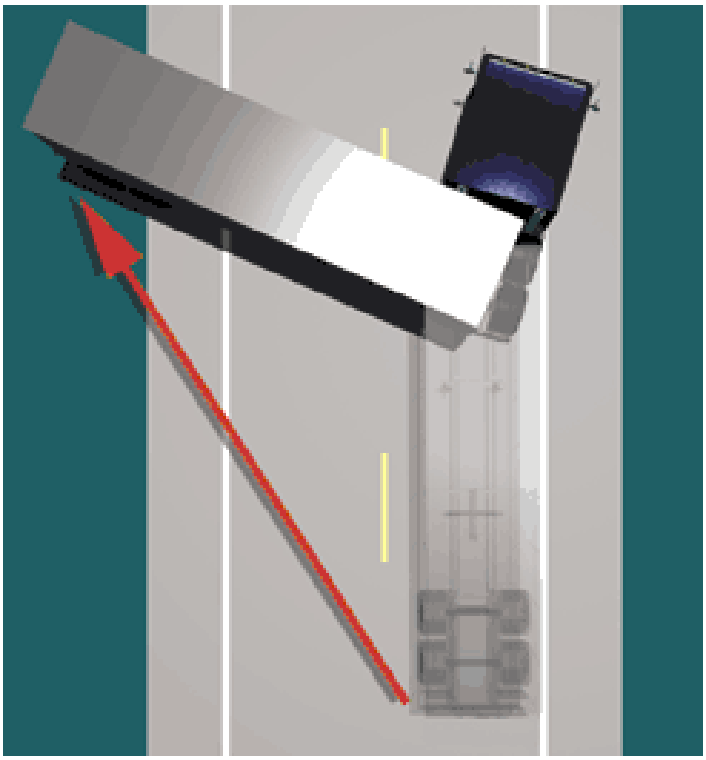

Figure 1-2: Trailer swing of a car and trailer combination

1.5 DESIGN OBJECTIVES OF AHV'S

Having mentioned the complex dynamics of the AHVs, it is necessary to note that the lateral performance is the critical issue in this study. On the other hand, longitudinal motion is not the primary concern of this study. The roll degree of freedom is indirectly involved through its relation to vehicle rollover, which may be associated with the lateral acceleration of the AHV at high speeds.

In order to examine the lateral performance of AHV's, some criteria have been proposed in the literature. Off-tracking (OT) is one of the most commonly-used performance measure for the investigation of the lateral dynamics of articulated vehicles. A generally accepted definition of OT is the radial difference between the path of the towing unit and the trailing unit during a specific turning maneuver [3]. Because of the excessive length of the articulated vehicles, the trailing units suffer from difficulties in following the leading vehicle unit, at both high and low forward speeds. If any steering action is not implemented at the trailing unit axles, the path of the two units most probably will not be the same. The driver steers the articulated vehicle based on his/her estimation of the trailer path.

Rearward amplification ratio (RWA) is another term frequently used in the literature as a performance measure of articulated heavy vehicles. The definition of the term is expressed as the peak lateral acceleration ratio of the trailing unit to that of the towing unit for an articulated vehicle [4]. The reason why RWA ratio has been a widely-used performance criterion is its utility in the roll study. As a rule of thumb, the lower RWA ratio implies the higher lateral stability of the articulated vehicle. That is, minimization of RWA ratio will serve the purpose of reducing the probability of rollover.

1.6 THESIS ORGANIZATION

In this introductory chapter, a brief overview of the types and characteristics of articulated heavy vehicles relevant to the basic subject of the thesis study is provided. Lateral dynamics and typical instabilities of AHVs are identified. Then, the explanation of major design objectives is given.

The second chapter mainly focuses on the review of the literature on trailer steering systems of the articulated heavy vehicles. In order to construct a background in the topic, relevant vehicle models and their verification methods are stated. Moreover, various trailer steering strategies found in the literature are examined.

The third chapter moves on to describe the dynamic model of the tractor and multi-axle semi-trailer. The derivation of the suggested dynamic model is explained and discussed in sufficient detail.

The fourth chapter introduces the active trailer steering (ATS) control strategies including both some classical and relatively more recent approaches in the literature, and the strategy proposed in this study. For each control strategy, the fundamental idea behind the methods is explained together with the derivation of the controller designs.

Chapter 5 includes the simulation results obtained for each of the controllers introduced in the previous chapter. The lateral performance of the tractor and semi-trailer combination is investigated at both low and high speed travel conditions.

The last chapter provides a brief summary of the comparative performance evaluation of the existing and the proposed ATS control strategies at low and high forward speeds.

CHAPTER 2

LITERATURE REVIEW

The rapid growth in the use of heavy commercial vehicles brings about the necessity of improved design of the AHV's. Thus, the topic of trailer steering in articulated heavy vehicles has been and still is an active research area of vehicle dynamics. Over the past years, a considerable amount of literature has been published on trailer steering systems of AHV's. It has become commonplace to distinguish the passive and active types of trailer steering systems. Although previous studies have primarily concentrated on passive trailer steering (PTS) systems, new developments give rise to studies that focus on the active steering systems for trailers.

Before proceeding to examine various kinds of trailer steering strategies, the vehicle models used in the previous studies, lateral performance measures and corresponding standard maneuvers will be presented.

2.1 ARTICULATED HEAVY VEHICLE MODELS

For a successful application of trailer steering, the proper modeling of articulated vehicle is required. Several studies investigating the trailer steering systems have made use of different vehicle models. The most frequently used vehicle models in the study of lateral performance of AHV's are linear yaw plane models[5][6][7][8][9][10]. As far as the lateral characteristics of the articulated vehicles concerned, the sufficiency of linear yaw plane models has been proved in the literature. The validation of linear yaw plane models of AHV's have been verified by the comparison with some advanced commercial software. Changfu et al. [11] performed the verification of a 6-axle linear articulated vehicle model in case of drastic handling situations. According

to their research, the responses obtained by the proposed linear yaw plane model has a decent agreement with those obtained by using TruckSim® software for the case of an extreme handling maneuver. Furthermore, higher order non-linear planar models are also investigated. Azadi et al. [12] suggested a higher order yaw plane model integrated with a nonlinear tire model.

In the recent studies, on the other hand, the additional degrees of freedom have been considered in the vehicle dynamics models. Especially, the researches including the roll dynamic of the vehicles require advanced models to be used [13]. Cebon et al. [14] used linear vehicle model comprising the roll degree of freedom in their study. Likewise, Islam utilized a similar roll/yaw vehicle model and performed its validation via TruckSim® reference model [15]. Further, a nonlinear roll/yaw vehicle model was used by Azadi, who verified the vehicle model via real test data [16].

To conclude with, researchers have examined several vehicle dynamic models for simulations and controller design. Review of the above literature shows that up to date studies focus on more improved models of AHVs. However, linear yaw/plane models are still quite popular due to their advantageous features of suitability for controller design and sufficient accuracy for simulation purposes.

2.2 PERFORMANCE MEASURES

For the assessment of lateral performance of articulated vehicles controlled with trailer steering strategies, various criteria have been developed. Commonly-used performance measures found in the literature for the AHV's lateral motion are listed in Table 2-1 together with their explanations.

As understood by the explanations on the Table 2-1, the performance measures are taken during standardized test maneuvers of AHVs. The specified standard test conditions mentioned in the explanation of the performance measures are provided in next section.

Table 2-1: Commonly used performance measures adapted from [17]

PERFORMANCE MEASURE	EXPLANATION
Low Speed Swept Path Width (SPW)	Maximum lateral offset between the paths of COG's of tractor & semi-trailer units during specific constant radius turning maneuver
Static Rollover Threshold	Maximum lateral acceleration just before the rollover of the articulated vehicle
Low-speed Off-tracking (LSOT)	Maximum width of the path swept by the AHV during specific 90-degree intersection turn
Yaw Damping Coefficient	Minimum damping ratio at the articulation joints of the vehicle during free oscillations
Rearward Amplification (RWA)	The ratio of the peak lateral acceleration at trailer COG to that of towing unit at specific high speed lane change maneuver
High-speed Transient Off-tracking (TOT)	Maximum lateral distance between the path of tractor front axle center and semi-trailer rear axle center during specific lane change maneuver
High-speed Steady State Off-tracking (HSOT)	Maximum lateral distance between the path of tractor front axle center and semi-trailer rear axle center during specific high speed steady state turning maneuver
Load Transfer Ratio	The ratio of the total lateral forces on either side of the articulated heavy vehicle
Steer Tire Friction Demand	The ratio of normalized horizontal force to the available peak friction
Tail Swing	Maximum lateral offset the rear corner of the vehicle travel outside of the front wheel path

As mentioned in the previous section, the most frequently used performance measures are RWA and PFOT (known as LSOT/HSOT at low/high speed conditions). In order to better understand these criteria, typical illustrations are presented in Figure 2-1 and Figure 2-2.

RWA is based on the peak values of lateral acceleration responses of the towing and trailing units. In Figure 2-1, P_r and P_f represent the peak values of lateral accelerations of trailer and tractor units. RWA value is calculated by taking the ratio of P_r to P_f.

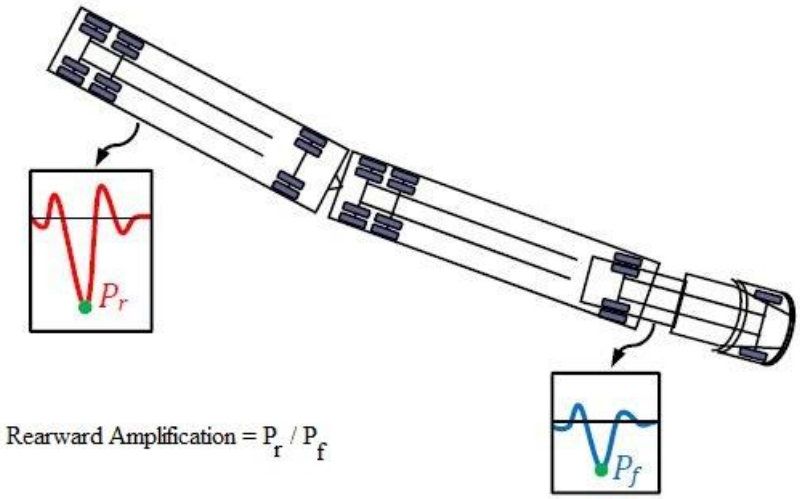

Figure 2-1: Illustration of rearward amplification ratio (RWA) [9]

PFOT is described as the maximum swept width between the paths followed by the tractor and semi-trailer units. In Figure 2-2, largest distance between the solid line and the dashed line identifies the PFOT measure.

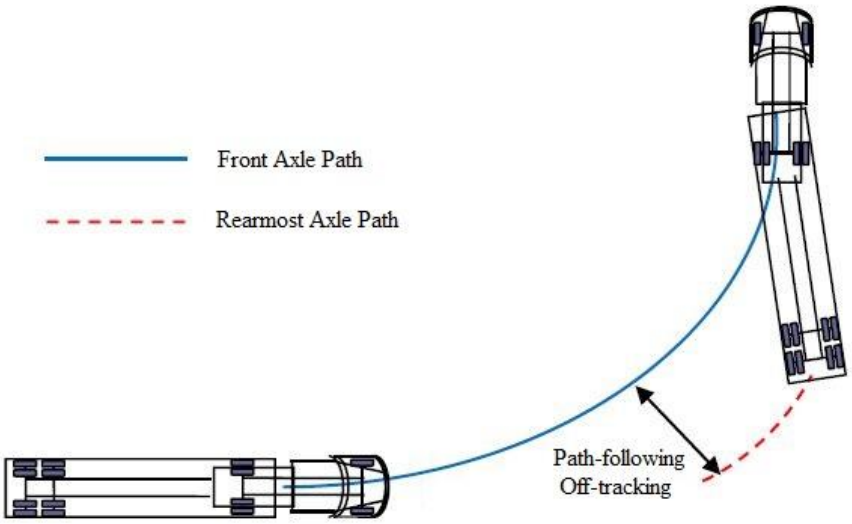

Figure 2-2: Illustration of path-following off-tracking (PFOT) [9]

2.3 STANDARD MANEUVERS

After reviewing general lateral performance measures for the AHV's, it is necessary to specify the standard maneuvers on which these measures are taken. Researchers have tried different maneuvers for both low and high speed cases, some of which have been standardized internationally. Below are some examples to commonly used standard maneuvers.

In the research conducted by Fancher and Winkler [4], the authors investigated the *single lane change maneuver* identified previously by International Standards Organization (ISO) in 2000. According to the study, the single sine-wave lateral acceleration input had been described as follows: A minimum lateral acceleration of 0.15g must be achieved at the front axle of the towing unit. The required steering input must be in the period of 0.4 Hz which can be converted to 2.5 seconds. The longitudinal speed of the vehicle combination should be 88 km/h. Similarly, SAE J2179 testing maneuver describes a single lane change at 88 km/h, allowing 1.464 m lateral offset for 61 m longitudinal distance [14]. In general, these maneuvers have been used for the evaluation of rearward amplification (RWA) ratio and transient state off-tracking (TOT) obtained by the relevant vehicle dynamic simulations.

High speed constant radius turning maneuver is described as traveling of the AHV at the speed of 100 km/h while the front axle centerline of the towing unit follows the path of a 393 m radius circle [17]. With this maneuver, the high-speed steady state off-tracking (HSOT) values can be obtained.

According to the study conducted by Jujnovich and Cebon [18], *low speed circle turning maneuver* and *low speed 90° intersection turn maneuver* are defined at a vehicle forward speed of 10 km/h. The towing unit of the AHV must follow the path of 11.25 m circle during both turning maneuvers. The lateral performance measure, low speed swept path, is obtained by using low speed circle turning maneuver. Also, low speed off-tracking (LSOT) is measured by implementing low speed 90° intersection turn maneuver.

2.4 PASSIVE TRAILER STEERING SYSTEMS

The lateral performance of the AHV's has been improved with the implementation of trailer steering systems. In order to resolve the lateral performance issue, a reasonable approach was introduced with the utilization of the passive trailer steering (PTS) systems. Several types of PTS systems have been proposed in the literature, consisting of self-steering, command steering, and pivotal bogie systems. As implied by its name, PTS systems apply the steering action to the corresponding trailer axles in a passive manner. For some PTS systems like self-steering, the forces created by the tire-road interactions determine the steering angle of the trailer wheels. However, the determination of trailer steering angle in PTS systems is generally done based on the value of the articulation angle between the vehicle units. Command steering and pivotal bogie systems make use of the rule mentioned above, i.e. the wheels of the trailer are steered at an angle proportional to the hitch angle.

2.4.1 Self-steering Systems

The first classic example of the passive trailer steering system is self-steering. According to LeBlanc et al. [19], self-steering systems were first developed to be used as a second axle of a tandem axle group on straight trucks. The major aim was to reduce off-tracking and tire scuffing in tight turns. The influences of self-steering axles on the steady-state handling performance of some AHV configurations are discussed in their research. A similar research conducted by Nisonger and Macadam has demonstrated that self-steering axles increase low-speed maneuverability as well as reducing the tire wear [20]. In another study, Luo examined the directional characteristics and performance of self-steered axles together with the liftable axles [21]. The results of his work reveal that self-steering axles possess large friction demand at both low and high speeds, suggesting high risk of jack-knifing.

2.4.2 Command-steering Systems

Command steering is another well-known example of PTS systems. For passive command steering systems, the rearmost trailer wheels are steered by an angle in relation to the articulation angle between the units via a mechanism. Figure 2-3 illustrates an example of a command steering mechanism.

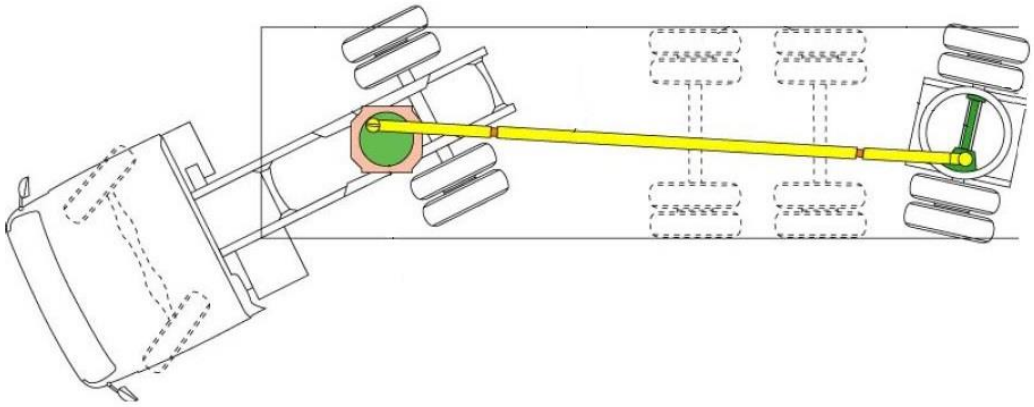

Figure 2-3: Command steering mechanism[2]

In 1991, Sankar et al. [22] published a paper in which they compared the lateral performance in cases of using command steering and self-steering systems. In their study, command steering is identified as forced steering, where the steering angle is expressed as a function of the articulation angle and the front wheel steering angle. In a more recent work, Özkan et al. [23] reported a study related to the minimization of tire wear with command-steering. An optimization procedure is used in their investigation to achieve a reduction of tire wear on AHV's without deteriorating the vehicle path. Both studies demonstrated that command trailer steering systems enhances the low-speed lateral performance of the articulated vehicles. The above finding is also consistent with the study carried out by Jujnovich and Cebon [18]. To conclude, the results of the studies reveal that low-speed maneuverability of the vehicle is improved as a consequence of the command steering.

2.4.3 Pivotal Bogie Steering Systems

Similar to command trailer steering, pivotal bogie systems utilize the trailer steering action depending on the articulation angle of the AHV. Pivotal bogie system differs from command steering in one main principle. In this PTS system, the whole bogie set is steered instead of individual axles of the trailer, causing additional complexity to the trailer steering system. An illustration of a pivotal bogie mechanism is given in Figure 2-4. Several bogie steering mechanisms have been patented in the past decade [24][25][26]. However, the implementation of modern bogie mechanism for the PTS systems has been introduced recently. Being a new type of pivotal bogie steering

system, Trackaxle® PTS system earned popularity in 2000's [27]. In the paper, Prem et al. indicated that the Trackaxle® PTS system offers enhanced safety and efficiency as well as reduced harm to the roads. In a different study[28], Prem and Atley mentioned potential benefits of the PTS system in many areas. They claimed that the Trackaxle® pivotal bogie system offers superior low speed off-tracking ability as well as reductions in road damage and tire scuffing. Furthermore, Jujnovich and Cebon [29] performed an experimental investigation on an articulated test vehicle in which its trailer is supported with pivotal bogie steering strategy. The outcome of their work was consistent with the results of the previous studies.

Figure 2-4: Pivotal bogie mechanism

2.5 ACTIVE TRAILER STEERING SYSTEMS

The primary goal of recent trailer steering researches is the development of a method, which can provide acceptable performance for a wide range of longitudinal vehicle speeds. Since all the previously stated PTS methods suffer from some serious limitations at high speeds, recent developments have emphasized the need for active trailer steering (ATS) strategies. Thus, recently, ATS systems have been one of the major research subjects on the articulated vehicle studies.

In order to accomplish the contradictory design objectives of AHVs at both low and high speeds, various active steering strategies have been proposed in the literature

[30][31][32]. These strategies can be classified under five categories as steer ratio principle, active command steering, reference model tracking, path-following and time-lag types. Following subsections identify the classified types of the control strategies found in the literature.

2.5.1 Steer Ratio Principle

In the past studies, steer ratio was a commonly-used trailer steering principle in articulated vehicles. In the literature, the term refers to the steering action on the towing units proportional to the steer angle of tractor unit or directional velocity. In the analysis of Wu and Lin, the influence of additional steerable trailer axles on the dynamic lateral performance was examined [33]. The control method suggested the steering of the trailer axle wheels in relation to the front steering angle of the tractor unit, concerning the forward vehicle speed. The corresponding steer ratio was determined by making the side slip angle equal to zero in steady state turning situations at all forward speeds. Three important conclusions of their study was the enhancement in lateral stability, reduction in phase delay of trailer unit, and improvement in maneuverability of vehicle. Furthermore, Wu [34] obtained similar findings in his next study, concerning the effect of roll degree of freedom in the investigation. In a more recent work, Rangavajhula and Tsao compared the off-tracking performance of AHV by implementing trailer steering at particular steer ratios [35]. The researchers have confirmed that trailer steering led to less off-tracking at all forward speeds. On the other hand, the researchers have observed the major weakness of steer ratio approach at high speeds.

2.5.2 Active Command Steering Strategy

Rangavajhula and Tsao proposed an active steering strategy mainly established with regard to a previously mentioned PTS method [5]. The trailer steering strategy was implemented on an AHV combination involving a number of trailers. The investigation of the command steering based active optimal control has utilized the geometric relation with the articulation angle, similar to the passive system. According to the study, the passive command steering is very effective in reducing off-tracking

only at low speeds, whereas the active one provides superior lateral performance at low to medium speeds.

2.5.3 Reference Model Tracking Strategy

Another strategy in active trailer steering systems can be identified as reference model tracking. Oreh et al. [32] have suggested an ATS strategy that tries to follow ideal reference responses of side slip, yaw rate, and articulation angle. Actually, they defined a desired set of vehicle states that the trailer should track. According to the study, the tracking of ideal side slip velocity and yaw rate characteristics is very effective in the lateral performance of the AHV only at high speed conditions. In contrast, this result in practically no improvement at low speeds. Furthermore, following the trajectory of proposed reference articulation angle exhibits good off-tracking performance at both low and high vehicle speeds. Another study conducted by Oreh, Kazemi and Azadi have suggested an ATS strategy, tracking a desired articulation angle between the units [12]. The authors have stated that the following of reference articulation angle provides a more direct method compared to the other techniques in terms of path-following. The reference hitch angle of the proposed method is calculated regarding the rear end of the semi-trailer to follow the fifth wheel path. A fuzzy logic controller (FLC) is implemented in the research to track the ideal trajectory of the hitch angle. As a conclusion, the lateral performance of the proposed method is effective in terms of off-tracking. In their next study [16], the authors have obtained similar findings by investigating another reference model tracking controller.

2.5.4 Path-following Type Strategies

Path-following ATS strategies are one of the most commonly used type in articulated vehicles. A considerable amount of literature has been published on that strategy up to now. In 1991, Notsu et al. [36] introduced an ATS strategy, called as path-following control method. The aim of the study was to suppress the swaying oscillations of trailers as well as providing better off-tracking performance. The basic idea behind the strategy was the steering of trailer axle wheels so that the rear end of the trailing unit should follow the front end of the towing unit. In the study, the required trailer steering angles are determined after the estimation of tractor path with the use of a

mathematical model. According to the research, the low speed off-tracking ability of the articulated test vehicle has improved with the utilization of the control method. However, there has been some discussion about the limitations and drawbacks of the study. After the introduction of the path-following strategy, many scientists pursue the development of Notsu's idea. In a recent work, Jujnovich and Cebon [37] have analyzed the CT-AT path following strategy, meaning an active trailer (AT) unit tracking its conventional tractor (CT) unit. The strategy has focused on the idea that the centerline of trailer rear end (follow point) should correctly track the articulation point (lead point). Detailed analyses at high speed cases are performed. However, the drawbacks of the method at low speed cases appeared. Furthermore, the researchers have concluded that the proposed strategy cannot make the fifth wheel to follow the front of the tractor unit. To preclude the situation, they have utilized an AT-AT strategy applying an additional steering action on the drive axles of the tractor unit. According to their conclusion, AT-AT strategy performed slightly better than the CT-AT strategy due to the extra steering action on tractor axles. In a similar study, Roebuck et al. [38] have designed a path-following controller for an AHV in case of high speed maneuvers. An AHV consisting of a truck, a dolly and a semi-trailer are first modeled for the implementation of the LQR controller. Afterwards, a Kalman filter is used to estimate all the vehicle states and the positions of the follow and lead points. The main objective of the optimal controller was to minimize the errors between the path of follow points and lead points of relevant vehicle units. In other words, the dolly tries to follow the path of the truck whereas the semi-trailer aims to follow the dolly path. Further investigation is performed via the implementation of the controller on a test vehicle, where the trailer axles are steered by hydraulic actuators. The results of the study have verified that the suggested path-following controller reduced the off-tracking and RWA of the vehicle. Different from the past studies, the research conducted by Cheng et al. [14] have examined a path-following controller in combination with a roll stability controller. The authors utilized optimal control methods, enhancing roll stability without deteriorating the path tracking ability. The relevant cost function of the LQR has regarded the path following error and RWA ratio as parameters to be minimized. The results demonstrated that the roll stability is

improved while keeping the path-following errors in an allowable ranges. Islam and He [3] proposed the lateral position deviation preview (LPDP) controller to prevent the unstable modes of the AHV's. The suggested model can also be considered as a path-following controller, offering a simpler way of path-tracking by appropriate matrix manipulations. All the papers published recently about the path-following controllers verifies the convenience of the approach in the field of active articulated trailer steering [39][40][41].

As distinct from other studies, Ding, Mikaric, and He tested the performance of an ATS system applying the optimal control in real time simulations [42]. A simulation environment is constructed consisting of a vehicle model on TruckSim®, an optimal controller, and the driver. In order to determine the active steering angles of the trailer wheels, a linear quadratic regulator (LQR) working in real time is used as ATS controller. The authors point out that the study has demonstrated the enhancement in low speed maneuverability. Also, improvement on high speed stability of the articulated vehicle is stated.

In his study, Islam has proposed a new approach called as two design loop (TDL) and single design loop (SDL) method [31]. In the study, the aim was to implement an active trailer steering system together with the design optimization of passive trailer variables. In order to better explain the approach, the main principle of TDL and SDL method is identified as follows: Optimal controller parameters are found for low speed and high speed cases, using Genetic Algorithm technique. Besides, the passive design variables of trailing unit such as the mass, inertia and distances between the trailer axles are determined in their allowable ranges. Both methods utilize the same principle with one significant difference. The TDL method computes the passive trailer variables after the controller design, whereas SDL performs the calculations in a single loop simultaneously. In his next study, Islam et al. [43] have concluded that the methods improve low speed maneuverability and high speed lateral stability.

2.5.5 Time-lag Strategy

Kharrazi et al. [44] proposed a different active trailer steering strategy. The approach was based on the regulation of the time delay between the steering action of the driver

and the creation of lateral forces on the trailing axle wheels. For any kind of vehicle, the lateral tire forces are developed as a reaction to the driver steering input. However, the formation of the tire forces on trailing units require some time after the instant the driver steers the towing vehicle unit. The steering-based controller aims to regulate the timing of active steering of the trailer wheels so that the formation of trailer tire forces would be compatible with the steering action of the driver. The performance of the proposed controller has been tested with the use of computer simulations as well as the implementation on a test vehicle. A significant reduction in RWA ratio and off-tracking, without deteriorating the maneuverability, has been observed. In their next study, Kharrazi, Lidberg and Fredriksson have applied the same ATS strategy, named as the generic controller at that time [45]. Implementing the time-delay controller approach, several different combinations of articulated heavy vehicles have been compared in terms of various lateral performance measures. As a result of the study, the suggested controller has been verified as effective for all vehicle combinations. The details of the both articles could be seen in the dissertation of Kharrazi [9].

2.6 MOTIVATION AND SCOPE OF THE STUDY

Regarding the significance of AHV's in transport technology, the proper design of articulated heavy vehicles is of great importance, particularly with respect to safety. The present study focuses on the modeling and active steering control of articulated vehicles with multi-axle semi-trailers. The improvement of the lateral performance of tractor semi-trailer combinations for both low and high speeds is the major focus of the study.

The fundamental design objectives for articulated heavy vehicles have been PFOT and RWA, at low and high vehicle longitudinal speeds, respectively. The high speed lateral performance of an AHV, as indicated by the design objectives, deteriorates while meeting the low speed design goals and vice versa [4]. Therefore, a successful method should be developed to meet both high and low speed requirements at the same time. The main subject of the study is to resolve the conflicting design objectives at different vehicle speeds by developing a strategy for the active steering of the semitrailer axles.

CHAPTER 3

MODELING

Having discussed the literature in the previous chapter, the purpose of this chapter is to provide a detailed explanation of modeling of the tractor and multi-axle semi-trailer combination. The derivation procedure of the 5 degree of freedom (DOF) yaw/roll vehicle model is expressed in detail.

First of all, the complete description of the AHV is provided. The modeled tractor comprises a steerable axle at the front and drive tandem axles at the back. The trailing unit is connected with the tractor unit by means of a fifth wheel located at the articulation point. The semi-trailer has three axles at the back side that are conventionally unsteered. In the Figure 3-1, however, all the semi-trailer axles are shown with steering angles in order to represent the forces created in case of active steering of each axle tires.

In the yaw/roll model demonstrated in Figure 3-1 and Figure 3-2, ISO reference coordinate system is used, meaning that the orientation of the X,Y and Z axes indicate the forward, upward and left side of the vehicle, respectively. In order to simplify the appearance of the model, each axle is represented by one equivalent wheel in the figure. The equations of motions are derived with the use of Newton's laws of dynamics.

The 5 DOFs of the yaw/roll vehicle model are expressed with the following terms: the side slip of the tractor v, the yaw rate of the tractor r, the roll angle of the tractor ϕ, the yaw rate of the semi-trailer r_t, and roll angle of semi-trailer ϕ_t. Note that the side

slip of semi-trailer is a depended term that can be represented as a combination of other states. For better understanding the terms denoted in the vehicle model, a brief look at the nomenclature (provided at the beginning of the thesis) may be necessary.

The basic assumptions in the derivation of the articulated vehicle model could be listed as follows:

- Body centered coordinate systems are fixed to the center of gravities (COG) of towing and trailing vehicle units.
- The total masses of the tractor and semi-trailer are lumped at their COGs as point masses.
- The stiffness of the tires is combined so that the equivalent cornering stiffness is the total stiffness of the wheels on the same axle.
- The lateral tire forces are assumed as a linear function of tire slip angles.
- Longitudinal tire forces such as traction and braking forces are ignored due to their relatively small influence on lateral dynamics of the AHV. That is, the tire forces on the x-directions are neglected.
- Pitch and bounce motion of both AHV units are irrelevant to the thesis topic and ignored.
- The velocities at the articulation point of towing and trailing units are compatible since both units are considered to travel at a constant forward speed U.

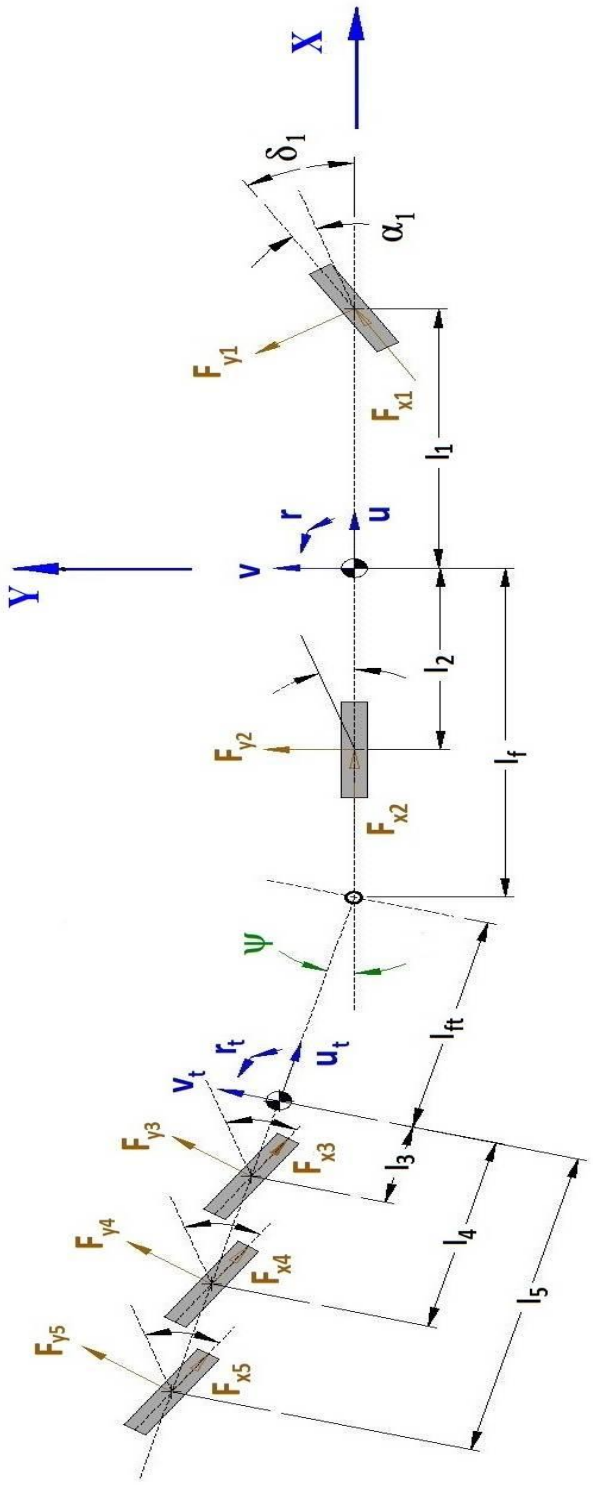

Figure 3-1: Bicycle model of the tractor and semi-trailer combination

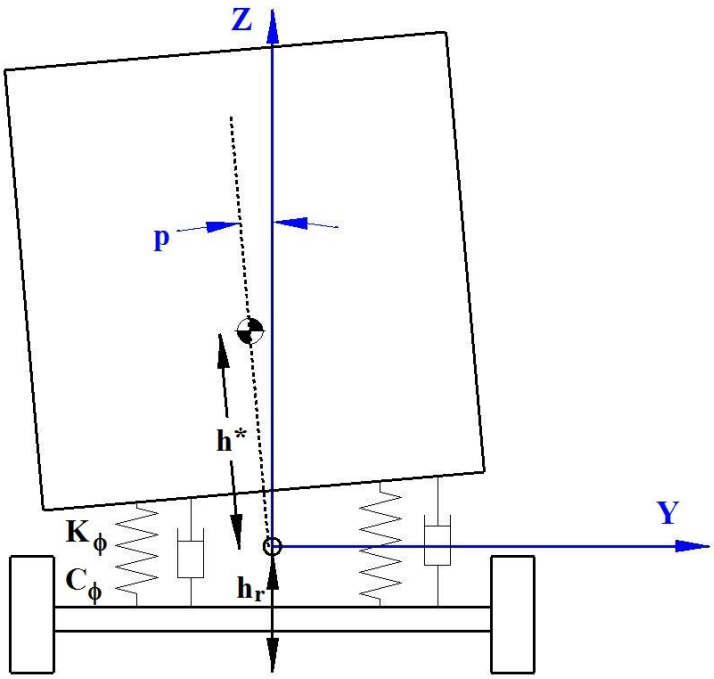

Figure 3-2: Additional roll degree of freedom of the combination

3.1 EQUATIONS OF MOTIONS

According to Figure 3-1, the full expressions of force and moment equilibrium regarding the side-slip, yaw and roll motions for *the tractor* are as follows:

$$m(\dot{v} + Ur) - m_s(h^*\dot{p}) = F_{y1}cos\delta_1 + F_{y2} + F_{yf} \tag{3.1}$$

$$-I_{sxz}\dot{p} + I_{zz}\dot{r} = l_1(F_{y1}cos\delta_1 + F_{x1}sin\delta_1) - l_2F_{y2} - l_fF_{yf} \tag{3.2}$$

$$I_{xx}\dot{p} - I_{xz}\dot{r} - m_sh^*(\dot{v} + Ur) = m_sgh^*sin\phi - (\sum K_\phi)\phi - (\sum C_\phi)p - h_{fr}F_{yf} + K_{12}(\phi_t - \phi) \tag{3.3}$$

Note that the force equilibrium in x direction stands for the longitudinal motion of the articulated heavy vehicle units. Due to the assumptions made in the previous pages, the longitudinal dynamics are irrelevant to the topic. Therefore, the equations of motion in x-direction for both vehicle units are skipped.

Similarly, the equations of motions corresponding to the side-slip, yaw and roll motions for *the semi-trailer* are expressed as follows:

$$m_t(\dot{v}_t + U_t r_t) - m_{st}({h_t}^* \dot{p}_t) = -F_{yf} cos\Psi + F_{y3} cos\delta_3 + F_{y4} cos\delta_4 + F_{y5} cos\delta_5 \quad (3.4)$$

$$-I_{sxzt}\dot{p}_t + I_{zzt}\dot{r}_t = -l_3 F_{y3} cos\delta_3 - l_4 F_{y4} cos\delta_4 - \mathrm{l}_5 F_{y5} cos\delta_5 - l_{ft} F_{yf} \cos\Psi \quad (3.5)$$

$$I_{xxt}\dot{p}_t - I_{xzt}\dot{r}_t - m_{st}{h_t}^*(\dot{v}_t + U_t r_t) = m_{st} g {h_t}^* sin\phi_t - \left(\sum K_{\phi t}\right)\phi_t - \left(\sum C_{\phi t}\right)\mathrm{p}_t + h_{frt} F_{yf} \cos\Psi - K_{12}(\phi_t - \phi) \quad (3.6)$$

In addition to the previous expressions, the compatibility equation for the velocities on the fifth wheel is expressed as follows:

$$U_t = U cos\Psi - v sin\Psi + l_f r sin\Psi \quad (3.7)$$

$$v_t = U sin\Psi + v cos\Psi - l_f r cos\Psi - l_{ft} r_t - h_{fr} p + h_{frt} p_t \quad (3.8)$$

Note that the tire lateral forces F_{yi}'s are assumed as a function of cornering stiffness and slip angles as indicated in Equation (3.9).

$$F_{yi} = \sum {C_s}^i \alpha_i = C_i \alpha_i \qquad for\ i = 1,2,3,4,5 \quad (3.9)$$

Furthermore, the non-linear expressions of the slip angles α_i for ith axle wheels are written in the following equations.

$$\alpha_1 = \tan^{-1}\left(\frac{v + l_1 r}{U}\right) - \delta_1 \quad (3.10)$$

$$\alpha_2 = \tan^{-1}\left(\frac{v - l_2 r}{U}\right) \quad (3.11)$$

$$\alpha_3 = \tan^{-1}\left(\frac{v_t - l_3 r_t}{U_t}\right) + \delta_3 \quad (3.12)$$

$$\alpha_4 = \tan^{-1}\left(\frac{v_t - l_4 r_t}{U_t}\right) + \delta_4 \quad (3.13)$$

$$\alpha_5 = \tan^{-1}\left(\frac{v_t - l_5 r_t}{U_t}\right) + \delta_5 \quad (3.14)$$

Manipulating the equations from (3.1) to (3.14), the final linearized version of the differential equations is obtained (see Appendix A for details) as follows:

$$\{m\}\dot{v} + \{m_t\}\dot{v}_t + \{-m_s h^*\}\dot{p} + \{-m_{st} {h_t}^*\}\dot{p}_t = \left\{\frac{C_1 + C_2}{U}\right\} v + \left\{\frac{C_3 + C_4 + C_5}{U}\right\} v_t + \left\{\frac{C_1 l_1 - C_2 l_2 - mU^2}{U}\right\} r + \left\{\frac{-C_3 l_3 - C_4 l_4 - C_5 l_5 - m_t U^2}{U}\right\} r_t + \{-C_1\}\delta_1 + \{C_3\}\delta_3 + \{C_4\}\delta_4 + \{C_5\}\delta_5 \quad (3.15)$$

$$\{ml_f\}\dot{v} + \{I_{zz}\}\dot{r} + \{-I_{sxz} - m_s h^* l_f\}\dot{p} = \left\{\frac{C_1 l_1 - C_2 l_2 + (C_1 + C_2) l_f}{U}\right\} v + \left\{\frac{C_1 {l_1}^2 + C_2 {l_2}^2 + (C_1 l_1 - C_2 l_2 - mU^2) l_f}{U}\right\} r + \{-C_1(\mathrm{l}_1 + l_f)\}\delta_1 \quad (3.16)$$

$$\{mh_{fr} - m_s h^*\}\dot{v} + \{-I_{sxz}\}\dot{r} + \{I_{sxx} - m_s h^* h_{fr}\}\dot{p} = \left\{\frac{(C_1 + C_2) h_{fr}}{U}\right\} v + \left\{\frac{(C_1 l_1 - C_2 l_2 - mU^2) h_{fr} + m_s U^2 h^*}{U}\right\} r + \{-\sum C_\phi\} p + m_s h^* g - \sum K_\phi - K_{12}\phi + \{K_{12}\}\phi_t + \{-C_1 h_{fr}\}\delta_1 \quad (3.17)$$

$$\{-m_t l_{ft}\}\dot{v}_t + \{I_{zzt}\}\dot{r}_t + \{I_{sxzt} + m_{st} {h_t}^* l_{ft}\}\dot{p}_t = \left\{\frac{-C_3(l_3 + l_{ft}) - C_4(l_4 + l_{ft}) - C_5(l_5 + l_{ft})}{U}\right\} v_t + \left\{\frac{C_3 l_3^2 + C_4 l_4^2 + C_5 l_5^2 + (C_3 l_3 + C_4 l_4 + C_5 l_5 + m_t U^2) l_{ft}}{U}\right\} r_t + \{-C_3(l_3 + l_{ft})\}\delta_3 + \{-C_4(l_4 + l_{ft})\}\delta_4 + \{-C_5(l_5 + l_{ft})\}\delta_5 \quad (3.18)$$

$$\{m_t h_{frt} - m_{st} h_t^*\}\dot{v}_t + \{-I_{sxzt}\}\dot{r}_t + \{I_{sxxt} - m_{st} h_t^* h_{frt}\}\dot{p}_t$$
$$= \left\{\frac{(C_3 + C_4 + C_5)h_{frt}}{U}\right\} v_t$$
$$+ \left\{\frac{-h_{frt}(C_3 l_3 + C_4 l_4 + C_5 l_5 + m_t U^2) + m_{st} U^2 h_t^*}{U}\right\} r_t$$
$$+ \{-\sum C_{\phi t}\}\mathrm{p}_t + \{K_{12}\}\phi + \{m_{st} h_t^* g - \sum K_{\phi t} - K_{12}\}\phi_t + \{C_3 h_{frt}\}\delta_3$$
$$+ \{C_4 h_{frt}\}\delta_4 + \{C_5 h_{frt}\}\delta_5 \quad (3.19)$$

$$\{-1\}\dot{v} + \{1\}\dot{v}_t + \{l_f\}\dot{r} + \{l_{ft}\}\dot{r}_t + \{-h_{fr}\}\dot{p} + \{h_{frt}\}\dot{p}_t = \{U\}r + \{-U\}r_t \quad (3.20)$$

$$\{1\}\dot{\phi} = \{1\}p \quad (3.21)$$

$$\{1\}\dot{\phi}_t = \{1\}p_t \quad (3.22)$$

These differential equations provide the base for the state space system modeling in the next section.

3.2 STATE-SPACE SYSTEM MODELING

Before proceeding to examine the construction of state-space matrices, it is crucial to address the theory behind the method. In control engineering, a state space system may be defined as a mathematical model of a physical system. The approach is said as a generalized time domain technique for modelling, analyzing and designing a wide range of control systems. A significant characteristics of state space modeling is its superior suitability with digital computational methods. The modeling in state space is preferred due to its ease of use on the software employed in this study, MATLAB®. In order to construct a state-space representation, the equations of motions should be expressed as a set of first-order differential equations in terms of the state and the input variables. If the original dynamic system is identified as linear time invariant equations, the application of state space representation on MATLAB® is simpler with the use of known matrix forms. A general mathematical form of the state space representation is provided as follows:

$$\dot{\boldsymbol{x}}(t) = \boldsymbol{A}\boldsymbol{x}(t) + \boldsymbol{B}\boldsymbol{u}(t) \quad (3.23)$$

$$\boldsymbol{y}(t) = \boldsymbol{C}\boldsymbol{x}(t) + \boldsymbol{D}\boldsymbol{u}(t) \quad (3.24)$$

where $\boldsymbol{x}(t), \boldsymbol{y}(t)$ and $\boldsymbol{u}(t)$ is called as state vector, output vector and input vector, respectively. The terms A, B, C and D represent the relevant matrices of the physical system, input etc.

In order to express the dynamics of the articulated vehicle as a state space model, the equations of motions pointed out in the previous section is used. The 8 state variables of the system is chosen as in the following matrix:

$$\boldsymbol{x} = \begin{bmatrix} v & v_t & r & r_t & p & p_t & \phi & \phi_t \end{bmatrix}^T \tag{3.25}$$

The state variables listed above indicates the side slip motions, yaw rates, roll rates and roll angles at the COGs of the tractor and semi-trailer units, respectively.

Using the states expressed above, the linear time invariant (LTI) state space model is written in the form of Equation (3.26).

$$\begin{Bmatrix} \dot{v} \\ \dot{v}_t \\ \dot{r} \\ \dot{r}_t \\ \dot{p} \\ \dot{p}_t \\ p \\ p_t \end{Bmatrix} = [A]_{8x8} \begin{Bmatrix} v \\ v_t \\ r \\ r_t \\ p \\ p_t \\ \phi \\ \phi_t \end{Bmatrix} + [B]_{8x4} \begin{Bmatrix} \delta_1 \\ \delta_3 \\ \delta_4 \\ \delta_5 \end{Bmatrix} \tag{3.26}$$

The elements of the state space matrices are supplied in the Appendix-A.

After completing the state space representation of the articulated vehicle, the trajectory of the vehicle may be determined in terms of states variables. The utilization of off-tracking as a performance measure necessitates the accurate computation of the trajectory of the articulated heavy vehicle. The path that the articulated vehicle follows can easily be obtained based on the information about the state variables.

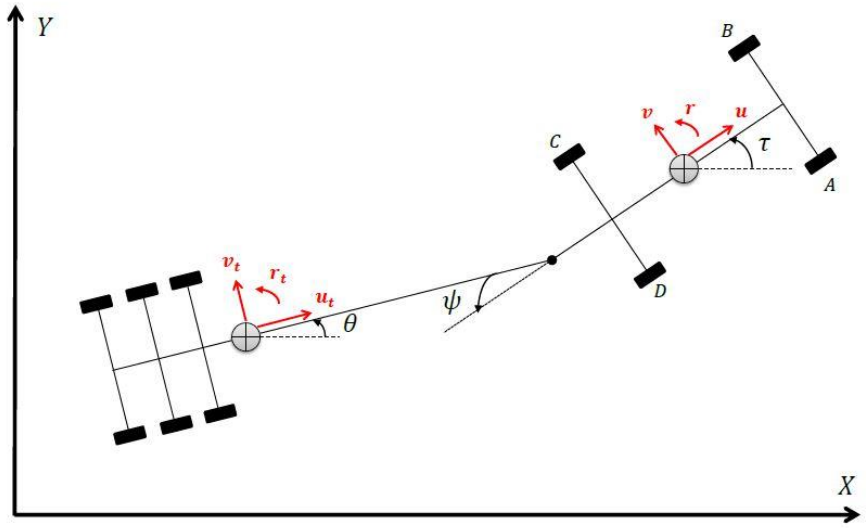

Figure 3-3: Trajectory coordinate system

The equations regarding the trajectory of the vehicle are derived with respect to the global coordinate system fixed to the ground (see Figure 3-3). First of all, the velocities on the x and y directions is determined with respect to the global coordinate system. Afterwards, the integral of that velocities help to obtain the position of the tractor and semi-trailer units. The corresponding velocities of the towing unit are written as in the following equations:

$$\dot{\tau} = r \tag{3.27}$$

$$\dot{x} = Ucos(\tau) - vsin(\tau) \tag{3.28}$$

$$\dot{y} = vcos(\tau) + Usin(\tau) \tag{3.29}$$

Integration of the equations (3.28) and (3.29) results in the position of the towing unit in a 2D environment. The semi-trailer velocities in all direction are determined in a similar manner.

In addition to this, equation (3.30) and (3.31) shows the approximated geometric relation between the adjacent units, providing the rate and angle of articulation between the tractor and semi-trailer:

$$\dot{\psi} = r - r_t \tag{3.30}$$

$$\psi = \tau - \theta \tag{3.31}$$

3.3 DRIVER MODEL

The standard test maneuvers have already been identified in the literature survey chapter previously. There are two ways of implementing active trailer steering depending on the maneuver type. In the first way, for the maneuvers except the *low speed 90° intersection turn*, the steering angles obtained by any ATS strategy are directly implemented on the trailer wheels. At the same time, a specified standard driver steering input is provided for the tractor. For the second way, however, guiding the articulated vehicle along a prescribed path requires a driver model to be used. In case of the intersection turn maneuver, the active trailer steering angles are implemented on the AHV model while the basic driver model also tries to keep the vehicle along the cornering path. In this study, the driver model used in the work of Işıklar is implemented to the suggested vehicle model [46]. The driver model can be seen in Figure 3-4 below:

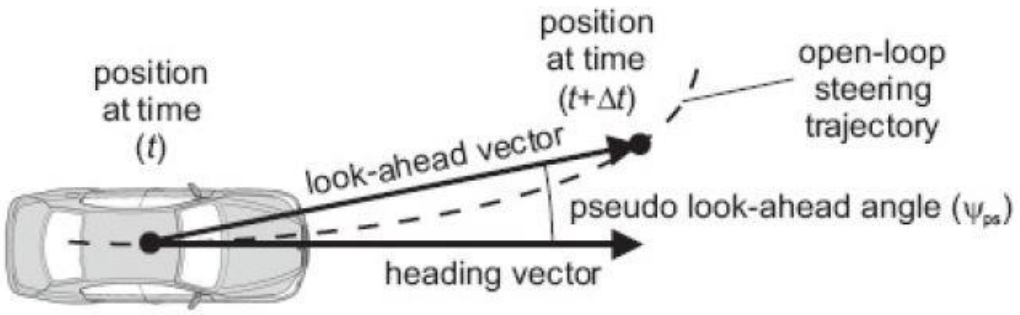

Figure 3-4: The illustration of basic driver model [46]

The driver model defines an error as the difference in the directions of heading vector and look-ahead vector. Then, the driver model drives the vehicle with a tractor steering input proportional to this error. In other words, as the articulated vehicle deviates from the prescribed path more, the modeled driver steers the front axle wheels of the tractor unit by greater angle.

According to this driver model, the steering angle is obtained by the following equation:

$$\delta_1 = K_s \, \psi_{ps} \tag{3.32}$$

where the terms K_s and ψ_{ps} refers to the driver steering sensitivity and pseudo look-ahead angle, respectively.

Using the identified steering angle for the tractor unit, low speed off-tracking (LSOT) analysis is conducted during low speed 90° intersection turning test maneuver.

3.4 STABILITY ANALYSIS

In this section, the stability analysis of the tractor & semi-trailer combination is investigated with the use of the vehicle model derived previously. As a rule of thumb, it is important for a physical system to maintain its stability in a wide range of parameter variations. In the proposed articulated vehicle model, forward speed of the tractor and semi-trailer combination is the main parameter changing the system matrix of the state-space representation. In order to investigate the dynamic stability of the conventional AHV, all the steering inputs for both units are considered to be zero. In other words, the state equation (Equation 3.26) is reduced to the following linear time invariant form:

$$\dot{\boldsymbol{x}} = \boldsymbol{A}\boldsymbol{x} \tag{3.33}$$

The eigenvalues of the system are obtained by finding the roots of the characteristic equation expressed in equation (3.34):

$$\det(s\boldsymbol{I} - \boldsymbol{A}) = 0 \tag{3.34}$$

In the characteristic equation, I, A and s refer to the identity matrix, system matrix and Laplace variable, respectively.

For an asymptotically stable system, it is essential to have a characteristic equation yielding all the roots with negative real parts. Any positive real part of the eigenvalues results in an unstable system. The solution of the equation (3.34) is expressed with the complex conjugate poles as follows:

$$p_{1,2} = -\sigma \pm i\omega_d \tag{3.35}$$

In the expression provided above, the real and imaginary parts σ and ω_d are respectively called as the damping coefficients and damped natural frequency. In addition to this, equation (3.36) shows the damping ratio of the corresponding poles:

$$\zeta = -\frac{\sigma}{\sqrt{\sigma^2 + \omega_d^2}} \tag{3.36}$$

Since system matrix A depends on the vehicle longitudinal speed, the poles and damping ratios have been continuously varying. A convenient way to indicate the stability of the system could be the identification of the damping ratios with the changing forward speed of the AHV. Figure 3-4 illustrates the damping ratios of the system as a function of vehicle longitudinal speed. Because of the 8x8 system matrix, there exist 4 complex conjugate poles as well as 4 different damping ratios. According to the Figure 3-5, only one damping ratio takes negative values after 185 km/h longitudinal speed, indicating an unstable system. Therefore, one can conclude that the conventional articulated vehicle has dynamic stability up to 185 km/h vehicle forward speed. Above this critical speed, any steering action by the driver or any lateral disturbance force will cause the articulated vehicle to experience the instability with non-decaying oscillations.

To summarize, the articulated vehicle model derived in the previous section brings about a stable state-space system up to some limiting longitudinal speed. The critical speed for the instability, which is approximately 185 km/h, seems to be a reasonable limit for an articulated vehicle. The standard test maneuvers does not reach such high forward speeds, implying that the vehicle model is valid for all the test conditions.

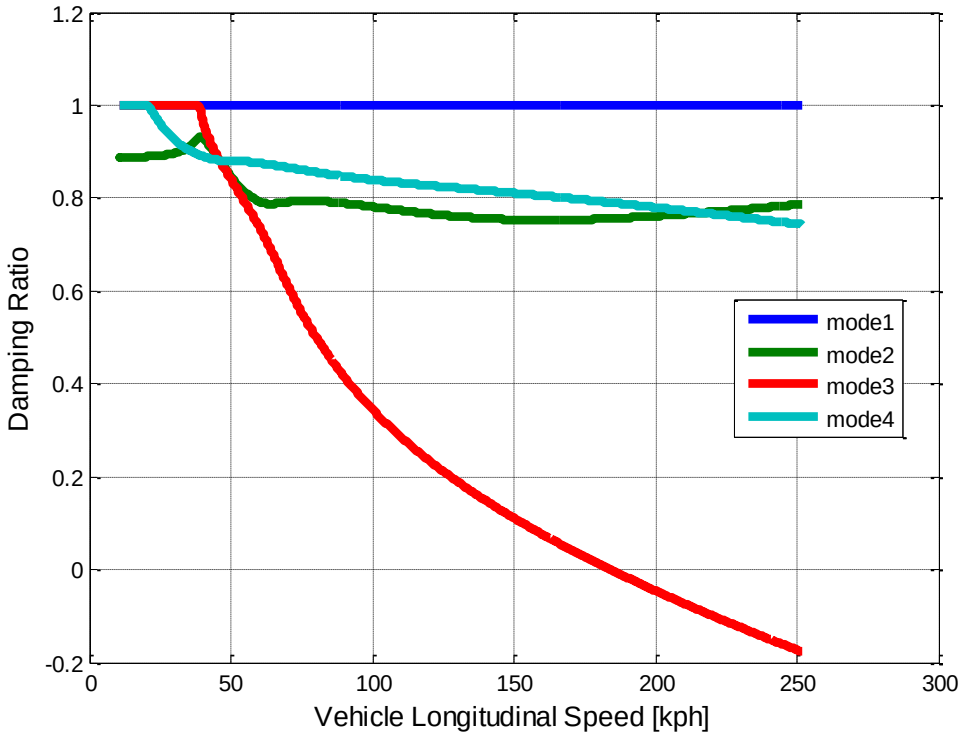

Figure 3-5: Damping ratios as a function of vehicle longitudinal speed

3.5 OPEN-LOOP SIMULATIONS

In this section, open loop responses of the conventional articulated vehicle during the standard maneuvers are investigated. Due to the cost of the field testing, it is more practical to use a vehicle model to simulate the real environment. For this reason, the articulated vehicle has been modeled in the previous subsection. The vehicle model utilizes an advance commercial programming tool, called MATLAB, to simulate the response of the tractor & semi-trailer combination.

For the open loop simulations, standard testing maneuvers described in Section 2.3 are implemented on the MATLAB program, within the simulation of the articulated vehicle model. Originally, the driver implements a specified steering angle only on the front axle wheels of the towing unit, without any active steering action on the semi-trailer axles.

The basic characteristics of the tractor and semi-trailer combination at both low and high speeds can be inferred by looking at the open loop responses. Knowing the

characteristics of the conventional AHV will help to identify the situations that are faced with in the design of ATS strategies at later sections.

3.5.1 Low Speed Characteristics of Tractor and Semi-trailer Combination

In general, an articulated heavy vehicle is exposed to the low speed driving situations during parking or turning on local roads. The main problematic characteristic that the AHV deals with is the swept path occupied by the longer combination vehicle. In case of highly off-tracking AHV's, the vehicle units take up very large spaces on the roads, raising the safety concerns about the vehicle. In order to avoid the negative effects during constant circle or corner turning maneuvers, the proper design of AHV may become crucial.

To simulate the standardized *low speed constant circle turning maneuvers*, the driver provides the ramped step steering input at 10 km/h vehicle forward speed, which is represented by the following equation.

$$\delta_1(t) = A\ tanh\left(\frac{2\pi}{T}t\right) \tag{3.37}$$

where the peak amplitude leads to 11.25 radius steady state turn and the time interval for reaching the peak amplitude corresponds to 3 seconds.

Figure 3-6 illustrates the path followed by center of gravities of the conventional tractor and semi-trailer units. The low speed circle swept path width (SPW) value associated with the standard maneuver is approximately 2.5 m.

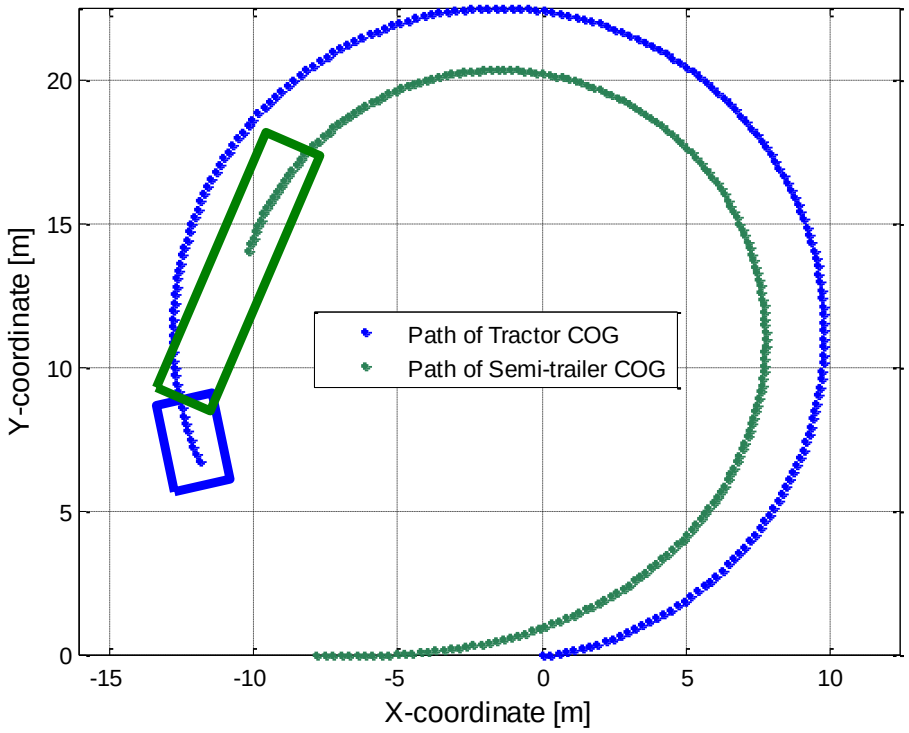

Figure 3-6: Trajectory of COG of the vehicle units during steady-state turning maneuver at 10 kph

Furthermore, the *low speed 90° intersection turning maneuver* have been carried out by the driver as identified previously in Section 3.3. The basic driver model guides the towing unit of the vehicle to turn a 90° intersection having an 11.25 m radius of curvature. The path swept by the COG's and the endpoints of the vehicle units can be seen in Figure 3-7 and 3-8, respectively.

According to the Figure 3-8, the low speed off tracking (LSOT) is measured as approximately 4.5 m in width.

The open-loop responses at low speed indicate that the ability of the trailing unit to follow the towing unit is not sufficiently satisfactory. In order to meet the maneuverability requirements better, the low speed swept path width or off-tracking values should be reduced to lower levels. As a consequence, active trailer steering may become an effective way of ensuring the desired improvement on the low speed lateral performance.

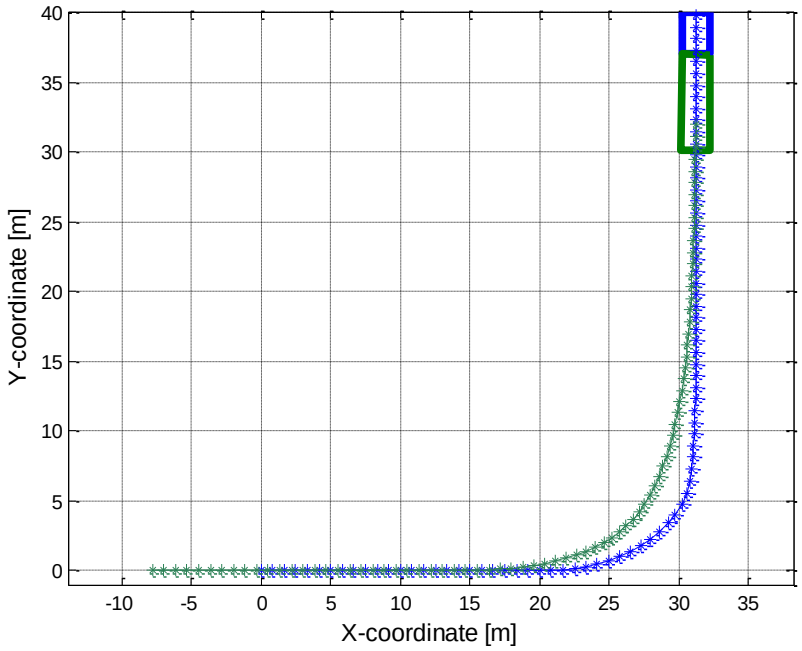

Figure 3-7: The path of the COG's of the tractor and semi-trailer during 90-degree turn at 10 kph

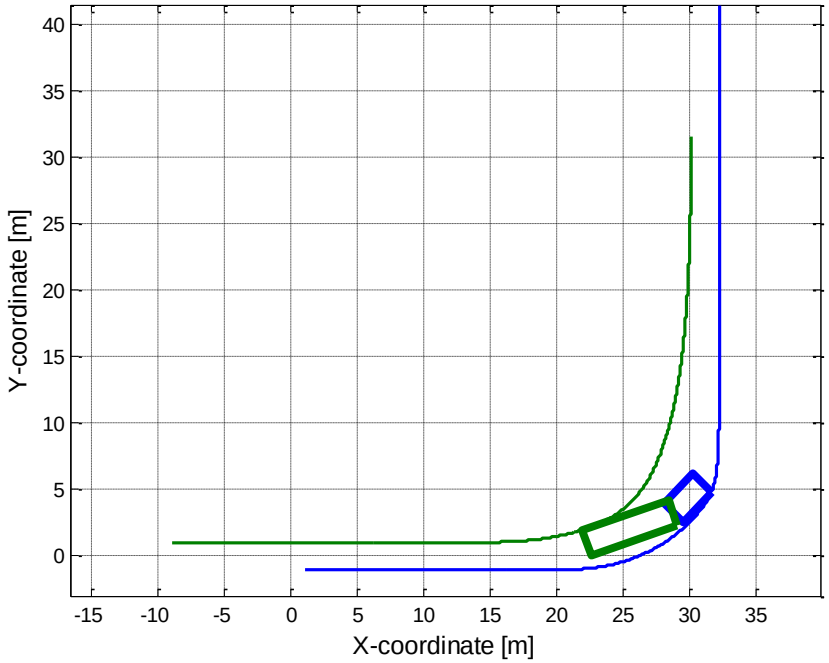

Figure 3-8: The path of the axle endpoints of the tractor and semi-trailer units during 90-degree turn at 10 kph

3.5.2 High Speed Characteristics of Tractor and Semi-trailer Combination

After examining the low speed characteristics of the AHV's, high speed behavior of the tractor and semi-trailer combination is investigated in this section. In most cases, articulated heavy vehicles are used to transport goods and materials on highways. As a result of this, AHV's have generally subjected to high speed driving conditions. Lane changes and turning of large radius curvatures are the two typical maneuvers that the AHV experience at high speed situations.

As indicated in Section 2.3, the standard maneuver for high speed lane change of longer combination vehicles are simulated at 88 km/h with a tractor steering input identified as follows:

$$\delta_1(t) = A\ sin\left(\frac{2\pi}{T}t\right) \tag{3.38}$$

In equation (3.38), the frequency of the sinusoidal input is standardized in the literature as 0.4 Hz, corresponding to a period of 2.5 seconds. Amplitude of the tractor steering input has been chosen in such a way that the minimum lateral acceleration at the front axle of the towing unit should be 0.15g. In this case, the peak amplitude of the steering input is chosen as 2 degrees, whereas the vehicle longitudinal speed is set to 88 km/h. The outcome of the simulations in response to the described maneuver is illustrated in the following figures (Figure 3-9, Figure 3-10, Figure 3-11).

According to the simulations, the rearward amplification ratio (RWA) is measured as 1.138, while the transient state off-tracking (TOT) value equals to 0.113 m. Furthermore, high speed steady state off-tracking (HSOT) is observed as 0.093 m in response to a standard high speed constant radius turn maneuver, in which the driver steering input is similar to the Equation 3.37.

The lateral movements of the towing and trailing units are not experienced simultaneously. The reason for this can be identified as follows: The lateral tire forces are developed on the tractor unit almost immediately in response to the driver steering action. On the other hand, the required lateral forces on semi-trailer tires cannot be generated until a side slip motion occurs. Since the lateral tire forces depend directly

on the slip angles, the situation can easily be noticed by looking at the timing of slip angle generation in Figure 3-9.

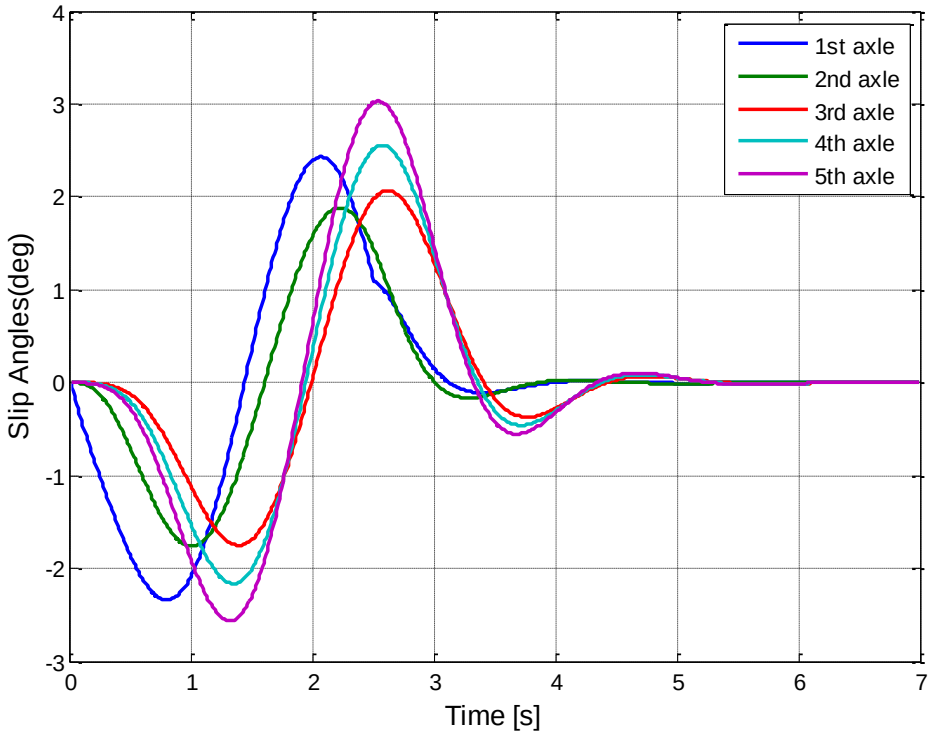

Figure 3-9: Slip angles generated by the tires on each axle of the tractor and semi-trailer combination during standard lane change maneuver

According to the Figure 3-9, there is a time lag between the development of slip angles on tractor (1st and 2nd) tires and semi-trailer (3rd, 4th and 5th) tires.

The time lag between the force generation lead to the amplification on the lateral acceleration of the trailing unit. As seen in the Figure 3-10, the lateral acceleration of the trailing unit follows that of towing unit after some time delay, with greater peak values. According to Figure 3-11, an overshoot is seen in the path of the semi-trailer COG, deteriorating the path-following ability.

To conclude, the main problem at high speed conditions can be said as the amplification of the lateral acceleration. Active trailer steering (ATS) systems can be serve the purpose of meeting the safety requirements by suppressing the RWA and improving path-following ability.

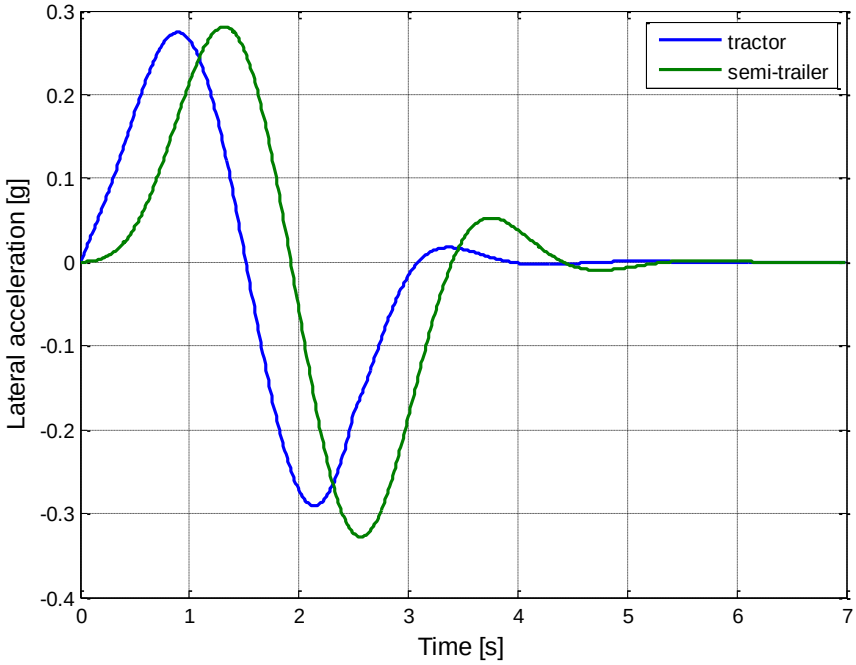

Figure 3-10: Lateral accelerations at the COG's of tractor and semi-trailer units at standard lane change maneuver

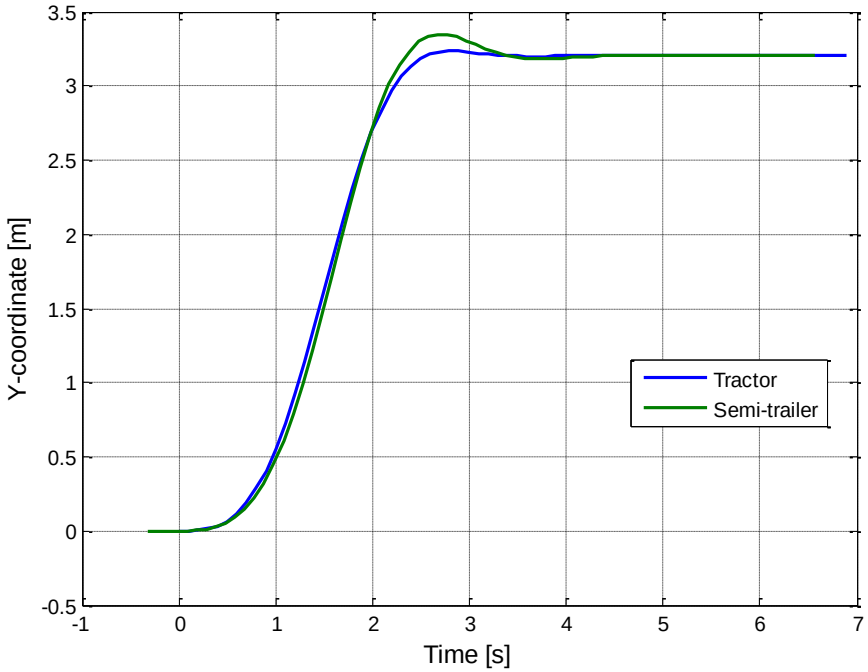

Figure 3-11: The paths of the COG's of tractor and semi-trailer units at standard lane change maneuver

CHAPTER 4

CONTROL STRATEGIES

Several kinds of control strategies are suggested in the literature, some of which are briefly introduced in Chapter 2. In this study, a new ATS control strategy effective at both low and high speed cases is proposed and compared with a number of the described ATS systems.

In this chapter, the theory behind the ATS strategies is examined in detail. Some of these methods are adjusted to be compatible with the comparison requirements of the current study. In the following, the list of active trailer steering approaches that are used in this study is provided:

- Steer Ratio Principle (SR)
- Command Steering Based Active Optimal Control (ACS)
- Virtual Driver Steering Control (VD)
- Lateral Position Deviation Preview Control (LPDP)
- Lead-Unit Following Control (LUF)

Steer ratio (SR) principle is the most basic control strategy and have been investigated in the literature for a long time. The second control strategy is similar to a passive trailer steering system known as command steering. VD and LPDP approaches can be identified as path-following type of ATS systems. The last strategy is based on the time lag approach, aiming the trailing unit and the lead unit to follow the same yaw characteristics. Although the first and second control strategies can be considered as

classical ones in the literature, the remaining approaches have been investigated more recently. In general, the previous approaches focuses on the low speed lateral performance of AHV's and are effective in that speed range. The new strategies, on the other hand, are designed to enhance mostly the high speed lateral performance. Therefore, the selection of both old and new approaches gives opportunity to compare the proposed method with strategies that are operational at both low and high speed conditions.

All of the explained control strategies can be implemented to the vehicle model obtained in Chapter 3 with a change in the state space matrices as follows:

$$\dot{\boldsymbol{x}} = A\boldsymbol{x} + B\delta_1 + B_u u \tag{4.1}$$

In the above expression, the conventional vehicle is turned into an AHV whose trailer wheels are steered actively. The only difference in the state-space form is the addition of the control input u, which represents the active steering angles of the semi-trailer unit and the corresponding control matrix, B_u. The term δ_1 represents the steering action to the tractor unit performed by the driver. Remaining terms indicate the same variables as in equation (3.26). Further details about the state space matrices for each control method are given in Appendix C.

In order to simplify the optimal control matrices and adjust the weightings easily, the three axles of the semi-trailer are combined to a virtual single axle. Then, the active steering input becomes:

$$u = \delta_s \tag{4.2}$$

In other words, the terms δ_1 and δ_s in equation (4.1) correspond to the tractor steering input given by the driver and the active trailer steering input determined by optimal controller, respectively.

In this study, the driver steering input is known for the standard test conditions whereas trailer steering angles are unknown quantities. The aim of all the control strategies is to determine the proper value of that active steering angles so that the lateral performance of the AHV is improved accordingly.

Before proceeding to examine the implementation of active trailer steering, it is necessary to explain the optimal control theory that will be used for the control strategies other than SR principle. As explained in the literature survey chapter, linear quadratic regulator (LQR) technique is the most commonly used control method in the study of active trailer steering. This is because the LQR offers a practical and convenient way of control as well as introducing superior performance.

According to the optimal control theory, the design of control system is usually associated with the choice of a control vector u minimizing a predetermined performance index. For a system described in equation (4.1), a quadratic performance index is written as follows:

$$J = \int_0^\infty (x^T Q x + u^T R u)\, dt \tag{4.3}$$

where both of the Q and R matrices should be positive definite Hermitian or real symmetric matrices. For the performance index given by (4.3), the quadratic cost function yields linear control laws that can be identified with the following expression:

$$u = -Kx \tag{4.4}$$

In equation (4.4), the optimal gain matrix K is defined as

$$K = R^{-1} B^T P \tag{4.5}$$

where the symmetric and positive definite matrix P is obtained with the algebraic Riccati equation given in equation (4.6):

$$A^T P + PA - PBR^{-1}BP + Q = 0 \tag{4.6}$$

In the optimal control theory, the selection of weighting factors is a vital procedure. In this study, the weighting factors are determined by looking at the responses obtained with each active steering control strategy. For each test maneuver, the weighting of ATS strategies that provides the best performance measure is calculated by using a trial-error approach.

4.1 STEER RATIO PRINCIPLE (SR)

Steer ratio principle is the most basic type of the active steering strategy that was introduced in 1980s for 4WS passenger cars. The control method was also used in the study of articulated heavy vehicles [33][34]. In the most recent studies, Rangavajhula and Tsao investigated the effect of different steer ratios on the lateral performance of articulated heavy vehicles.

The control method is based on the fundamental idea of making the active trailer steering in proportional to the tractor front wheel angle. Therefore, the control strategy is written as the following basic formula:

$$\delta_s = \mu\, \delta_1 \tag{4.7}$$

where the terms δ_s, δ_1 and μ refer to active trailer steering angle, tractor front wheel steering angle applied by the driver, and the proportionality constant, respectively.

The most important concern of this control strategy is to determine the proportionality constant connecting the two steering angles. In most cases, the term μ is defined in a way such that the steady state side slip angle of the corresponding vehicle unit equals to zero. Since the system matrix of the vehicle model depends on the vehicle forward speed, there must be a unique proportionality constant for a specific vehicle speed. As a result, system matrices given by equation (3.26) should be solved by applying the zero side slip criteria in steady state conditions.

Figure 4-1 illustrates the change of the steer ratio with respect to the vehicle forward speed.

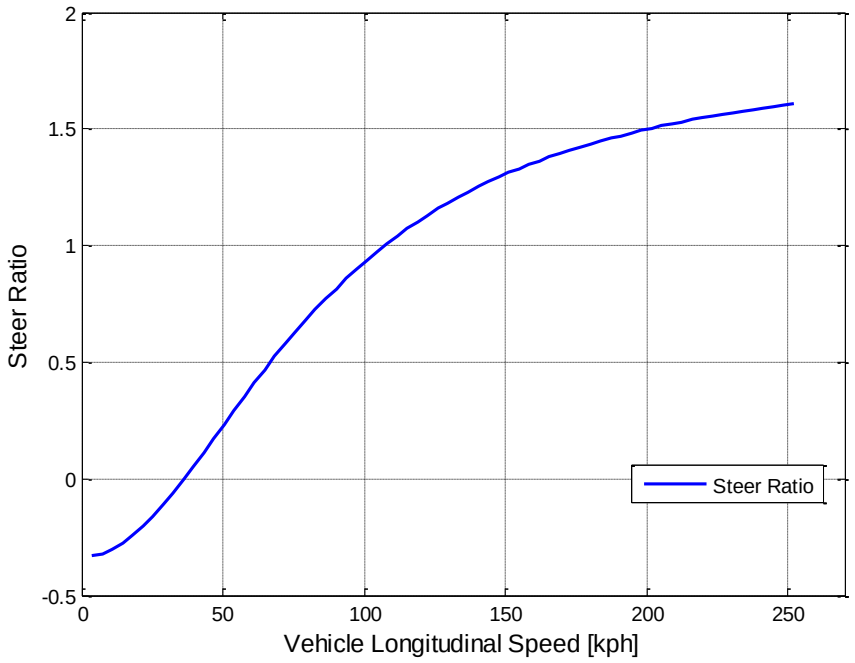

Figure 4-1: Steer ratio as a function of vehicle longitudinal speed

Because of large matrix sizes of the state space system, the steer ratios are calculated using MATLAB® program. The implementation of SR principle requires the following state space form:

$$\dot{\boldsymbol{x}} = \boldsymbol{A}\boldsymbol{x} + \boldsymbol{B}\delta_1 + \boldsymbol{B_u}u \tag{4.8}$$

where the control input u equals to the active trailer steering input defined in equation (4.9) as follows:

$$u = \mu\, \delta_1 \tag{4.9}$$

Note that the corresponding proportionality constant for specific vehicle speed can be obtained by observing the steer ratios given in Figure 4-1. The details of the matrices associated with the control strategy are given in Appendix C.

4.2 COMMAND STEERING BASED ACTIVE OPTIMAL CONTROL (ACS)

In this section, a command steering based active trailer steering strategy is investigated. In classical passive command steering approach, a mechanism is directly used to produce trailer steering action in proportion to articulation angle between the

units. The active type of command steering utilizes the same principal with the use of optimal control and varying proportionality. Rangavajhula and Tsao suggested the command steering based active optimal control strategy, comparing its performance with the classical command steering [5]. In their study, tractor with three full-trailer combinations is modeled to investigate the behavior at low and medium speed conditions. The basic geometrical relation used for the determination of each trailer steering angles in their study is illustrated in Figure 4-2.

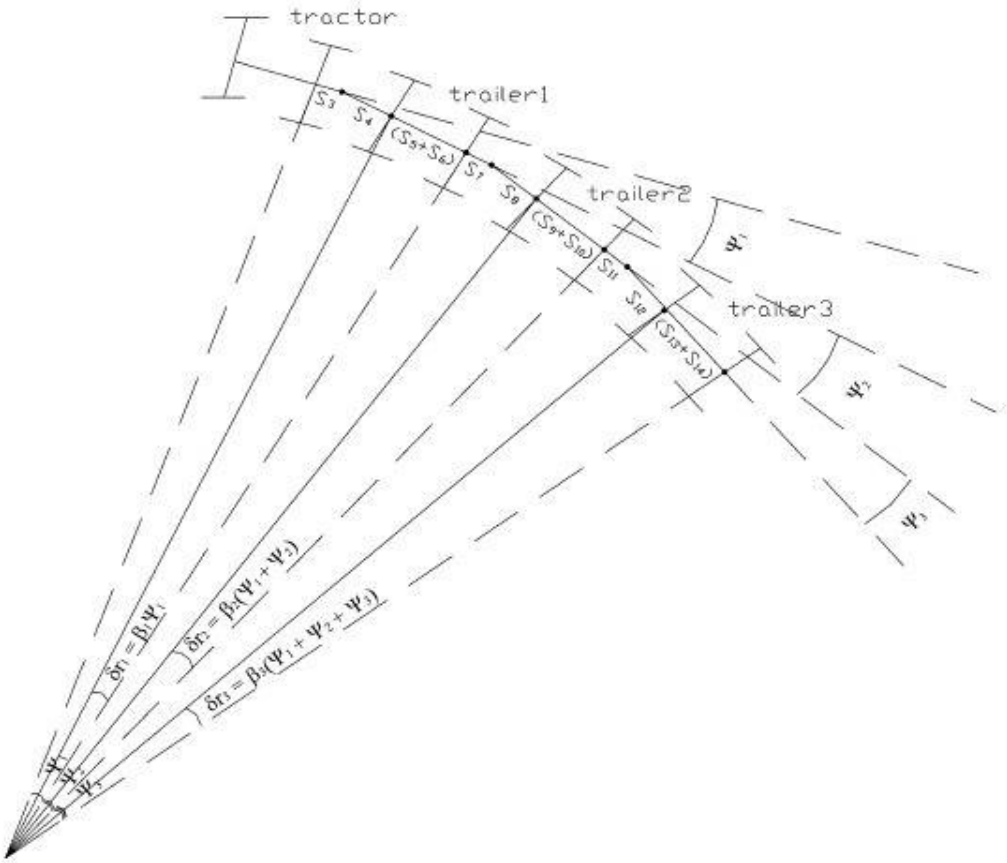

Figure 4-2: Active command steering geometry for multiple full-trailers

In the research conducted by Rangavajhula and Tsao, the active steering angles for each of the full-trailers are expressed as a function of hitch angles between the adjacent vehicle units. Afterwards, the active steering angles are replaced with the corresponding hitch angles on their optimal controller. In this study, the same approach is adopted for a tractor and semi-trailer model. The derivation procedure of the optimal controller is as follows:

First of all, the geometrical relation is expressed as in the following equation.

$$\delta_s = \beta\, \psi \tag{4.10}$$

In equation (4.10), β is determined by the geometrical relation, and ψ stands for the articulation angle between the adjacent vehicle units.

In the method of active command steering, the state-space system given by equation (4.1) turns out to be the equation (4.11):

$$\dot{\boldsymbol{x}} = \boldsymbol{A}\boldsymbol{x} + \boldsymbol{B}\delta_1 + \boldsymbol{B_{ACS}}u \tag{4.11}$$

where the control input, in that case, is the command steering based articulation angle given by equation (4.12):

$$u = \psi \tag{4.12}$$

In their work, Rangavajhula and Tsao minimize the states of the system while satisfying minimum control energy criterion. An identity matrix is used for the weighting of Q matrix in their study. This indicates that all the states of their system have the same importance. Therefore, the use of equally important states is investigated in this study, too. The performance index given by equation (4.3) is directly used in the research with appropriate weighting factor of active steering angle, giving the best lateral performance.

4.3 VIRTUAL DRIVER STEERING CONTROLLER (VD)

In recent studies, path-following type of control strategies becomes widespread. Virtual driver steering controller was proposed by Cebon et al. [14]. In this strategy, the authors assume that a virtual driver sitting at the rear end of the trailing unit aims to follow the path of the articulation point. In other words, by using active trailer steering, the virtual driver guides the vehicle aiming the rear end of the semi-trailer to pass through the route of the fifth wheel. As a result, the major purpose of this control strategy is to minimize the corresponding path-tracking error. An illustration of virtual driver steering controller approach is given in Figure 4-3.

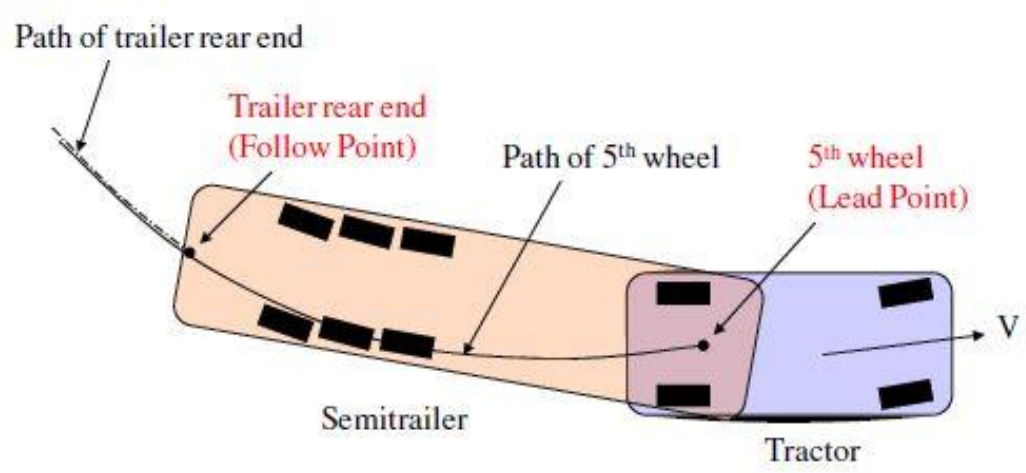

Figure 4-3: Virtual driver steering controller suggested by Cebon et al. [14]

Obviously, follow point at the trailing unit passes from the lead point after some time. This requires keeping the path information of the lead point in the memory.

In this study, the approach is adopted with the modification of system matrices so that the resultant states of the system become as equation (4.13):

$$\boldsymbol{x_{VD}} = [v \quad v_t \quad r \quad r_t \quad p \quad p_t \quad \phi \quad \phi_t \quad y_e \quad y_{5th} \quad y_{5th\Delta} \quad \dots \quad y_{5thm\Delta}]^T \quad (4.13)$$

In the above expression, first 8 terms correspond to the original system states, whereas the other terms are related to the lateral position of the fifth wheel, lateral position of semi-trailer rear end, and the lateral positions of the fifth wheel at previous times, respectively.

The system matrices are manipulated by using forward difference formula as in reference [3]. The lateral velocity of the fifth wheel can be described with respect to the coordinate system fixed to the center of gravities of the vehicle units as in the following equation:

$$\dot{y}_{5th}(t) = v(t) - l_f r(t) \quad (4.14)$$

In a similar way, the lateral velocity of the rear end of the trailing unit can be written as in the expression given below:

$$\dot{y}_e(t) = v_t(t) - l_5 r_t(t) \quad (4.15)$$

In addition to this, the points where the fifth wheel passed at the previous time can be stored by using forward difference formula with appropriate time step.

$$\dot{y}_{5thi}(t - i\Delta) = \frac{1}{\Delta}[y_{5th}(t - (i-1)\Delta) - y_{5th}(t - i\Delta)] \tag{4.16}$$

where $i = 1,2,3 \ldots, m$ and $\Delta = (l_{ft} + l_5)/U$.

Using the equations (4.14), (4.15) and (4.16), the final state-space system is derived with the states given by equation (4.13), where the details of the matrices are given in Appendix C.

In their study, the authors aim to minimize the path-following error that can be written by equation (4.17). The error is defined as the lateral difference between the path of the fifth wheel maintained in the memory and path of the rear end of the semi-trailer.

$$e(t) = y_{5thm\Delta}(t) - y_e(t) \tag{4.17}$$

As a result, the quadratic performance index related to the path-tracking error minimization via virtual driver steering controller is defined as follows:

$$J = \int_0^\infty \rho_1[e(t)]^2 + \rho_2[\delta_s(t)]^2 \, dt \tag{4.18}$$

In the expression above, the terms ρ_1 and ρ_2 corresponds to the weighting factors associated with the path-tracking error and the active steering input, respectively.

4.4 LATERAL POSITION DEVIATION PREVIEW (LPDP)

As another type of path-following strategy, lateral position deviation preview suggested by Islam and He [3] is a similar approach to virtual driver steering control system. The major difference between the control strategies is the selection of lead and follow point.

For LPDP controller, the path of the tractor front axle center should be followed by the semi-trailer axle centers. Figure 4.3 illustrates the approach used in the study of Islam and He [3].

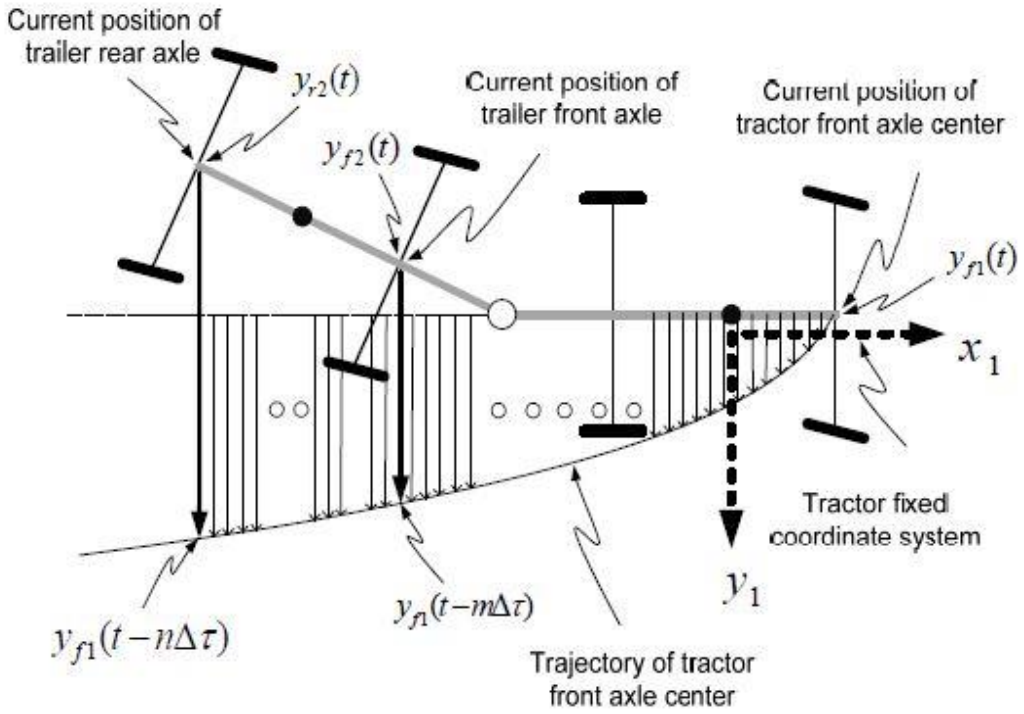

Figure 4-4: Lateral position deviation preview (LPDP) approach suggested by Islam and He[3]

In this case, the preview path information of the tractor front end is maintained as a state variable so that the rear axle passes through this path with a time delay. The approach is adopted with the modification of matrices, yielding the resultant states of the system be as follows:

$$\boldsymbol{x_{LPDP}} = [v \quad v_t \quad r \quad r_t \quad p \quad p_t \quad \phi \quad \phi_t \quad y_r \quad y_f \quad y_{f\Delta} \quad \dots \quad y_{fn\Delta}]^T \qquad (4.19)$$

In the expression written above, the additional states y_f and y_r are related to the lateral positions of tractor front axle center and semi-trailer active axle center. Also, the remaining states are associated with the positions of tractor front axle center, considering the time delay.

In order to construct the state-space system, the supplementary equations are written. For instance, the lateral velocity of the front axle center is described with respect to the coordinate system fixed to the center of gravity of tractor:

$$\dot{y}_f(t) = v(t) + l_1 r(t) \qquad (4.20)$$

Similarly, the lateral velocity at the rearmost axle center with respect to the coordinate system fixed to the COG of the semi-trailer is written as in the expression (4.21):

$$\dot{y}_r(t) = v_t(t) - l_3 r_t(t) \tag{4.21}$$

Moreover, the lateral positions passed by the front axle center at previous times are maintained as state variables by using forward difference formula with suitable time step.

$$\dot{y}_f(t - j\Delta) = \frac{1}{\Delta}\left[y_f(t - (j-1)\Delta) - y_f(t - j\Delta)\right] \tag{4.22}$$

where $j = 1,2,3 \ldots, n$ and $\Delta = (l_1 + l_f + l_{ft} + l_t)/U$.

After explaining the constructed state-space representation, it is necessary to identify the corresponding performance index that will be used for the linear quadratic regulator. The purpose of Islam and He in their paper was to minimize the cost function related to the lateral position deviation between the units. Using the same approach, the lateral position error is defined by equation (4.23) for our case:

$$e(t) = y_{fn\Delta}(t) - y_r(t) \tag{4.23}$$

As a result, the quadratic performance index associated with the minimization of lateral position error is defined as follows:

$$J = \int_0^\infty \rho_1[e(t)]^2 + \rho_2[\delta_s(t)]^2 \, dt \tag{4.24}$$

It can be noticed that the quadratic performance index is the same as the one used in the previous control method. On the other hand, the definition of the error for the two control method is different, resulting in dissimilar responses in the simulations.

4.5 LEAD-UNIT FOLLOWING CONTROLLER (LUF)

Being proposed by Kharazzi [9], lead-unit following controller offers a characteristic-following approach different from the other control methods. In this control strategy, the target of the trailing unit is to track the yaw characteristics of the towing unit of an articulated heavy vehicle with a certain time lag.

In the research conducted by Kharazzi [9], the mechanism behind the time-lag phenomenon is defined as follows:

First of all, the driver of the articulated vehicle performs the steering action leading to the lateral motion of the towing unit. This lateral motion produces a lateral force on the articulation joint between the vehicle units. Then, the process is followed by the yaw motion and side slip of the trailing unit. After the sufficient side slip, the slip angles of the tires reach a certain level, generating large enough lateral tire forces to regulate the yaw motion of the trailing unit.

Figure 4-5 illustrates the flowchart explaining the dynamics of the force generation on the trailing units in response to the driver steering input.

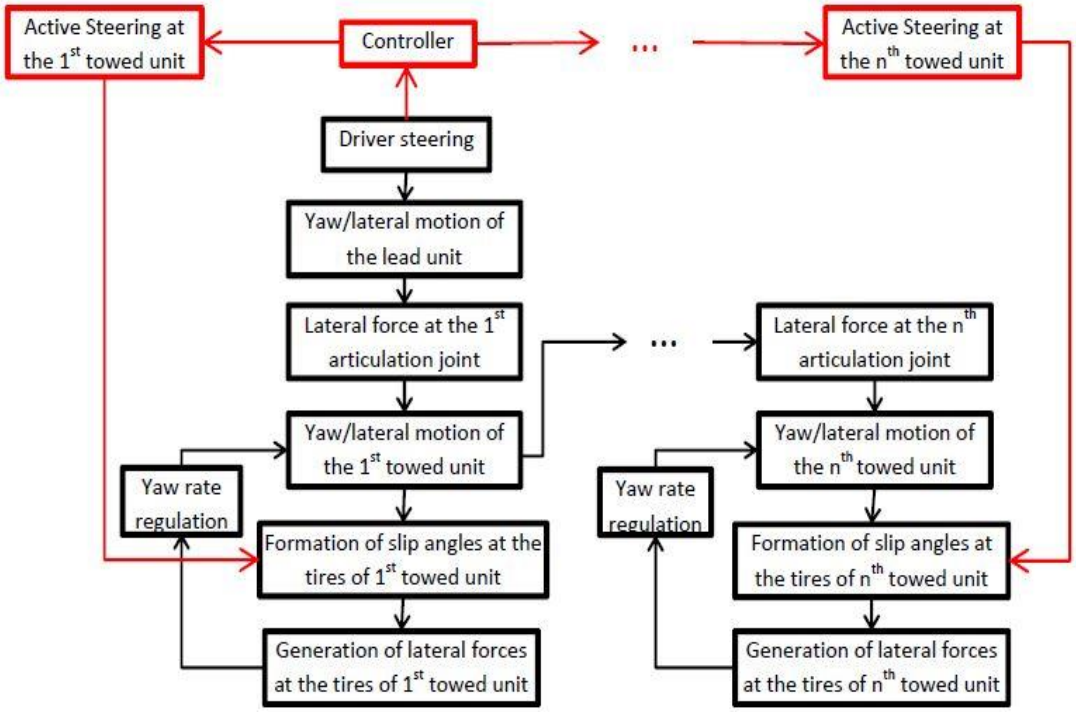

Figure 4-5: Dynamic flowchart of the lateral and yaw motion of the AHV units [9]

It is noticed by examining the Figure 4-5 that the red lines indicating the active steering input is another variable effecting the generation of the lateral tire forces on the towed unit axles.

In the study, the author indicates that if the time delay between the driver steering input and the force generation on semi-trailer axles lessen, suppression of the rearward amplification can be achieved.

According to the study, the lateral tire force to control the yaw motion of the trailing units can be produced earlier with the implementation of active steering on the trailer wheels. As a result of this, rearward amplification can be suppressed before the yaw rates of the towed unit become large. Furthermore, off-tracking problem can be solved by generating the lateral tire forces with active steering rather than side slip of the vehicle unit.

In order to implement this approach to the proposed vehicle model, the original state equations are adjusted. In that case, the states of the system become as follows:

$$\boldsymbol{x_{LUF}} = [v \quad v_t \quad r \quad r_t \quad p \quad p_t \quad \phi \quad \phi_t \quad r_\Delta \quad \dots \quad r_{k\Delta}]^T \tag{4.25}$$

In the above expression, the additional states represent the yaw rate characteristics of the leading unit with the implementation of time lag approach.

Using forward difference formula, the corresponding differential equation can be expressed as follows:

$$\dot{r}(t - i\Delta) = \frac{1}{\Delta}[r(t - (i-1)\Delta) - r(t - i\Delta)] \tag{4.26}$$

where $i = 1,2,3 \dots, k$

In this case, the approximate time delay is obtained by averaging the yaw difference between the units of the conventional AHV.

In the lead-unit following case, the error is the difference between the yaw characteristics of the semi-trailer unit at the present time and that of tractor unit at a specific previous time.

$$e(t) = r_t(t) - r_{k\Delta}(t) \tag{4.27}$$

Therefore, the quadratic performance index offering the minimization of characteristic-following error is written as follows:

$$J = \int_0^{\infty} \rho_1[e(t)]^2 + \rho_2[\delta_s(t)]^2 \, dt \tag{4.28}$$

In the expression above, the terms ρ_1 and ρ_2 correspond to the weighting factors associated with the error and the active steering input, respectively.

4.6 PROPOSED CONTROLLER: LATERAL ACCELERATION CHARACTERISTICS FOLLOWING (LACF)

Having mentioned different control methods used in the literature, it is time to explain the control strategy proposed in this study. The newly introduced control method is called as lateral acceleration characteristics following (LACF). Actually, the suggested control strategy is based on the time lag approach like the previous method (LUF). On the other hand, this strategy offers further dominance on the lateral acceleration characteristics of AHVs at both low and high speed conditions. The expectation from the proposed controller is improved lateral performance at transient state conditions additional to steady state conditions.

In the previous method implemented by Kharazzi, the yaw rate characteristic was the only parameter that the author concerned. However, the lateral acceleration of the vehicle units are not only dependent on the yaw rates but also influenced by the side-slip and roll motions of the vehicle. In most general terms, lateral accelerations of the vehicle units can be defined with the following expressions:

$$\ddot{y}(t) = \dot{v}(t) + Ur(t) - \frac{m_s h^*}{m}\dot{p}(t) \tag{4.29}$$

$$\ddot{y}_t(t) = \dot{v}_t(t) + U_t r_t(t) - \frac{m_{st} h_t^*}{m_t}\dot{p}_t(t) \tag{4.30}$$

In order to investigate the lateral acceleration characteristic precisely, the vehicle simulation results given by Figure 3-9 are separated to its effective components. The overall lateral acceleration of the tractor unit is illustrated together with the contributions of the three independent motion components in Figure 4-6.

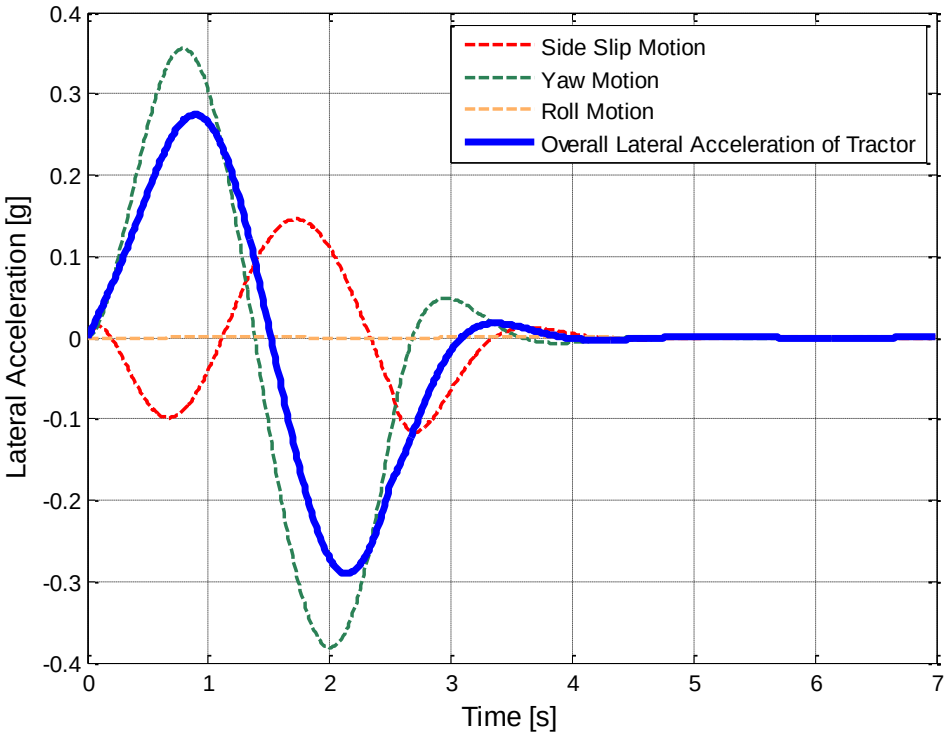

Figure 4-6: Contribution of the side slip, yaw and roll motions on the lateral acceleration characteristics of tractor unit

It should be noted lateral acceleration of semi-trailer unit is not shown in the figure to reduce the complexity. In Figure 4-6, it is seen that the side slip and yaw motions are the dominant components that have large influence on the lateral acceleration characteristics.

Since the roll degree of freedom have little effect on the lateral acceleration characteristics of both vehicle units, the equations stated above are reduced to the following form:

$$\ddot{y}(t) = \dot{v}(t) + Ur(t) \tag{4.31}$$

$$\ddot{y}_t(t) = \dot{v}_t(t) + U_t r_t(t) \tag{4.32}$$

The terms $\dot{v}$ and r are the two important parameters effecting the lateral acceleration characteristics at transient state and steady state conditions, respectively.

The proposed controller has contribution to the previously mentioned lead-unit following controller, concerning both $\dot{v}$ and r terms. Recall that the only concern of the lead-unit following control was the yaw characteristics (r).

In order to construct a state-space system that can be utilized for the proposed control method, the following states are obtained:

$$\boldsymbol{x_{LACF}} = [\ \boldsymbol{x}\ \dot{\boldsymbol{x}}\ \dot{v}_{\Delta}\ \ldots\ \dot{v}_{l\Delta}\ \ r_{\Delta}\ \ldots\ r_{k\Delta}\ ]^{T} \tag{4.33}$$

where the first and second terms represent the original states used on the conventional vehicle and the derivatives of these states, respectively.

To obtain the derivatives as state variables, the matrix manipulation given by equation (4.34) is applied:

$$\dot{\boldsymbol{x}}_{\boldsymbol{LACF}} = \begin{bmatrix} \boldsymbol{A} & \boldsymbol{0} \\ \boldsymbol{0} & \boldsymbol{A} \end{bmatrix} \boldsymbol{x_{LACF}} + \begin{bmatrix} \boldsymbol{B} & \boldsymbol{0} \\ \boldsymbol{0} & \boldsymbol{B} \end{bmatrix} \boldsymbol{\delta_1} + \begin{bmatrix} \boldsymbol{B_u} & \boldsymbol{0} \\ \boldsymbol{0} & \boldsymbol{B_u} \end{bmatrix} \boldsymbol{u} \tag{4.34}$$

Using forward difference formula, the time-delayed states of the system can be obtained. Then, the corresponding differential equations can be written as in the equations (4.35) and (4.36):

$$\ddot{v}(t - i\Delta) = \frac{1}{\Delta}[\dot{v}(t - (i-1)\Delta) - \dot{v}(t - i\Delta)] \tag{4.35}$$

where $i = 1,2,3\ \ldots, l$

$$\dot{r}(t - i\Delta) = \frac{1}{\Delta}[r(t - (i-1)\Delta) - r(t - i\Delta)] \tag{4.36}$$

where $i = 1,2,3\ \ldots, k$

The approximate time delays are obtained by averaging the yaw difference and side-slip rate differences between the units of the conventional AHV. The derivation steps of the state space system for the proposed controller are provided in Appendix C in detail.

Recall that, in the LACF strategy, the lateral acceleration characteristics of the semi-trailer should track that of the tractor with a time delay between the two units. Therefore, the error definition in this case is written as in equation (4.37):

$$e(t) = \{\dot{v}_t(t) + U_t r_t(t)\} - \{\dot{v}_{n\Delta}(t) + U r_{m\Delta}(t)\} \tag{4.37}$$

The quadratic cost function minimizing the error in the lateral acceleration characteristics become:

$$J = \int_0^\infty \rho_1[e(t)]^2 + \rho_2[\delta_s(t)]^2 \; dt \tag{4.38}$$

Then, the error expression is simplified to avoid the non-diagonal elements in the weighting matrix. This simplification also helps with observing the effect of each component during weighting factor adjustment. As a result of this, the error is separated into two components as follows:

$$e_1(t) = \dot{v}_t(t) - \dot{v}_{n\Delta}(t) \tag{4.39}$$

$$e_2(t) = r_t(t) - r_{m\Delta}(t) \tag{4.40}$$

The resulting quadratic performance index is given in equation (4.41):

$$J = \int_0^\infty \rho_1[e_1(t)]^2 + \rho_2[e_2(t)]^2 + \rho_3[\delta_s(t)]^2 \; dt \tag{4.41}$$

Having identified the state space system and defined the quadratic performance index, a linear quadratic regulator (LQR) now can be used for the proposed controller.

To summarize, the proposed active trailer steering strategy is a time lag type ATS strategy, which is a completion of the LUF method. Considering an additional variable, it is expected to show better performance than LUF method both and low and high speed conditions. The simulation results and their comparison are presented in the next chapter.

CHAPTER 5

SIMULATION RESULTS

In this chapter, the lateral response of the vehicle model to the specified standard test maneuvers is investigated. MATLAB® platform is used for the vehicle dynamic simulations. The relevant standard maneuvers stated in the literature survey chapter are used to test the lateral performance associated with each active strategy. The comparison of the performances of ATS strategies is provided.

The standard maneuvers introduced in the study of lateral performance evaluation are explained in the previous chapters. In this study, the most popular test maneuvers are utilized for the assessment of the lateral performance of the modeled articulated vehicle. At high and low vehicle speed conditions, the applied maneuvers are summarized as in the following table:

Table 5-1: Summary of standard maneuvers implemented for the simulation

STANDARD MANEUVER TYPE	**DRIVER STEERING INPUT**	**VEHICLE FORWARD SPEED**
Low Speed Constant Radius Turning Maneuver	Ramped Step Steering Input	10 km/h
Low Speed 90° Intersection Turning Maneuver	Driver Model Steering Input	10 km/h
High Speed Constant Radius Turning Maneuver	Ramped Step Steering Input	100 km/h
High Speed Lane Change Maneuver	Sinusoidal Steering Input	88 km/h

In the following sections, the high speed and low speed cases are investigated separately. The performance evaluation of the articulated vehicle controlled with active trailer steering strategies is provided.

5.1 LATERAL PERFORMANCE OF THE AHV AT LOW SPEED CONDITIONS

Articulated heavy vehicles are generally used in highways at medium to high forward speed situations. On the other hand, narrow local roads and parking conditions bring about the necessity of sufficient lateral performance of the AHVs at low speeds.

As stated in literature survey section, the low speed performance of an AHV is evaluated at 10 km/h, turning an 11.25 m radius of curvature circle in steady state conditions. Therefore, a ramped step steering input with an amplitude providing the specified constant radius is used in the simulations. Figure 5.1 illustrates the ramped step steering input associated with the low speed turning maneuver.

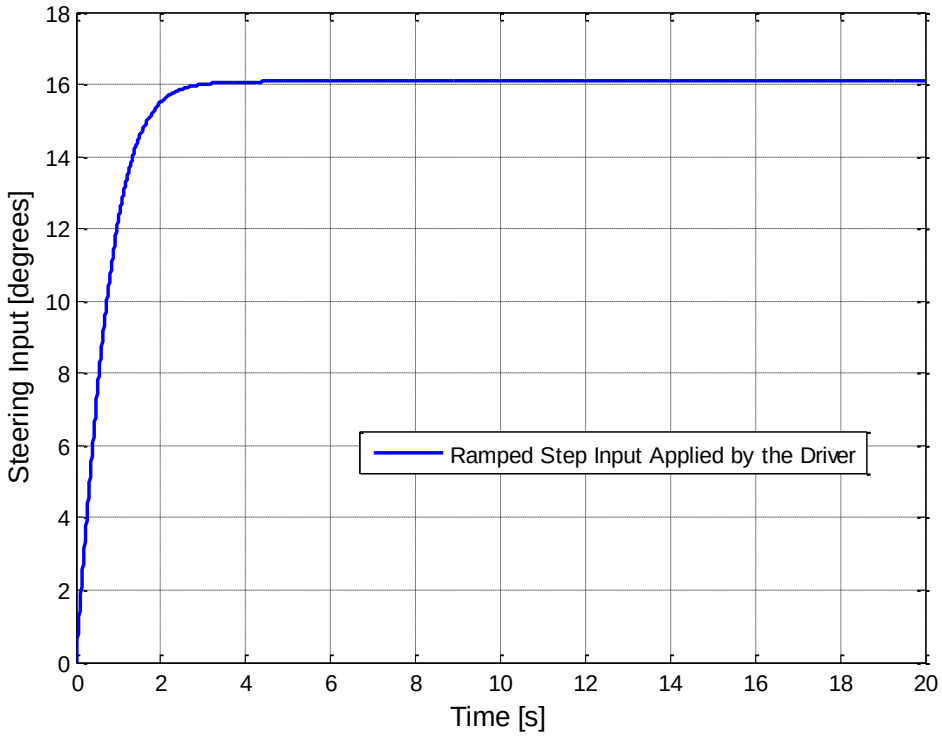

Figure 5-1: Steering input applied by the driver during low speed 360° constant radius turn

In this standard test maneuver, it can be noticed that the amplitude of the driver steering input goes up to 16 degrees due to the turning of small radius of curvature. Such large steering inputs are reasonable and non-problematic because of the very low vehicle longitudinal speeds.

The performance evaluation in this maneuver is carried out with the determination of the low speed circle swept path width (SPW). The steady state circle SPW is defined as the lateral position deviation between the paths of the COG's of each unit. Therefore, the difference between the steady state turning radii of the two units give the expression related to the specified performance measure. Equation (5.1) is used to determine the value of low speed circle steady state SPW at the indicated test condition.

$$SPW = R_t - R_s \tag{5.1}$$

where the terms R_t and R_s refers to the turning radii of tractor and semitrailer units after both units reached the steady state conditions, respectively.

Due to the imposed large driver steering angles, the vehicle dynamic simulations are expected to give huge SPW values at low speed maneuvers. After implementing all of the control strategies stated in Chapter 4, responses to the standard low speed 360° constant radius turning test maneuver are summarized in Table 5-2.

Table 5-2: SPW values obtained by the simulations for each control strategy

	Conv.	**SR**	**ACS**	**VD**	**LPDP**	**LUF**	**LACF**
SPW	2.432 m	1.651 m	2.100 m	2.243 m	2.297 m	0.013 m	0.008 m
Initial Error	zero	zero	zero	zero	zero	0.982 m	0.990 m

As can be inferred from the Table 5-2, the LUF and the proposed LACF control strategies behave better in terms of steady-state off-tracking performance at the expense of some position error in the initial path. Furthermore, the recently used path-following methods, VD and LPDP, provides unsatisfactory results compared to the

steer ratio principle (SR) and active command steering (ACS). This is because the new methods are generally interested in the high speed lateral performance whereas the old strategies mainly focus on low speed conditions.

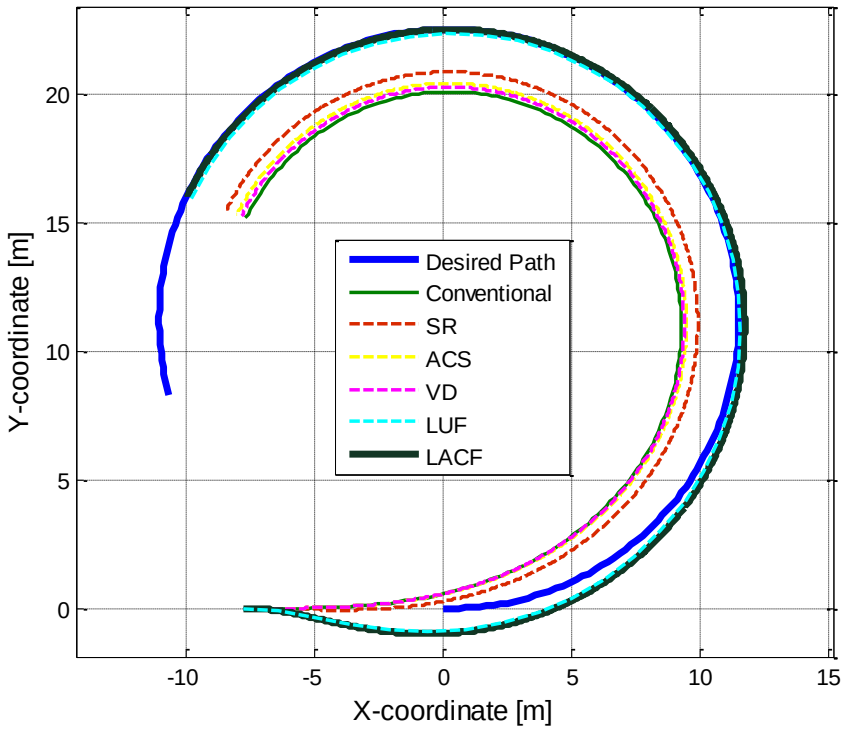

Figure 5-2: Trajectories of the semi-trailer unit at low speed circle turning maneuver for each control strategy

The low speed circle turning trajectory of the semi-trailer units for each control strategy is illustrated in Figure 5-2. It should be noted that the desired path is the collection of points from which the center of gravity of the towing unit passes. Despite the initial error, the LUF and LACF methods entail very successful steady-state circle SWP performance.

Similar to the low speed steady state circle swept path width, low speed 90° intersection turn has to be performed at a longitudinal speed of 10 km/h. Also, the corresponding radius of curvature should be 11.25 m [18].

In the simulations, the basic driver model indicated in Chapter 3 drives the articulated heavy vehicle so that an intersection turn is achieved. Different from the other

maneuvers, the steering input for the tractor front axle is determined by the driver model in that case. Figure 5-3 illustrates the corresponding steering input which is generated by the basic driver model.

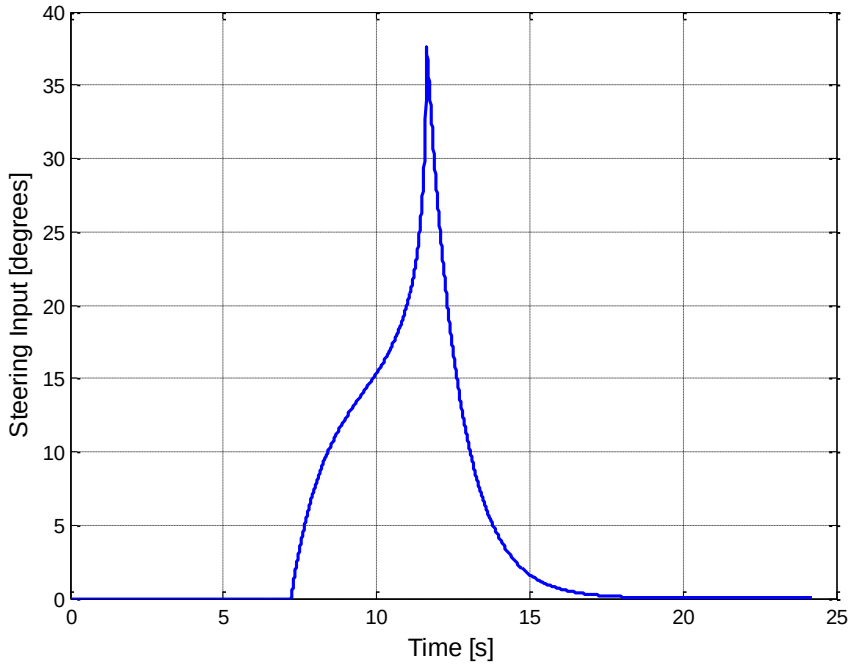

Figure 5-3: Steering input applied by the driver during low speed 90° intersection turn maneuver

During the specified maneuver, the assessment of the vehicle lateral performance has been performed by measuring the path swept by the endpoints of vehicle units. In the simulations, the paths of the left side of the rearmost axle of the semi-trailer have been kept in the memory as well as the path of the right side of the front axle of the tractor. Afterwards, the maximum difference between the swept path is identified as the low speed off-tracking (LSOT) value, given by the equation below:

$$LSOT = max(R_{tr} - R_{sl}) \tag{5.2}$$

Table 5-3: The LSOT values obtained by the simulations for each control strategy

	Con	**SR**	**ACS**	**VD**	**LPDP**	**LUF**	**LACF**
LSOT	4.76 m	4.37 m	4.75 m	4.76 m	4.76 m	4.20 m	4.16 m

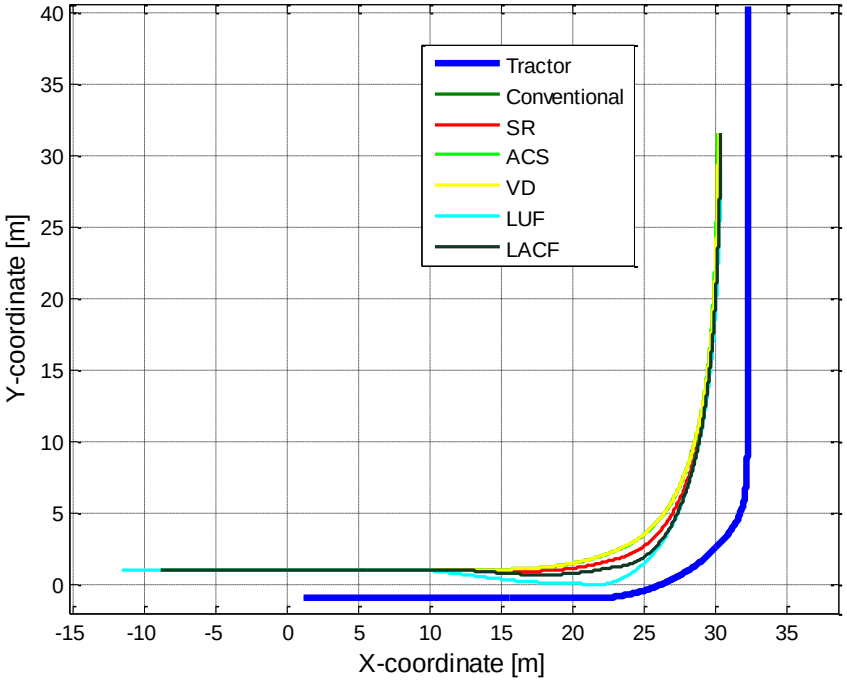

Figure 5-4: The area swept by the endpoints of the vehicle units during 90° intersection turn maneuver at low speed

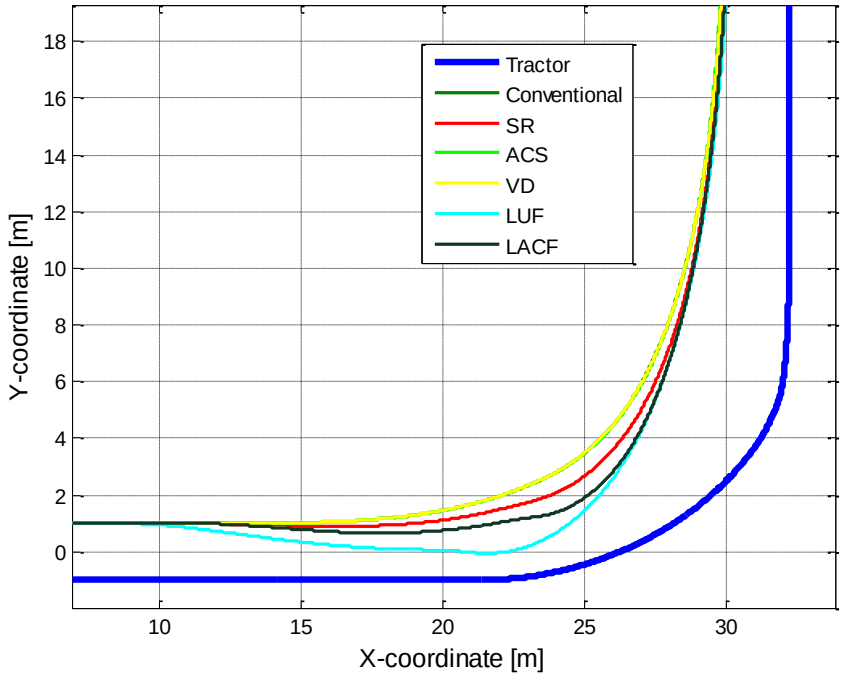

Figure 5-5: Zoomed view of the swept area by the vehicle units during 90° intersection turn maneuver at low speed

The LSOT results of the simulation are illustrated in Table 5.3 above. According to the results, proposed LACF method and LUF approach provide better results among the other strategies. In addition, steer ratio principle can be said as satisfactory when compared to the other methods. Remaining control strategies result in almost no change in the low speed off-tracking performance of the articulated heavy vehicle.

The area swept by the left side of the semi-trailer rearmost axle and the right side of the tractor front axle is illustrated in Figure 5-4 and Figure 5-5.

5.2 LATERAL PERFORMANCE OF THE AHV AT HIGH SPEED CONDITIONS

Most of the time, articulated heavy vehicles is exposed to high speed driving conditions on highways, especially in the steady state turning and lane change maneuvers. Therefore, a suitable design of the longer combination vehicles at high speed situations becomes vital for the efficiency and safety issues. That is the reason for the recent trend in the field: the active trailer steering control strategies to be designed for high speed conditions.

In high speed cases, there are two commonly used standard maneuvers to evaluate the lateral acceleration performance of the AHVs, which are the high speed turning maneuvers and the high speed lane changes. As explained in the Chapter 2, the important performance measures in the range of high forward speeds are the steady state high speed off-tracking (HSOT), transient state high-speed off-tracking (TOT) and rearward amplification ratio (RWA).

According to the standard maneuvers used in the literature, high-speed steady state off-tracking is evaluated at the speed of 100 km/h when the tractor front axle center of follows the circle of 393 m radius [17]. A ramped step steering input is implemented by the driver to the tractor front wheels. Figure 5.6 shows the corresponding steering input applied by the driver.

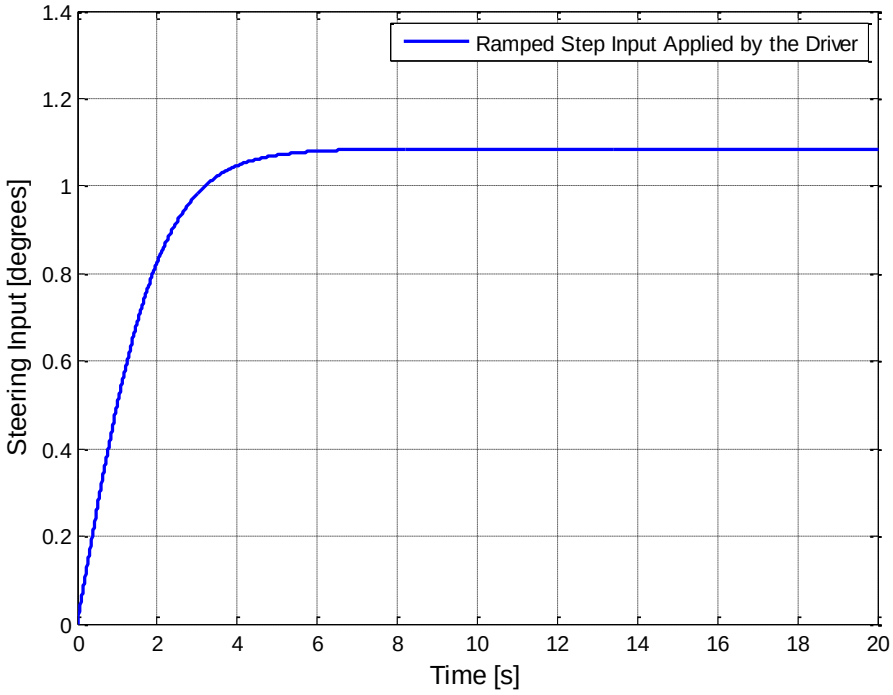

Figure 5-6: Steering input applied by the driver during high speed 360° constant radius turn

Different from the low speed constant circle turning maneuver, the steering angles implemented by the driver are smaller in that case. This is because the AHV turns very large radius of curvature at high forward speeds. Regarding such large radius of curvatures and small steering action, it can be implied that the vehicle combination is subjected to the situations that is somewhat near to straight ahead driving condition. As a result, the high speed off-tracking (HSOT) values obtained from the simulations are expected to be smaller compared to the low speed conditions. The HSOT values is calculated with the following expression:

$$HSOT = R_t - R_s \tag{5.3}$$

Table 5-4: The HSOT values obtained by the simulations for each control strategy

	Con	**SR**	**ACS**	**VD**	**LPDP**	**LUF**	**LACF**
HSOT	0.093 m	0.010 m	0.055 m	0.016 m	0.030 m	0.022 m	0.022 m

According to the table illustrated above, almost all of the control strategies provide satisfactory results in terms of HSOT, except the active command steering. Proposed LACF method is among the one of the most effective strategies, whereas the best approaches are the steer ratio principle and virtual driver steering controller.

The second and the most frequently used driving situation for the AHV is the high speed lane change maneuver. Having been clarified in the literature survey chapter, the standard lane change maneuver is investigated using the following maneuver identified by Fancher and Winkler [4]: A sinusoidal wave steering input should be applied by the driver to the front axle of the towing unit at a constant forward speed of 88 km/h. The frequency of the wave has to be 0.4 Hz, whereas the lane change maneuver produces a minimum 0.15g lateral acceleration at the front axle of the tractor unit.

According to the specified maneuvers, the following steering input is applied by the driver in the vehicle simulations:

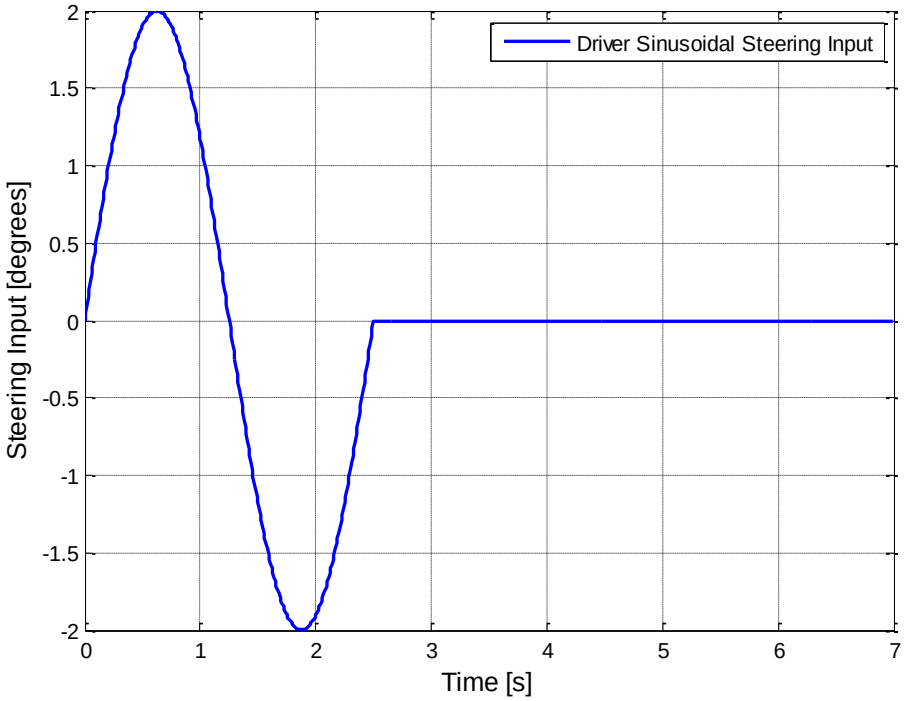

Figure 5-7: Driver steering input during lane change maneuver at 88 kph

From the specified lane change maneuver, two different lateral performance measure is obtained by the simulations. In fact, rearward amplification ratio (RWA) is an important lateral performance measure as well as the high speed transient off-tracking (TOT). The simulations yield the values of RWA and TOT, which are defined as in the following equations:

$$RWA = \frac{peak(\ddot{y}_s)}{peak(\ddot{y}_t)} \tag{5.4}$$

$$TOT = peak(y_s) - peak(y_t) \tag{5.5}$$

The active trailer steering control strategies aim to reduce the TOT as much as possible, while suppressing the RWA to unity. In the literature, the RWA implies increased roll stability near to the value of unity.

Different from the other standard maneuvers, two independent lateral performance measures are taken during high speed lane change maneuver, which are RWA and TOT. As a consequence, the adjustment of the weighting factors leads to various combinations of RWA and TOT pairs. In general, the designer prefers appropriate weighting factors regarding his own concerns. Showing the trade-off relationship between RWA and TOT values on a map (see Figure 5-8) helps the designer to observe all possibilities to be chosen.

According to the Figure 5-8, the most successful control strategies in terms of path-following are VD, LPDP, and LACF since the high speed transient off-tracking (TOT) is almost reduced to zero. Furthermore, VD, LPDP, LUF, and LACF methods can suppress the rearward amplification (RWA) to its ideal level of unity.

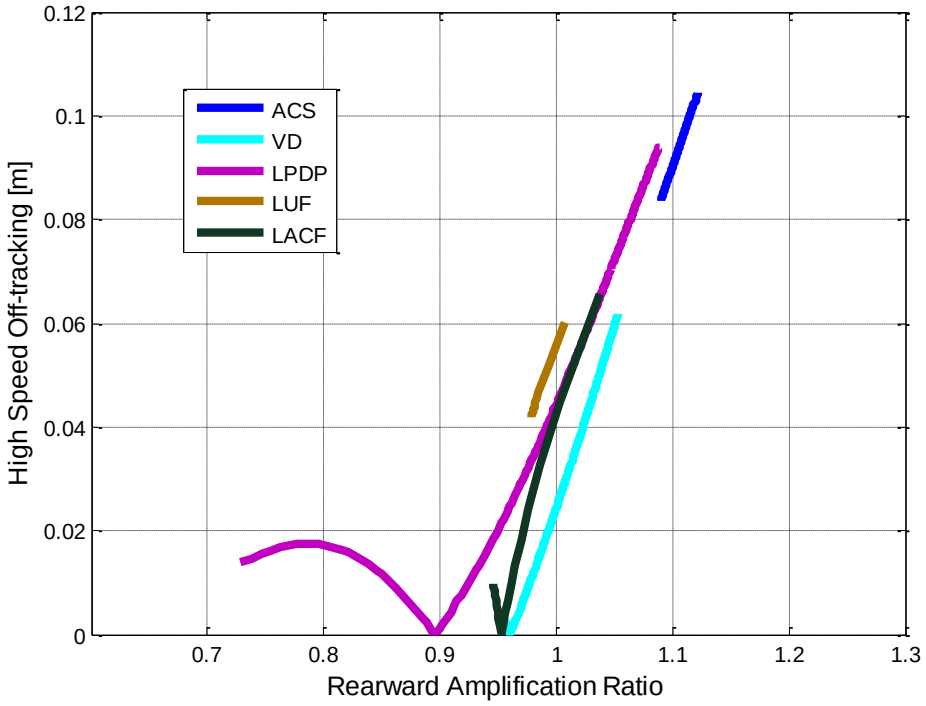

Figure 5-8: HSOT and RWA map showing the trade-off relationship associated with the changing weight factors

Table 5-5 is constructed using the responses obtained from the vehicle dynamic simulation during high speed lane change maneuver. Note that the RWA and TOT pair corresponds to the weighting factors for minimum off-tracking case, while RWA* and TOT* is obtained with the weighting factors for the ideal amplification level.

Table 5-5: Rearward amplification (RWA) and transient off-tracking (TOT) values obtained by the simulations for each control strategy

	Con	**SR**	**ACS**	**VD**	**LPDP**	**LUF**	**LACF**
RWA	1.138	1.675	1.090	0.961	0.895	0.978	0.953
TOT	0.113 m	0.110 m	0.084 m	zero	zero	0.042 m	zero
RWA*	1.138	1.675	1.090	1.000	1.000	1.000	1.000
TOT*	0.113 m	0.110 m	0.084 m	0.024 m	0.045 m	0.056 m	0.043 m

According to the Table 5-5, the control strategies VD, LPDP and LACF behave well among the others, almost zeroing the transient path-following off-tracking of the tractor and semi-trailer combination. Although the SR principle has almost no effect on the transient off-tracking performance, LUF and ACS methods make improvement in the reduction of TOT. Likewise, the path-following type controllers VD & LPDP and the time-lag type controllers LUF and LACF suppresses the rearward amplification ratio below the unity.

The path where the COG's of tractor and semi-trailer units follows during high speed lane change is illustrated in Figure 5-5. To examine the path-following errors correctly, zoomed view of the upper and lower parts of the figure are provided (see Figure 5-6 and Figure 5-7).

Having observed the bottom part of the vehicle paths, the SR strategy seems to be unsatisfactory at tracking the towing unit. Looking at the zoomed view of the top, on the other hand, enhanced path-following ability of VD, LPDP, and LACF are justified.

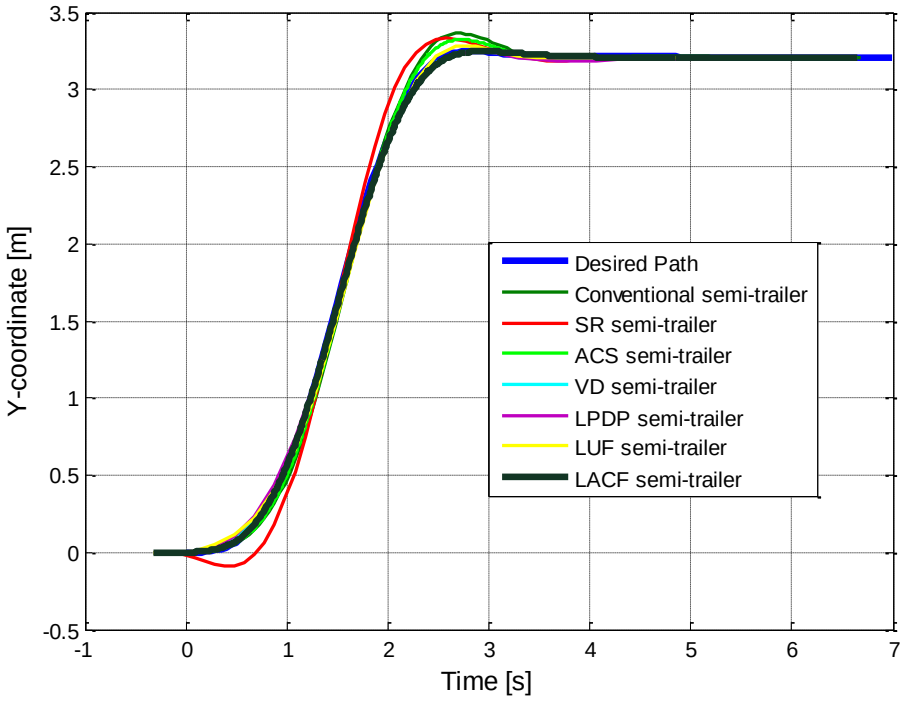

Figure 5-9: Lateral paths of the COGs of the vehicle units during high speed lane change maneuver

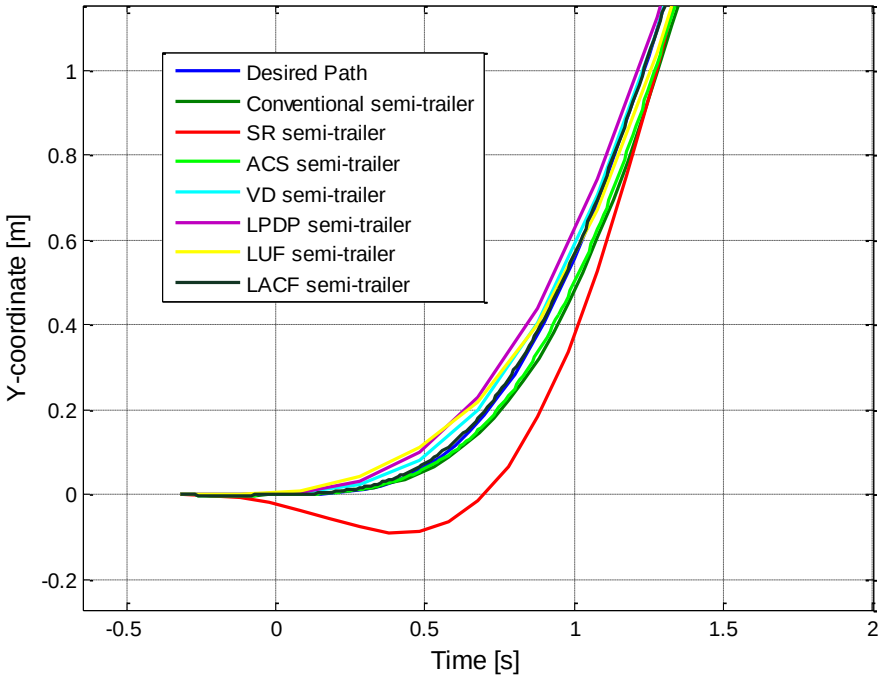

Figure 5-10: Zoomed bottom view of the lateral paths of the COGs of the vehicle units during high speed lane change maneuver

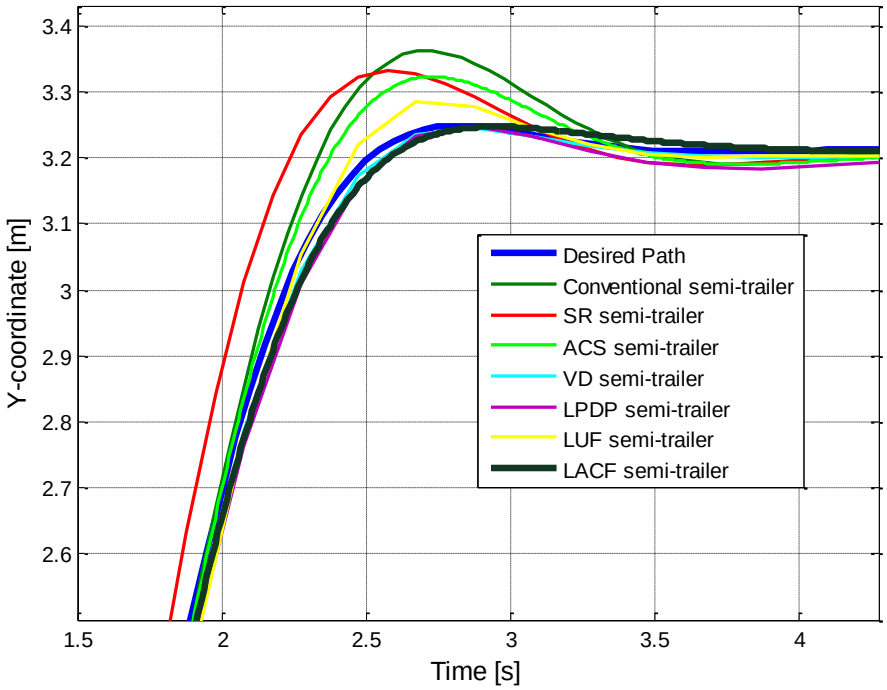

Figure 5-11: Zoomed top view of the lateral paths of the COGs of the vehicle units during high speed lane change maneuver

Figure 5-12 and Figure 5-13 illustrate the lateral acceleration and yaw velocity characteristics of the vehicle units, respectively. According to the Figure 5-12, the lateral acceleration of semi-trailer unit tries to follow the tractor lateral acceleration characteristics with a time lag for LACF strategy. Consequently, suppressed RWA and less off-tracking due to the non-oscillatory behavior are verified. The non-oscillatory behavior is also observed in the yaw characteristics and articulation angle given by Figure 5-13 and Figure 5-14.

Similar to the proposed control strategy, LPDP, VD, and LUF also accomplish the suppression of RWA, while ACS is not sufficient in that performance measure. Note that the results obtained with the SR principle are not shown in Figure 5-12, since the large amplitudes hide other variations on the figure.

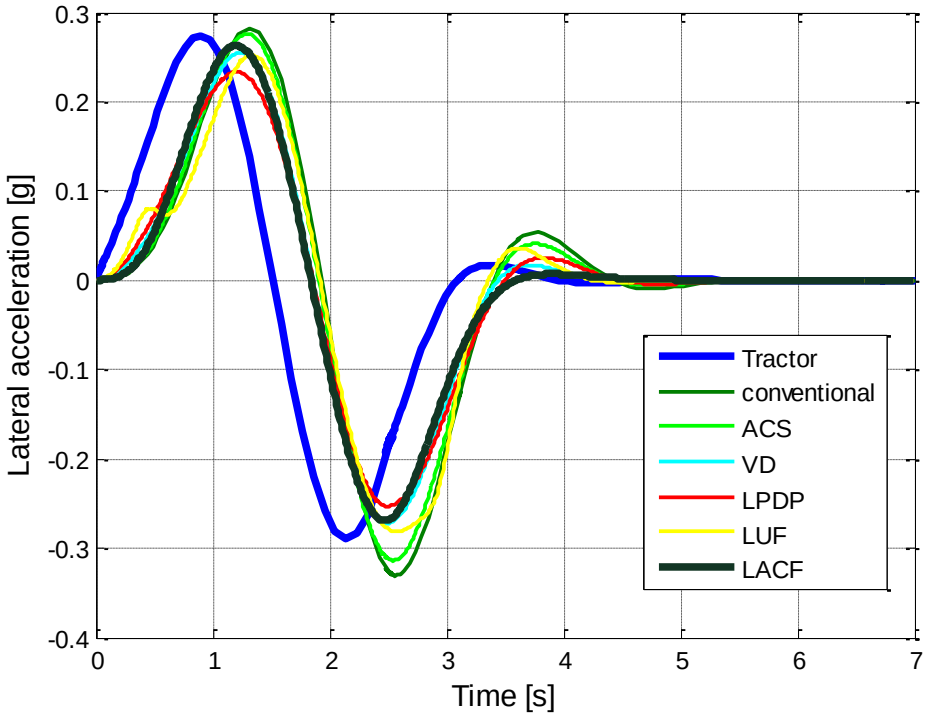

Figure 5-12: Lateral accelerations at the COGs of the vehicle units during high speed lane change maneuver

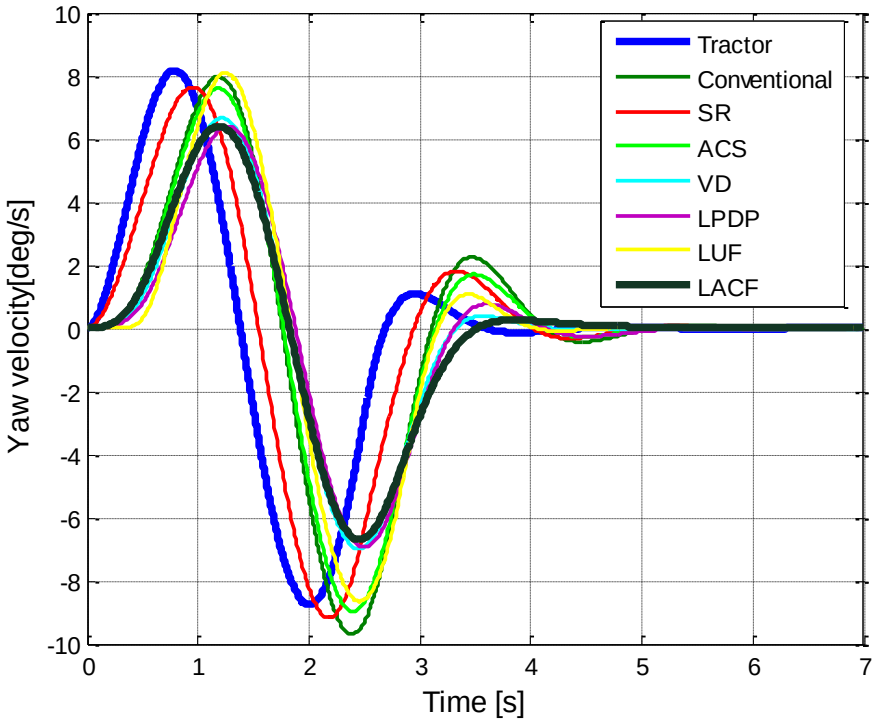

Figure 5-13: Yaw velocities at the COGs of the vehicle units during high speed lane change maneuver

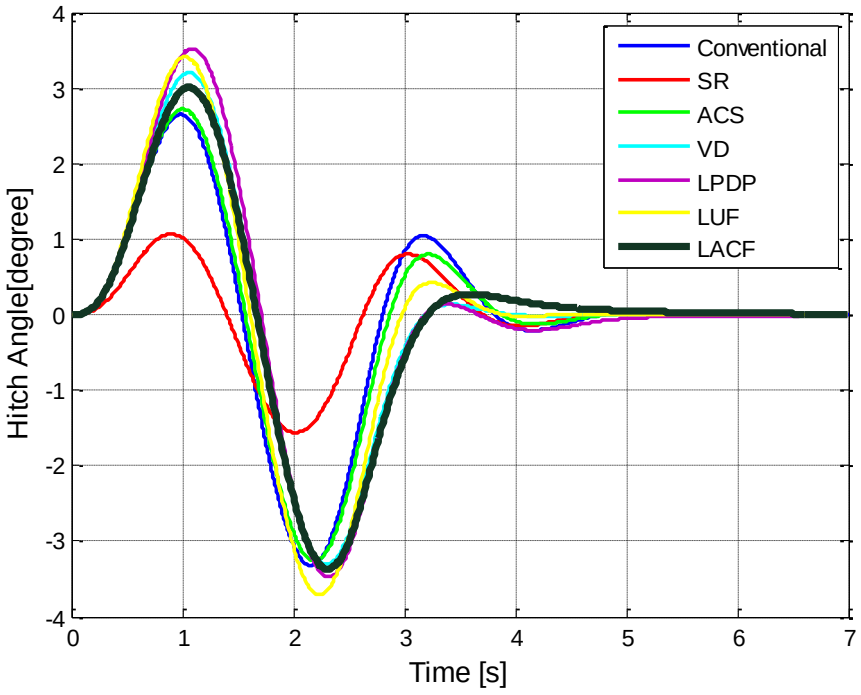

Figure 5-14: Articulation angle between the tractor and semi-trailer during high speed lane change maneuver

In addition, Figure 5-15 illustrates the roll angles during the high speed lane change maneuver. The proposed LACF strategy makes improvement on the oscillatory characteristics of the roll angles. All the strategies except the SR and ACS provide satisfactory roll behavior that may be seen as an indication of the enhanced roll characteristics.

Table 5-6: Peak roll angles values obtained for each control strategy

	Con	**SR**	**ACS**	**VD**	**LPDP**	**LUF**	**LACF**
Peak Roll Angle	0.8503°	1.063°	0.8564°	0.8186°	0.7845°	0.7900°	0.8364°

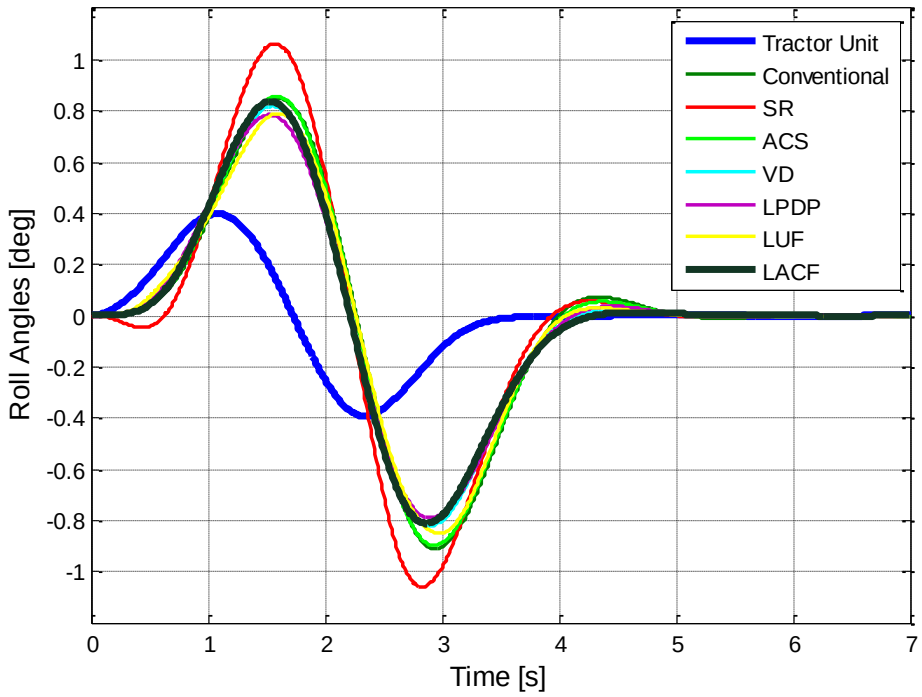

Figure 5-15: Roll angles of the vehicle units during high speed lane change maneuver

Table 5-7: Lateral performance measures obtained for each control strategy

Measure	Control Strategy						
	Conv.	**SR**	**ACS**	**VD**	**LPDP**	**LUF**	**LACF**
SPW	2.432 m	1.651 m	2.100 m	2.243 m	2.297 m	0.013 m	0.008 m
Initial SPW	zero	zero	zero	zero	zero	0.982 m	0.990 m
LSOT	4.76 m	4.37 m	4.75 m	4.76 m	4.76 m	4.20 m	4.16 m
RWA	1.138	1.675	1.090	0.961	0.895	0.978	0.953
RWA*	1.138	1.675	1.090	1.000	1.000	1.000	1.000
TOT	0.113 m	0.110 m	0.084 m	zero	zero	0.042 m	zero
TOT*	0.113 m	0.110 m	0.084 m	0.024 m	0.045 m	0.056 m	0.043 m
HSOT	0.093 m	0.010 m	0.055 m	0.016 m	0.030 m	0.022 m	0.022 m

Table 5-7 summarizes the lateral performance measures obtained for the applied control strategies. The vehicle dynamic simulations provide the following conclusions:

- Steer ratio (SR) behaves well at low forward speeds, whereas its high speed lateral performance is not good enough compared to the conventional AHV. However, the control strategy gives the best response in terms of high speed off-tracking and provides successful response in terms of low speed swept path width.
- Among the strategies, active command steering (ACS) provides an average performance in terms of combined low and high speed conditions. Although all the performance measures are improved by the implementation of ACS, the effect of the improvement is not sufficient. Indeed, there are alternative strategies that improve each of the performance measures to a greater extent.

- The path-following types of control methods, VD and LPDP, provide superior response at high speed test conditions. In fact, VD controller gives the best overall high speed performance among all the strategies. The weakness of these methods, on the other hand, is the poor lateral performance they offer at low forward speeds.
- By looking at the values of RWA*, it is concluded that VD, LPDP, LUF and LACF can suppress the rearward amplification to its ideal level. The adjustment of weighting factors results in a RWA* ratio of unity. In this case, however, the corresponding transient off-tracking TOT* values deteriorate.
- Lead unit following (LUF) strategy provides sufficient performance at both low and high speed situations, giving the second best results among the control strategies, after LACF. One weakness of LUF and LACF is the initial error in the SPW during low speed turning test conditions. However, this initial error causes increased steady state circle turning performance.
- The weakness of LUF strategy in transient state can directly be seen by looking at the TOT value. While the other path-following types and the proposed control strategy can reduced the off-tracking to zero, LUF strategy is not sufficiently successful.
- Proposed control strategy, LACF, is more successful than the existing strategies when evaluated on the basis of combined overall low and high speed performance. The control strategy gives the best response in terms of SPW, LSOT, and TOT. Furthermore, HSOT and RWA values are close to the best values obtained in the simulations.

CHAPTER 6

CONCLUSION

The aim of this study is to design an active trailer steering control strategy for articulated heavy vehicles. Among the various combinations of towing and trailing vehicle units, a combination consisting of a tractor and a multi-axle semi-trailer is selected for this study. The selected combination is the most commonly used type of the AHV. In order to prevent the unstable motion modes, which are jack-knifing, trailer swing, and roll over; lateral performance of the AHV should meet certain criteria. A number of active trailer steering systems have been proposed in the literature to improve the performance of AHV.

When the dynamic models of AHV used in the literature are examined in detail, it is noted that each model has its positive and negative characteristic features depending on the application considered. After reviewing these models, a 5 DOF nonlinear yaw/roll dynamic model of a tractor and multi-axle semi-trailer combination was developed for this study.

The ATS control strategy proposed in this study is based on the Lead Unit Following (LUF) control method. LUF has been implemented such that the yaw velocity of the trailing unit follows the yaw velocity of the tractor. The main feature of the proposed strategy, Lateral Acceleration Characteristic Following (LACF) control, is that the trailing unit tries to follow the lateral acceleration characteristics of the towing unit involving both the side slip acceleration and the yaw velocity of the towing unit rather than just the yaw velocity. Thus the trailing unit is effectively following the lateral acceleration of the towing unit.

In order to evaluate the lateral performance of an AHV controlled by the proposed method, a couple of classical and a couple of more recent strategies in the literature are implemented. Simulations using these strategies and the proposed strategy with the standard test conditions have been performed. Then the results from the simulations are compared to assess the performance of each strategy.

The simulation results reveal that the existing strategies do not consistently provide satisfactory lateral performance when both low and high speeds are considered. The classical steer ratio (SR) strategy provides good performance with respect to off-tracking both at low and high speeds. However, its performance with respect to rearward amplification is not satisfactory at high speeds. Active command steering (ACS) strategy results in probably the poorest overall performance among the strategies included in the analyses at low and high speeds. On the other hand, the virtual driver (VD) and lateral position deviation preview (LPDP) show better performance generally in high speed conditions than low speed conditions. Therefore they are more suited for high speeds. The lead unit following method (LUF) may provide the best performance for combined low and high speed conditions when compared to the strategies analyzed above even though the VD strategy is superior with respect to high speed behavior. The proposed strategy LACF is shown to provide better performance when both low and high speed behavior are taken into account among all the strategies. Its superiority is due to the fact that it can provide a much faster response in transient off-tracking conditions as well as better path following ability.

To summarize, an active trailer steering control strategy, Lateral Acceleration Characteristic Following LACF, is designed for a tractor and multi-axle semi-trailer combination. The lateral performance of the vehicle combination is enhanced with the implementation of the proposed active trailer steering strategy. The basic superiority of the proposed method with respect to major classical and recent control strategies is its performance when both low and high speed behavior are concerned.

The study detailed in the thesis study may be improved by using a more sophisticated model for the tractor semi-trailer combination. In particular the use of non-linear tire

models would make it possible to apply a wider range of weighting factors so that the limiting cases without considering the linearity assumptions. Further, the proposed controller can be implemented on different combinations of AHVs. As a result, the success and limitations of the LACF controller can be verified on various vehicle configurations. A set of weighting factors as a function of forward speed of the combination may also be searched for an adaptive application of the strategy.

REFERENCES

[1] OECD, *Moving Freight with Better Trucks: Improving Safety, Productivity and Sustainability*. OECD Publishing, 2011.

[2] I. Knight, T. Robinson, B. Robinson, T. Barlow, I. McCrae, A. Odhams, R. L. Roebuck, and C. Cheng, "The likely effects of permitting longer semi-trailers in the UK: vehicle specification, performance and safety," *TRL Publ. Proj.*, 2010.

[3] M. M. Islam and Y. He, "Design of a Preview Controller for Articulated Heavy Vehicles," *J. Mech. Eng. Autom.*, vol. 3, pp. 661–676, 2013.

[4] P. Fancher and C. Winkler, "Directional performance issues in evaluation and design of articulated heavy vehicles," *Veh. Syst. Dyn.*, vol. 45, no. 7–8, pp. 607–647, 2007.

[5] K. Rangavajhula and H.-S. J. Tsao, "Command steering of trailers and command-steering-based optimal control of an articulated system for tractor-track following," *Proc. Inst. Mech. Eng. Part D J. Automob. Eng.*, vol. 222, no. 6, pp. 935–954, 2008.

[6] X. Ding, Y. He, J. Ren, and T. Sun, "A Comparative Study of Control Algorithms for Active Trailer Steering Systems of Articulated Heavy Vehicles," *Am. Control Conf.*, pp. 3617–3622, 2012.

[7] Z. Tianjun and Z. Changfu, "Modelling and active safe control of heavy tractor semi-trailer," *2nd Int. Conf. Intell. Comput. Technol. Autom. ICICTA*, vol. 2, pp. 112–115, 2009.

[8] A. Hac, D. Fulk, and H. Chen, "Stability and Control Considerations of Vehicle-Trailer Combination," *SAE Int. J. Passeng. Cars - Mech. Syst.*, no. 724, pp. 776–790, 2008.

[9] S. Kharrazi, "Steering based lateral performance control of long heavy vehicle combinations," 2012.

[10] S. H. Tamaddoni, "Yaw Stability Control of Tractor Semi-Trailers," 2008.

[11] Z. Tianjun, S. Xiaojun, and Z. Changfu, “Development of a Tractor-Semitrailer Stability,” *Int. Conf. Power Electron. Intell. Transp. Syst.*, pp. 102–105, 2009.

[12] S. H. Tabatabaei Oreh, R. Kazemi, and S. Azadi, “A new desired articulation angle for directional control of articulated vehicles,” *Proc. Inst. Mech. Eng. Part K J. Multi-body Dyn.*, 2012.

[13] D. Oberoi, “Enhancing roll stability and directional performance of articulated heavy vehicles based on anti-roll control and design optimization.,” 2011.

[14] C. Cheng, R. Roebuck, A. Odhams, and D. Cebon, “High-speed optimal steering of a tractor–semitrailer,” *Veh. Syst. Dyn. Int. J. Veh. Mech. Mobil.*, 2011.

[15] M. Manjurul Islam, “Parallel Design Optimization of Multi-Trailer Articulated Heavy Vehicles with Active Safety Systems Md . Manjurul Islam,” 2013.

[16] S. H. Tabatabaei Oreh, R. Kazemi, and S. Azadi, “A sliding mode controller for directional control of articulated vehicles,” *Proc. Inst. Mech. Eng. Part K J. Multi-body Dyn.*, 2012.

[17] F. Distribution, M. Using, and S. Grids, “Performance Standards for Heavy Vehicles in Australia,” 2001.

[18] B. Jujnovich and D. Cebon, “Comparative Performance of Semi-trailer Steering,” *Int. Symp. Heavy Veh. Weight. Dimens.*, 2002.

[19] P. LeBlanc, M. El-Gindy, and J. Woodrooffe, “Self-Steering Axles: Theory and Practice.” 1989.

[20] R. L. Nisonger and C. C. Macadam, “Influence of Self-steering Axles on the Directional Response of Commercial Vehicles,” *Veh. Syst. Dyn. Int. J. Veh. Mech. Mobil.*, pp. 289–291, 2002.

[21] S. Luo, “Relative Performance Analysis of Articulated Vehicles with Multiple Conventional Liftable and Self-steering Axles,” 2004.

[22] S. Sankar, S. Rakheja, and A. Piche, “Directional Dynamics of a Tractor-Semitrailer with Self and Forced-Steering Axles.” 1991.

[23] B. Özkan, E. Aptoula, T. Heren, H. Mandacı, and Ç. Can, “Minimization of Tire Wear for Tractor Semi-trailers with Command Steering,” *Otomotiv Teknol. Kongresi*, pp. 1–8, 2014.

[24] H. W. J. Onkhoff and O. F. Begkenham, “Automatic Steering Device For Swiveling Bogies,” 1932.

[25] H. W. Jonkhoff, “Bogie Vehicle Steering Mechanism,” 1937.

[26] C. S. Abbott, “Steering Mechanism for Trucks and Trailers,” 1933.

[27] H. Prem, L. Mai, and K. Atley, “Application of Trackaxle to Multi-Combination Vehicles,” 2006.

[28] H. Prem and E. Ramsey, “Performance evaluation of the Trackaxle Self-Steering System,” *Int. Symp. Heavy Veh. Weight. Dimens.*, pp. 405–422, 2002.

[29] B. Jujnovich and D. Cebon, “Validation of a semi-trailer steering model,” *Int. Symp. Heavy Veh. Weight. Dimens.*, 2004.

[30] A. Percy and I. Spark, “A numerical control algorithm for a B-double truck-trailer with steerable trailer wheels and active hitch angles,” *Proc. Inst. Mech. Eng. Part D J. Automob. Eng.*, vol. 226, no. 3, pp. 289–300, 2012.

[31] M. M. Islam, “Design synthesis of articulated heavy vehicles with active trailer steering systems,” 2010.

[32] S. H. T. Oreh, R. Kazemi, S. Azadi, and A. Zahedi, “A New Method for Directional Control of a Tractor Semi-trailer,” vol. 6, no. 12, pp. 396–409, 2012.

[33] D. H. Wu and J. Hai, “Analysis of dynamic lateral response for a multi-axle-steering tractor and trailer,” *Int. J. Heavy Veh. Syst.*, vol. 10, no. 4, p. 281, 2003.

[34] D.-H. Wu, “A theoretical study of the yaw/roll motions of a multiple steering articulated vehicle,” *Proc. Inst. Mech. Eng. Part D J. Automob. Eng.*, vol. 215, no. 12, pp. 1257–1265, 2005.

[35] K. Rangavajhula and H. S. J. Tsao, “Effect of multi-axle steering on off-tracking and dynamic lateral response of articulated tractor-trailer combinations,” *Int. J. Heavy Veh. Syst.*, vol. 14, no. 4, p. 376, 2007.

[36] I. Notsu, S. Takahashi, and Y. Watanabe, “Investigation into Turning Behaviour of Semi-trailer with Additional Trailer-wheel Steering.” 1991.

[37] B. A. Jujnovich and D. Cebon, “Path-Following Steering Control for Articulated Vehicles,” *J. Dyn. Syst. Meas. Control*, vol. 135, no. 3, 2013.

[38] R. Roebuck, A. Odhams, K. Tagesson, C. Cheng, and D. Cebon, “Implementation of trailer steering control on a multi-unit vehicle at high speeds,” *J. Dyn. Syst. Meas. Control*, vol. 136, no. 2, p. 021016, 2013.

[39] B. Jujnovich, R. Roebuck, A. Odhams, and D. Cebon, “Implementation of active rear steering of a tractor-semi-trailer,” 2007.

[40] A. M. C. Odhams, R. L. Roebuck, B. A. Jujnovich, and D. Cebon, “Active steering of a tractor-semi-trailer,” *Proc. Inst. Mech. Eng. Part D J. Automob. Eng.*, vol. 225, no. 7, pp. 847–869, 2011.

[41] A. M. C. Odhams, R. L. Roebuck, D. Cebon, and C. B. Winkler, “Dynamic safety of active trailer steering systems,” *Proc. Inst. Mech. Eng. Part K J. Multi-body Dyn.*, vol. 222, no. 4, pp. 367–380, 2008.

[42] X. Ding, S. Mikaric, and Y. He, “Design of an active trailer-steering system for multi-trailer articulated heavy vehicles using real-time simulations,” *Proc. Inst. Mech. Eng. Part D J. Automob. Eng.*, 2012.

[43] M. M. Islam, X. Ding, and Y. He, “A closed-loop dynamic simulation-based design method for articulated heavy vehicles with active trailer steering systems,” *Veh. Syst. Dyn.*, vol. 50, no. 5, pp. 675–697, 2012.

[44] S. Kharrazi, M. Lidberg, R. Roebuck, J. Fredriksson, and A. Odhams, “Implementation of active steering on longer combination vehicles for enhanced lateral performance,” *Veh. Syst. Dyn.*, no. July 2015, pp. 1–22, 2012.

[45] S. Kharrazi, M. Lidberg, and J. Fredriksson, “A generic controller for improving lateral performance of heavy vehicle combinations,” *Proc. Inst. Mech. Eng. Part D J. Automob. Eng.*, 2012.

[46] G. Isiklar and I. Besselink, “Simulation of complex articulated commercial vehicles for different driving manoeuvres,” 2007.

APPENDIX A

VEHICLE MODEL

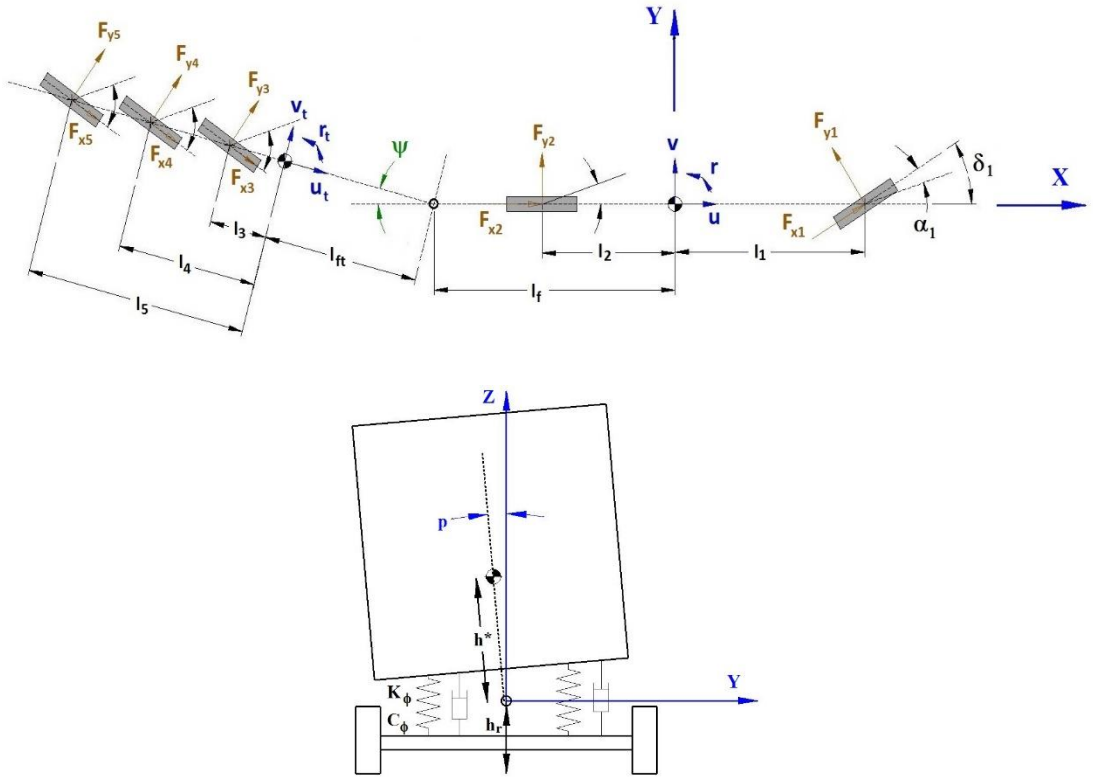

Figure A-1: Vehicle model of a tractor and semi-trailer combination

In order to obtain the lateral response of the vehicle during specific maneuvers, a proper implementation of the vehicle model is essential. Figure 1A illustrates the bicycle model of the articulated heavy vehicle including the roll degree of freedom. To derive the necessary AHV model, Newton 2nd law of dynamics are used. In the Figure 1A, a body centered coordinate system is fixed to the center of gravity of each

vehicle unit, assuming that all the masses of the tractor and semi-trailer are lumped at that points. Either side of the AHV have brought together at the centerline to represent the combination as a bicycle model. In other words, the right and left tires are represented as only one wheel, considering the overall cornering stiffness being equal to the total stiffness of all the wheels on the same axle.

Note that the steering angles and slip angles of the wheels are denoted as δ_i and α_i for the i[th] axle of the vehicle, respectively. The corresponding longitudinal-lateral-yaw velocities at the COG points of the vehicle units are described as u, v, r and u_t, v_t, r_t in their positive x-y-z directions.

The relevant lengths between the axles or articulation points are expressed as l_i , whereas the tire forces at the ith axle are written as F_{xi} and F_{yi} .

For all the other variables and symbols, looking at the Nomenclature section will help.

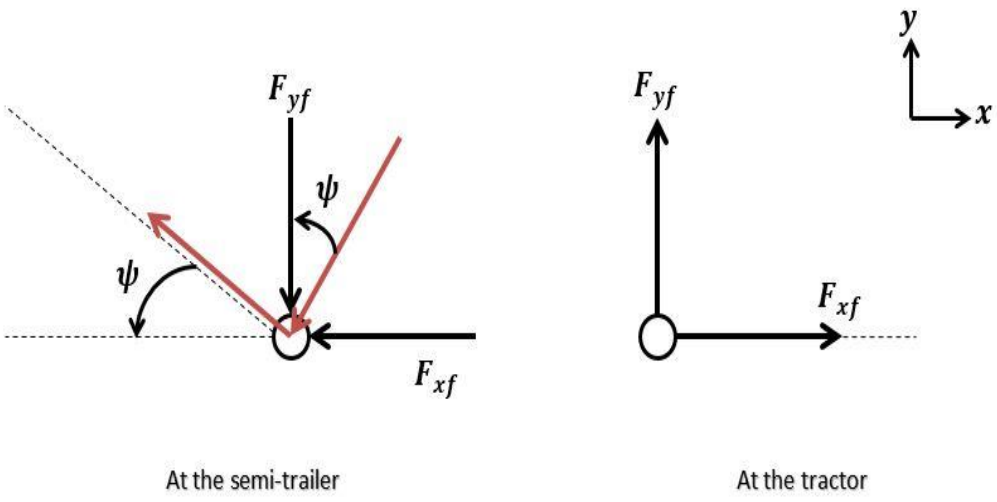

Figure A-2: The reaction forces created at the vehicle articulation point

Illustration of the vehicle combination as separate vehicle units will help us to easily obtain the equations of motions for tractor and semi-trailer. As a result, the reaction force at the articulation point should act to each unit as an action-reaction pair. Figure A2 reveals the forces at the hitch point of the vehicle.

After the separation, the equations of motions for the *tractor* can be identified as the following equations. According to the Figure A1, the full expressions of force and moment equilibrium in both translational and rotational directions is written using Newton 2nd law as follows:

$$m(\dot{U} - vr) + m_s(h^* rp) = -F_{y1} sin\delta_1 + F_{x1} cos\delta_1 + F_{x2} + F_{xf} \quad (A1)$$

$$m(\dot{v} + Ur) - m_s(h^* \dot{p}) = F_{y1} cos\delta_1 + F_{x1} sin\delta_1 + F_{y2} + F_{yf} \quad (A2)$$

$$I_{zz}\dot{r} - I_{sxz}\dot{p} = l_1(F_{y1}\cos\delta_1 + F_{x1}\sin\delta_1) - \mathrm{l}_2\mathrm{F}_{y2} - \mathrm{l}_f\mathrm{F}_{yf} \quad (A3)$$

$$I_{xx}\dot{p} - I_{xz}\dot{r} - m_s h^*(\dot{v} + Ur) = m_s g h^* sin\phi - \left(\sum K_\phi\right)\phi - \left(\sum C_\phi\right)\mathrm{p} - h_{fr}\mathrm{F}_{yf} + K_{12}(\phi_t - \phi) \quad (A4)$$

Note that the Equation (A4) stands for the motion about the roll degree of freedom of the tractor unit.

Similarly, the equation of motions for the *semi-trailer* can be written as follows:

$$m_t(\dot{U}_t - v_t r_t) + m_{st}({h_t}^* r_t p_t) = -F_{xf} cos\Psi + F_{yf} sin\Psi + F_{x3} cos\delta_3 + F_{x4} cos\delta_4 + F_{x5} cos\delta_5 + F_{y3} sin\delta_3 + F_{y4} sin\delta_4 + F_{y5} sin\delta_5 \quad (A5)$$

$$m_t(\dot{v}_t + U_t r_t) - m_{st}({h_t}^* \dot{p}_t) = -F_{xf} sin\Psi - F_{yf} cos\Psi - F_{x3} sin\delta_3 - F_{x4} sin\delta_4 - F_{x5} sin\delta_5 + F_{y3} cos\delta_3 + F_{y4} cos\delta_4 + F_{y5} cos\delta_5 \quad (A6)$$

$$I_{zzt}\dot{r}_t - I_{sxzt}\dot{p}_t = l_3(F_{x3} sin\delta_3 - F_{y3} cos\delta_3) + l_4(F_{x4} sin\delta_4 - F_{y4} cos\delta_4) + \mathrm{l}_5(F_{x5} sin\delta_5 - F_{y5} cos\delta_5) - l_{ft} F_{yf} \cos\Psi - l_{ft} F_{xf} sin\Psi \quad (A7)$$

$$I_{xxt}\dot{p}_t - I_{xzt}\dot{r}_t - m_{st}{h_t}^*(\dot{v}_t + U_t r_t) = m_{st} g {h_t}^* sin\phi_t - \left(\sum K_{\phi t}\right)\phi_t - \left(\sum C_{\phi t}\right)\mathrm{p}_t + h_{frt} F_{yf} \cos\Psi + h_{frt} F_{xf} sin\Psi - K_{12}(\phi_t - \phi) \quad (A8)$$

Additionally, the lateral and longitudinal velocities at the articulation point of the AHV should be compatible. Equations (A9) and (A10) refers to the velocity expressions of semi-trailer derived with the help of the constraint at the hitch point.

$$U_t = Ucos\Psi - vsin\Psi + l_f rsin\Psi \qquad (A9)$$

$$v_t = Usin\Psi + vcos\Psi - l_f rcos\Psi - l_{ft} r_t - h_{fr} p + h_{frt} p_t \qquad (A10)$$

The derivatives of the above expressions will be used to convert the differential equations to a state space model. Therefore, a differentiation procedure has been applied to express the equations as follows:

$$\dot{U}_t = \dot{U}cos\Psi - U\dot{\Psi}sin\Psi - \dot{v}sin\Psi - v\dot{\Psi}cos\Psi + l_f \dot{r}sin\Psi + l_f r\dot{\Psi}cos\Psi \qquad (A11)$$

$$\dot{v}_t = \dot{U}sin\Psi + U\dot{\Psi}cos\Psi + \dot{v}cos\Psi - v\dot{\Psi}sin\Psi - l_f \dot{r}cos\Psi + l_f r\dot{\Psi}sin\Psi - l_{ft}\dot{r}_t - h_{fr}\dot{p} + h_{frt}\dot{p}_t \qquad (A12)$$

Since the fundamental research subject is the lateral performance of the AHV in the dissertation, the major consideration of the model have been the motion of the vehicle combination in y-direction. Hence, the tractive & braking effects can be neglected to simplify the vehicle model i.e. x-components of the forces are not regarded in the expressions from (A1) to (A8). After the elimination of Equations (A1) and (A5) and the effects of longitudinal forces, the resultant expressions reduced to the following form:

$$m(\dot{v} + Ur) - m_s(h^*\dot{p}) = F_{y1}cos\delta_1 + F_{y2} + F_{yf} \qquad (A13)$$

$$I_{zz}\dot{r} - I_{sxz}\dot{p} = l_1\left[F_{y1}\cos\delta_1\right] - \mathrm{l_2F_{y2}} - \mathrm{l}_f\mathrm{F}_{yf} \qquad (A14)$$

$$(I_{x'x'})\dot{p} - I_{x'z'}\dot{r} - m_s h^*(\dot{v} + Ur) = m_s g h^* \phi - \left(\sum K_\phi\right)\phi - \left(\sum C_\phi\right)\mathrm{p} - \mathrm{F}_{yf}h_{fr} + K_{12}(\phi_t - \phi) \qquad (A15)$$

$$m_t(\dot{v}_t + U_t r_t) - m_{st}(h_t{}^*\dot{p}_t) = -F_{yf}cos\Psi + F_{y3}cos\delta_3 + F_{y4}cos\delta_4 + F_{y5}cos\delta_5 \qquad (A16)$$

$$-I_{sxzt}\dot{p}_t + I_{zzt}\dot{r}_t = l_3\left[-F_{y3}cos\delta_3\right] + l_4\left[-F_{y4}cos\delta_4\right] + \mathrm{l}_5\left[-F_{y5}cos\delta_5\right] - l_{ft}F_{yf}\cos\Psi \quad (A17)$$

$$(I_{xxt})\dot{p}_t - I_{xzt}\dot{r}_t - m_{st}h_t{}^*(\dot{v}_t + U_t r_t) = m_{st}gh_t{}^* sin\phi_t - \left(\sum K_{\phi t}\right)\phi_t - \left(\sum C_{\phi t}\right)\mathrm{p}_t + F_{yf}h_{frt} - K_{12}(\phi_t - \phi) \quad (A18)$$

In order to convert the identified equations of motions to a state-space system, all the terms should be replaced by the state variables. At first, the lateral force F_{yi}'s on the above expressions is written in terms of corresponding slip angles and cornering stiffness as follows:

$$F_{yi} = C_s{}^{ith\ axle}\alpha_i = C_i\alpha_i \quad (A19)$$

For further details, the full expressions of the slip angle α_i's are written as the following equations from (A20) to (A24):

$$\alpha_1 = \tan^{-1}\left(\frac{v + l_1 r}{U}\right) - \delta_1 \quad (A20)$$

$$\alpha_2 = \tan^{-1}\left(\frac{v - l_2 r}{U}\right) \quad (A21)$$

$$\alpha_3 = \tan^{-1}\left(\frac{v_t - l_3 r_t}{U_t}\right) + \delta_3 \quad (A22)$$

$$\alpha_4 = \tan^{-1}\left(\frac{v_t - l_4 r_t}{U_t}\right) + \delta_4 \quad (A23)$$

$$\alpha_5 = \tan^{-1}\left(\frac{v_t - l_5 r_t}{U_t}\right) + \delta_5 \quad (A24)$$

For the above equations, the sign convention related to the slip angles are denoted as follows: When going from centerline of the wheel to direction of motion, clockwise rotation means positive slip angle whereas counter-clockwise rotation refers to negative slip angle.

In order to decrease the level of complexity of the model for the controller design, small angle assumptions have been used for the linearization of the vehicle model. According to the assumption, steering angles, slip angles and hitch angles are considered as very small so that the equations (A25) and (A26) can be written in that case.

$$\sin(\delta) = \delta \cong 0 \quad \& \quad \cos(\delta) = 1 \tag{A25}$$

$$\sin(\Psi) = \Psi \cong 0 \quad \& \quad \cos(\Psi) = 1 \tag{A26}$$

Also, the slip angles have been reduced to the following form:

$$\alpha_1 = \frac{v + l_1 r}{U} - \delta_1 \tag{A27}$$

$$\alpha_2 = \frac{v - l_2 r}{U} \tag{A28}$$

$$\alpha_3 = \frac{v_t - l_3 r_t}{U_t} + \delta_3 \tag{A29}$$

$$\alpha_4 = \frac{v_t - l_4 r_t}{U_t} + \delta_4 \tag{A30}$$

$$\alpha_5 = \frac{v_t - l_5 r_t}{U_t} + \delta_5 \tag{A31}$$

Furthermore, the linearization of the velocity compatibility equations and their derivatives are written as follows:

Then,

$$U_t = U - v\Psi + l_f r\Psi \tag{A32}$$

$$v_t = U\Psi + v - l_f r - l_{ft} r_t - h_{fr} p + h_{frt} p_t \tag{A33}$$

$$\dot{U}_t = \dot{U} - U\dot{\Psi}\Psi - \dot{v}\Psi - v\dot{\Psi} + l_f \dot{r}\Psi + l_f r\dot{\Psi} \tag{A34}$$

$$\dot{v}_t = \dot{U}\Psi + U\dot{\Psi} + \dot{v} - v\dot{\Psi}\Psi - l_f \dot{r} + l_f r\dot{\Psi}\Psi - l_{ft}\dot{r}_t + h_{fr}\dot{p} - h_{frt}\dot{p}_t \tag{A35}$$

To avoid the state by state multiplications, products of small variables have been neglected in the above equations as follows:

$$U_t = U \tag{A36}$$

$$v_t = U\Psi + v - l_f r - l_{ft} r_t - h_{fr} p + h_{frt} p_t \tag{A37}$$

$$\dot{U}_t = \dot{U} - v\dot{\Psi} + l_f r\dot{\Psi} \tag{A38}$$

$$\dot{v}_t = Ur - Ur_t + \dot{v} - l_f \dot{r} - l_{ft}\dot{r}_t + h_{fr}\dot{p} - h_{frt}\dot{p}_t \tag{A39}$$

In addition to this, it will be helpful to express the geometric relations of the yaw rates with the articulation angle as Equation (A40):

$$\dot{\Psi} = r - r_t \tag{A40}$$

The reaction forces at the articulation point can be eliminated by combining the tractor equations of motions with the ones for the semi-trailer unit. After the elimination procedure, a state-space model is ready to be constructed. The necessary manipulations on the equations result in overall differential equations related to the state-space model in terms of state variables. The final form of the equations is given as seen from equation (A41) to equation (A48):

$$\begin{aligned}\{m\}\dot{v} + \{m_t\}\dot{v}_t + \{-m_s h^*\}\dot{p} + \{-m_{st} {h_t}^*\}\dot{p}_t \\ = \left\{\frac{C_1 + C_2}{U}\right\} v + \left\{\frac{C_3 + C_4 + C_5}{U}\right\} v_t + \left\{\frac{C_1 l_1 - C_2 l_2 - mU^2}{U}\right\} r \\ + \left\{\frac{-C_3 l_3 - C_4 l_4 - C_5 l_5 - m_t U^2}{U}\right\} r_t + \{-C_1\}\delta_1 + \{C_3\}\delta_3 + \{C_4\}\delta_4 \\ + \{C_5\}\delta_5\end{aligned} \tag{A41}$$

$$\begin{aligned}\{ml_f\}\dot{v} + \{I_{zz}\}\dot{r} + \{-I_{sxz} - m_s h^* l_f\}\dot{p} \\ = \left\{\frac{C_1 l_1 - C_2 l_2 + (C_1 + C_2) l_f}{U}\right\} v \\ + \left\{\frac{C_1 {l_1}^2 + C_2 {l_2}^2 + (C_1 l_1 - C_2 l_2 - mU^2) l_f}{U}\right\} r \\ + \{-C_1(\mathrm{l}_1 + l_f)\}\delta_1\end{aligned} \tag{A42}$$

$$\{mh_{fr} - m_s h^*\}\dot{v} + \{-I_{sxz}\}\dot{r} + \{I_{sxx} - m_s h^* h_{fr}\}\dot{p}$$
$$= \left\{\frac{(C_1 + C_2)h_{fr}}{U}\right\} v + \left\{\frac{(C_1 l_1 - C_2 l_2 - mU^2)h_{fr} + m_s U^2 h^*}{U}\right\} r$$
$$+ \{-\sum C_\phi\} p + m_s h^* g - \sum K_\phi - K_{12}\phi + \{K_{12}\}\phi_t$$
$$+ \{-C_1 h_{fr}\}\delta_1 \qquad (A43)$$

$$\{-m_t l_{ft}\}\dot{v}_t + \{I_{zzt}\}\dot{r}_t + \{I_{sxzt} + m_{st} h_t^* l_{ft}\}\dot{p}_t$$
$$= \left\{\frac{-C_3(l_3 + l_{ft}) - C_4(l_4 + l_{ft}) - C_5(l_5 + l_{ft})}{U}\right\} v_t$$
$$+ \left\{\frac{C_3 l_3^2 + C_4 l_4^2 + C_5 l_5^2 + (C_3 l_3 + C_4 l_4 + C_5 l_5 + m_t U^2) l_{ft}}{U}\right\} r_t$$
$$+ \{-C_3(l_3 + l_{ft})\}\delta_3 + \{-C_4(l_4 + l_{ft})\}\delta_4$$
$$+ \{-C_5(l_5 + l_{ft})\}\delta_5 \qquad (A44)$$

$$\{m_t h_{frt} - m_{st} h_t^*\}\dot{v}_t + \{-I_{sxzt}\}\dot{r}_t + \{I_{sxxt} - m_{st} h_t^* h_{frt}\}\dot{p}_t$$
$$= \left\{\frac{(C_3 + C_4 + C_5)h_{frt}}{U}\right\} v_t$$
$$+ \left\{\frac{-h_{frt}(C_3 l_3 + C_4 l_4 + C_5 l_5 + m_t U^2) + m_{st} U^2 h_t^*}{U}\right\} r_t$$
$$+ \{-\sum C_{\phi t}\} p_t + \{K_{12}\}\phi + \{m_{st} h_t^* g - \sum K_{\phi t} - K_{12}\}\phi_t + \{C_3 h_{frt}\}\delta_3$$
$$+ \{C_4 h_{frt}\}\delta_4 + \{C_5 h_{frt}\}\delta_5 \qquad (A45)$$

$$\{-1\}\dot{v} + \{1\}\dot{v}_t + \{l_f\}\dot{r} + \{l_{ft}\}\dot{r}_t + \{-h_{fr}\}\dot{p} + \{h_{frt}\}\dot{p}_t = \{U\}r + \{-U\}r_t \qquad (A46)$$

$$\{1\}\dot{\phi} = \{1\}p \qquad (A47)$$

$$\{1\}\dot{\phi}_t = \{1\}p_t \qquad (A48)$$

In order to construct the mathematical model of the physical vehicle, a linear time invariant (LTI) state space system of the following form is studied.

$$\dot{\boldsymbol{x}}(t) = \boldsymbol{A}\boldsymbol{x}(t) + \boldsymbol{B}\boldsymbol{u}(t)$$

$$\boldsymbol{y}(t) = \boldsymbol{C}\boldsymbol{x}(t) + \boldsymbol{D}\boldsymbol{u}(t)$$

$\boldsymbol{x}(t)$: state variables vector

$\boldsymbol{y}(t)$: output variables vector

$\boldsymbol{u}(t)$: input variables vector

$\boldsymbol{A}$: system matrix

$\boldsymbol{B}$: input matrix

$\boldsymbol{C}$: output matrix

$\boldsymbol{D}$: disturbance or feedforward matrix

The following definitions provides the explanations of the 8 states used in the derivation of the linear yaw & roll articulated vehicle model:

$$\boldsymbol{x} = \left[v \;\; v_t \;\; r \;\; r_t \;\; p \;\; p_t \;\; \phi \;\; \phi_t \right]^T$$

v : Lateral velocity of COG of tractor

v_t : Lateral velocity of COG of semi-trailer

r : Yaw rate of the COG of tractor

r_t : Yaw rate of the COG of semi-trailer

p : Roll rate of the sprung mass COG of the tractor

p_t : Roll rate of the sprung mass COG of the semi-trailer

ϕ : Roll angle of the sprung mass COG of the tractor

ϕ_t : Roll angle of the sprung mass COG of the semi-trailer

The equations provided from (A41) to (A48) should be rearranged to have the following matrix form:

$$[A_i]_{8x8}\begin{Bmatrix}\dot{v}\\ \dot{v}_t\\ \dot{r}\\ \dot{r}_t\\ \dot{p}\\ \dot{p}_t\\ p\\ p_t\end{Bmatrix} = [B_i]_{8x8}\begin{Bmatrix}v\\ v_t\\ r\\ r_t\\ p\\ p_t\\ \phi\\ \phi_t\end{Bmatrix} + [C_i]_{8x4}\begin{Bmatrix}\delta_1\\ \delta_3\\ \delta_4\\ \delta_5\end{Bmatrix} \quad (A49)$$

In the matrices, all the elements are zero except for the ones that are listed as follows:

$A_i(1,1) = m$

$A_i(1,2) = m_t$

$A_i(1,5) = -m_s h^*$

$A_i(1,6) = -m_{st} {h_t}^*$

$A_i(2,1) = m l_f$

$A_i(2,3) = I_{zz}$

$A_i(2,5) = -I_{sxz} - m_s h^* l_f$

$A_i(3,1) = m h_{fr} - m_s h^*$

$A_i(3,3) = -I_{sxz}$

$A_i(3,5) = I_{sxx} - m_s h^* h_{fr}$

$A_i(4,2) = -m_t l_{ft}$

$A_i(4,4) = I_{zzt}$

$A_i(4,6) = -I_{sxzt} + m_{st} {h_t}^* l_{ft}$

$A_i(5,2) = m_t h_{frt} - m_{st} {h_t}^*$

$A_i(5,4) = -I_{sxzt}$

$A_i(5,6) = I_{sxxt} - m_{st} h_t^* h_{frt}$

$$A_i(6,1) = -1$$

$$A_i(6,2) = 1$$

$$A_i(6,3) = l_f$$

$$A_i(6,4) = l_{ft}$$

$$A_i(6,5) = -h_{fr}$$

$$A_i(6,6) = h_{frt}$$

$$A_i(7,7) = 1$$

$$A_i(8,8) = 1$$

$$B_i(1,1) = \frac{C_1 + C_2}{U}$$

$$B_i(1,2) = \frac{C_3 + C_4 + C_5}{U}$$

$$B_i(1,3) = \frac{C_1 l_1 - C_2 l_2 - mU^2}{U}$$

$$B_i(1,4) = \frac{-C_3 l_3 - C_4 l_4 - C_5 l_5 - m_t U^2}{U}$$

$$B_i(2,1) = \frac{C_1 l_1 - C_2 l_2 + (C_1 + C_2) l_f}{U}$$

$$B_i(2,3) = \frac{C_1 {l_1}^2 + C_2 {l_2}^2 + (C_1 l_1 - C_2 l_2 - mU^2) l_f}{U}$$

$$B_i(3,1) = \frac{(C_1 + C_2) h_{fr}}{U}$$

$$B_i(3,2) = \frac{(C_1 l_1 - C_2 l_2 - mU^2) h_{fr} + m_s U^2 h^*}{U}$$

$$B_i(3,5) = -\sum C_\phi$$

$$B_i(3,7) = m_s h^* g - \sum K_\phi - K_{12}$$

$$B_i(3,8) = K_{12}$$

$$B_i(4,2) = \frac{-C_3(l_3 + l_{ft}) - C_4(l_4 + l_{ft}) - C_5(l_5 + l_{ft})}{U}$$

$$B_i(4,4) = \frac{C_3 l_3^2 + C_4 l_4^2 + C_5 l_5^2 + (C_3 l_3 + C_4 l_4 + C_5 l_5 + m_t U^2) l_{ft}}{U}$$

$$B_i(5,2) = \frac{(C_3 + C_4 + C_5) h_{frt}}{U}$$

$$B_i(5,4) = \frac{-h_{frt}(C_3 l_3 + C_4 l_4 + C_5 l_5 + m_t U^2) + m_{st} U^2 {h_t}^*}{U}$$

$$B_i(5,6) = -\sum C_{\phi t}$$

$$B_i(5,7) = K_{12}$$

$$B_i(5,8) = m_{st} {h_t}^* g - \sum K_{\phi t} - K_{12}$$

$$B_i(6,3) = U$$

$$B_i(6,4) = -U$$

$$B_i(7,5) = 1$$

$$B_i(8,6) = 1$$

$$C_i(1,1) = -C_1$$

$$C_i(1,2) = C_3$$

$$C_i(1,3) = C_4$$

$$C_i(1,4) = C_5$$

$$C_i(2,1) = -C_1(\mathrm{l}_1 + l_f)$$

$$C_i(3,1) = -C_1 h_{fr}$$

$$C_i(4,2) = -C_3(l_3 + l_{ft})$$

$$C_i(4,3) = -C_4(l_4 + l_{ft})$$

$$C_i(4,4) = -C_5\left(l_5 + l_{ft}\right)$$

$$C_i(5,2) = C_3 h_{frt}$$

$$C_i(5,3) = C_4 h_{frt}$$

$$C_i(5,4) = C_5 h_{frt}$$

In the form of standard state space representation, the matrices are expressed as follows:

$$\dot{\boldsymbol{x}} = \boldsymbol{A}\boldsymbol{x} + \boldsymbol{B}\boldsymbol{\delta} \qquad (A50)$$

where $A = [A_i]^{-1}[B_i]$ and $B = [A_i]^{-1}[C_i]$

APPENDIX B

VEHICLE DATA

Table B- 1: Vehicle data adapted from reference [5]

SYMBOL	EXPLANATION	VALUE	UNIT
m	Whole mass of the tractor unit	6769	kg
m_s	Sprung mass of the tractor unit	4819	kg
m_t	Whole mass of the semi-trailer unit	32151	kg
m_{st}	Sprung mass of the semi-trailer unit	30821	kg
I_{sxx}	Roll moment of inertia of sprung mass of tractor unit about the COG of its sprung mass center	4348	kgm^2
I_{zz}	Yaw moment of inertia of whole mass of tractor unit about the COG of its whole mass center	20606	kgm^2
I_{sxz}	Yaw/roll product of moment of inertia of sprung mass of tractor unit about the COG of its sprung mass center	2176	kgm^2
I_{sxxt}	Roll moment of inertia of sprung mass of semi-trailer unit about the COG of its sprung mass center	42025	kgm^2

I_{zzt}	Yaw moment of inertia of whole mass of semi-trailer unit about the COG of its whole mass center	226272	kgm^2
I_{sxzt}	Yaw/roll product of moment of inertia of sprung mass of semi-trailer unit about the COG of its sprung mass center	18497	kgm^2
g	Gravitational acceleration constant	9.81	m/s^2
l_1	Distance between the whole mass COG of tractor unit and 1st axle center	1.115	m
l_2	Distance between the whole mass COG of tractor unit and 2nd axle center	1.959	m
l_3	Distance between the whole mass COG of the semi-trailer unit and 3rd axle center	1.047	m
l_4	Distance between the whole mass COG of the semi-trailer unit and 4th axle center	2.457	m
l_5	Distance between the whole mass COG of the semi-trailer unit and 5th axle center	3.767	m
l_f	Distance between the COG of the tractor unit and the articulation point	1.959	m
l_{ft}	Distance between the COG of the semi-trailer unit and the articulation point	5.853	m
h_f	Height of the fifth wheel measured from the ground	1.100	m
h_s	Height of the sprung mass center of gravity of the tractor unit measured from the ground	1.058	m
h_{st}	Height of the sprung mass center of gravity of the semi-trailer unit measured from the ground	0.900	m
h_r	Height of the roll center of sprung mass of the tractor measured from the ground	0.558	m
h_{rt}	Height of the roll center of sprung mass of the semi-trailer measured from the ground	0.723	m

h^*	Difference in height of roll center of sprung mass of the tractor unit and its sprung mass COG	0.500	m
$h_t{}^*$	Difference in height of roll center of sprung mass of the semi-trailer unit and its sprung mass COG	0.177	m
h_{fr}	Difference in height of roll center of sprung mass of the tractor unit and the height of fifth wheel	0.542	m
h_{frt}	Difference in height of roll center of sprung mass of the semi-trailer unit and the height of fifth wheel	0.377	m
$\sum K_\phi$	Total roll stiffness of suspensions and tires of the tractor unit	1948060	Nm/rad
$\sum K_{\phi t}$	Total roll stiffness of suspensions and tires of the semi-trailer unit	515660	Nm/rad
$\sum K_{12}$	Total roll stiffness of coupling point between tractor and semi-trailer	114590	Nm/rad
$\sum C_\phi$	Total roll damping of suspensions and tires of the tractor unit	320000	Nms/rad
$\sum C_{\phi t}$	Total roll damping of suspensions and tires of the semi-trailer unit	270000	Nms/rad
C_1	Total cornering stiffness of the tires on the front axle of the tractor	277200	N/rad
C_2	Total cornering stiffness of the tires on the rear axle of the tractor	740280	N/rad
C_3	Total cornering stiffness of the tires on the front axle of the semi-trailer	882000	N/rad
C_4	Total cornering stiffness of the tires on the middle axle of the semi-trailer	882000	N/rad
C_5	Total cornering stiffness of the tires on the rear axle of the semi-trailer	882000	N/rad

APPENDIX C

MATRICES FOR THE CONTROL STRATEGIES

In this section, the state space matrices related to each control strategy is provided in a detailed way. Recall the linear time invariant (LTI) state space system given by equation (A50) in Appendix A.

$$\dot{\boldsymbol{x}} = \boldsymbol{A}\boldsymbol{x} + \boldsymbol{B}\boldsymbol{\delta} \qquad (C1)$$

Implementation of active trailer steering on the vehicle model brings about the necessity of the modification of the matrices identified in Appendix A. For each control strategy, the matrices associated with the articulated vehicle model controlled by ATS systems are provided in Appendix C. The control strategies proposed by other researchers is adopted to the vehicle model so that a comparison of the approaches could be applied.

Matrices Related To the AHV Controlled with Steer Ratio Principle (SR):

In the study, the steer ratio principle is stated as an ATS strategy described with the equation (4.9) previously. Rewrite the equation as follows:

$$\delta_s = \mu\, \delta_1 \qquad (C2)$$

Written for the steer ratio principle, the equation (C1) become in the form of the following equation.

$$\dot{\boldsymbol{x}} = \boldsymbol{A}\boldsymbol{x} + \boldsymbol{B}\delta_1 + \boldsymbol{B_u}\delta_s \qquad (C3)$$

where the matrices are constructed as

$$[A]_{8x8} = [A_i]_{8x8}{}^{-1}[B_i]_{8x8}$$

$$[B]_{8x1} = [A_i]_{8x8}{}^{-1}[C_i]_{8x1}$$

$$[B_u]_{8x1} = [A_i]_{8x8}{}^{-1}[C_{iu}]_{8x1}$$

The matrices $[A_i]_{8x8}$ and $[B_i]_{8x8}$ is the same as the previously mentioned matrices in Appendix A. On the other hand, $[C_i]_{8x1}$ and $[C_{iu}]_{8x1}$ is identified with the following matrix elements. Note that the matrices have elements having the value of zero except the provided ones.

$$C_i(1,1) = -C_1$$

$$C_i(2,1) = -C_1(\mathrm{l}_1 + l_f)$$

$$C_i(3,1) = -C_1 h_{fr}$$

$$C_{iu}(1,1) = C_t$$

$$C_{iu}(4,1) = -C_t(l_t + l_{ft})$$

$$C_{iu}(5,1) = C_t h_{frt}$$

where the equivalent cornering stiffness of the semi-trailer C_t and equivalent distance on which the actively steered axle is put on the semi-trailer l_t is provided below.

$$C_t = C_3 + C_4 + C_5$$

$$l_t = \frac{l_3 + l_4 + l_5}{3}$$

Since the active steering angle directly related to the driver steering input, the matrices turns out to be the equation (C4) as follows.

$$\dot{\boldsymbol{x}} = \boldsymbol{A}\boldsymbol{x} + \boldsymbol{B_{SR}}\delta_1 \qquad (C4)$$

where the driver input matrix changed as $\boldsymbol{B_{SR}} = \boldsymbol{B} + \mu\boldsymbol{B_u}$

Matrices Related To the AHV Controlled with Active Command Steering (ACS): Command steering based active trailer steering is identified in the previous section, having the following relation given by equation (C5):

$$\delta_s = \beta\, \psi_s \qquad (C5)$$

The form given in equation (C3) is valid for that ATS strategy, too. However, the matrix associated with the active steering input is replaced as in the following equation:

$$\dot{\boldsymbol{x}} = \boldsymbol{A}\boldsymbol{x} + \boldsymbol{B}\delta_1 + \boldsymbol{B_{ACS}}\psi_s \qquad (C6)$$

where the matrix associated with the command steering based active input is expressed as $\boldsymbol{B_{ACS}} = \beta \boldsymbol{B_u}$. In this relation, the value of β is determined as

$$\beta = \frac{l_t}{l_t + l_{ft}}$$

In this control strategy, the quadratic performance index is based on the minimization of the states of the vehicle.

Matrices Related To the AHV Controlled with the Virtual Driver Steering Controller (VD):

For the implementation of virtual driver steering controller (VD), recall the previously mentioned states of the system.

$$\boldsymbol{x_{VD}} = [\boldsymbol{x} \quad y_e \quad y_{5th} \quad y_{5th\Delta} \quad \cdots \quad y_{5thm\Delta}]^T \qquad (C7)$$

where the first terms refers to the 8 original system states provided in Appendix A. The other terms corresponds to the position of the rearmost point of the semi-trailer, position of the fifth wheel and the time delayed positions of the fifth wheel, respectively.

The additional differential equations are written as follows:

$$\dot{y}_e(t) = v_t(t) - l_5 r_t(t) \qquad (C8)$$

$$\dot{y}_{5th}(t) = v(t) - l_f r(t) \qquad (C9)$$

$$\dot{y}_{5thi}(t - i\Delta) = \frac{1}{\Delta}[y_{5th}(t - (i-1)\Delta) - y_{5th}(t - i\Delta)] \qquad (C10)$$

where $i = 1,2,3 \ldots, m$ and $\Delta = (l_{ft} + l_5)/U$.

The resultant matrices for the implementation of virtual driver steering controller are expressed in the form of equation (C11):

$$\begin{Bmatrix} \dot{\boldsymbol{x}} \\ \dot{y}_e \\ \dot{y}_{5th} \\ \dot{y}_{5th\Delta} \\ \vdots \\ \dot{y}_{5thm\Delta} \end{Bmatrix} = \begin{bmatrix} [A]_{8x8} & [0]_{8x(m)} \\ [T]_{(m+2)x8} & [I]_{(m+2)x(m)} \end{bmatrix} \begin{Bmatrix} \boldsymbol{x} \\ y_e \\ y_{5th} \\ y_{5th\Delta} \\ \vdots \\ y_{5thm\Delta} \end{Bmatrix} + \begin{bmatrix} [B]_{8x1} \\ [0]_{(m+2)x1} \end{bmatrix} \delta_1 + \begin{bmatrix} [B_u]_{8x1} \\ [0]_{(m+2)x1} \end{bmatrix} \delta_s \qquad (C11)$$

where

$$[T]_{(m+2)x8} = \begin{bmatrix} 0 & 1 & 0 & -l_5 & 0 & 0 & 0 & 0 \\ 1 & 0 & -l_f & 0 & 0 & 0 & 0 & 0 \\ 0 & 0 & 0 & 0 & 0 & 0 & 0 & 0 \\ \vdots & \vdots & \vdots & \vdots & \vdots & \vdots & \vdots & \vdots \\ 0 & 0 & 0 & 0 & 0 & 0 & 0 & 0 \end{bmatrix}$$

$$[I]_{(m+2)x(m)} = \begin{bmatrix} 1/\Delta & -1/\Delta & 0 & 0 & 0 & 0 \\ 0 & 1/\Delta & -1/\Delta & 0 & 0 & 0 \\ 0 & 0 & 1/\Delta & -1/\Delta & 0 & 0 \\ \vdots & \ddots & \ddots & \ddots & \ddots & \vdots \\ 0 & 0 & 0 & 0 & 1/\Delta & -1/\Delta \end{bmatrix}$$

The quadratic performance index used in the LQR aims to minimize the lateral position error between the lead point and the follow point, as explained in Section 4.

Matrices Related To the AHV Controlled with the Lateral Position Deviation Preview Controller (LPDP):

For this control strategy, the modified states of the system are written as follows:

$$\boldsymbol{x_{LPDP}} = [\boldsymbol{x} \quad y_r \quad y_f \quad y_{f\Delta} \quad \cdots \quad y_{fn\Delta}]^T \qquad (C12)$$

where the additional states are the position of the centerline of the active semi-trailer axle, position of the centerline of the tractor front axle, and its time delayed states, respectively.

In addition to this, the relevant differential equations to be used with the original equations of motions are given by equation (C13), (C14) and (C15):

$$\dot{y}_r(t) = v_t(t) - l_3 r_t(t) \tag{C13}$$

$$\dot{y}_f(t) = v(t) + l_1 r(t) \tag{C14}$$

$$\dot{y}_f(t - j\Delta) = \frac{1}{\Delta}\left[y_f(t - (j-1)\Delta) - y_f(t - j\Delta)\right] \tag{C15}$$

where $j = 1,2,3 \ldots, n$ and $\Delta = (l_1 + l_f + l_{ft} + l_t)/U$.

As a result, the final form of the state-space matrices for the LPDP controller become as follows:

$$\begin{Bmatrix} \dot{\boldsymbol{x}} \\ \dot{y}_r \\ \dot{y}_f \\ \dot{y}_{f\Delta} \\ \vdots \\ \dot{y}_{fn\Delta} \end{Bmatrix} = \begin{bmatrix} [A]_{8x8} & [0]_{8x(n)} \\ [T]_{(n+2)x8} & [I]_{(n+2)x(n)} \end{bmatrix} \begin{Bmatrix} \boldsymbol{x} \\ y_r \\ y_f \\ y_{f\Delta} \\ \vdots \\ y_{5fn\Delta} \end{Bmatrix} + \begin{bmatrix} [B]_{8x1} \\ [0]_{(n+2)x1} \end{bmatrix} \delta_1 + \begin{bmatrix} [B_u]_{8x1} \\ [0]_{(n+2)x1} \end{bmatrix} \delta_s \tag{C16}$$

where

$$[T]_{(n+2)x8} = \begin{bmatrix} 0 & 1 & 0 & -l_3 & 0 & 0 & 0 & 0 \\ 1 & 0 & l_1 & 0 & 0 & 0 & 0 & 0 \\ 0 & 0 & 0 & 0 & 0 & 0 & 0 & 0 \\ \vdots & \vdots & \vdots & \vdots & \vdots & \vdots & \vdots & \vdots \\ 0 & 0 & 0 & 0 & 0 & 0 & 0 & 0 \end{bmatrix}$$

$$[I]_{(n+2)x(n)} = \begin{bmatrix} 1/\Delta & -1/\Delta & 0 & 0 & 0 & 0 \\ 0 & 1/\Delta & -1/\Delta & 0 & 0 & 0 \\ 0 & 0 & 1/\Delta & -1/\Delta & 0 & 0 \\ \vdots & \ddots & \ddots & \ddots & \ddots & \vdots \\ 0 & 0 & 0 & 0 & 1/\Delta & -1/\Delta \end{bmatrix}$$

For LPDP controller, the quadratic performance index used in the LQR try to minimize the lateral position error between the position of tractor front axle centerline and active semi-trailer axle centerline.

Matrices Related To the AHV Controlled with the Lead Unit Following Controller (LUF):

For the implementation of lead unit following controller (LUF), the states of the system is identified as equation (C17).

$$\boldsymbol{x_{LUF}} = [\boldsymbol{x} \quad r_{\Delta} \quad \dots \quad r_{k\Delta}]^T \tag{C17}$$

where the first term corresponds to original states and the other terms refer to the time delayed states. The additional states is obtained using the differential equation written as follows:

$$\dot{r}(t - i\Delta) = \frac{1}{\Delta}[r(t - (i-1)\Delta) - r(t - i\Delta)] \tag{C18}$$

where $i = 1,2,3 \dots, k$ and Δ is approximated by averaging the yaw difference between the units of the conventional AHV.

The final from of matrices is written as equation (C19):

$$\begin{Bmatrix} \dot{\boldsymbol{x}} \\ \dot{r}_{\Delta} \\ \vdots \\ \dot{r}_{k\Delta} \end{Bmatrix} = \begin{bmatrix} [A]_{8x8} & [0]_{8xk} \\ [T]_{kx8} & [I]_{kxk} \end{bmatrix} \begin{Bmatrix} \boldsymbol{x} \\ r_{\Delta} \\ \vdots \\ r_{k\Delta} \end{Bmatrix} + \begin{bmatrix} [B]_{8x1} \\ [0]_{kx1} \end{bmatrix} \delta_1 + \begin{bmatrix} [B_u]_{8x1} \\ [0]_{kx1} \end{bmatrix} \delta_s \tag{C19}$$

where

$$[T]_{kx8} = \begin{bmatrix} 0 & 0 & 1/\Delta & 0 & 0 & 0 & 0 & 0 \\ 0 & 0 & 0 & 0 & 0 & 0 & 0 & 0 \\ 0 & 0 & 0 & 0 & 0 & 0 & 0 & 0 \\ \vdots & \vdots & \vdots & \vdots & \vdots & \vdots & \vdots & \vdots \\ 0 & 0 & 0 & 0 & 0 & 0 & 0 & 0 \end{bmatrix}$$

$$[I]_{kxk} = \begin{bmatrix} 0 & -1/\Delta & 0 & 0 & 0 & 0 \\ 0 & 1/\Delta & -1/\Delta & 0 & 0 & 0 \\ 0 & 0 & 1/\Delta & -1/\Delta & 0 & 0 \\ \vdots & \ddots & \ddots & \ddots & \ddots & \vdots \\ 0 & 0 & 0 & 0 & 1/\Delta & -1/\Delta \end{bmatrix}$$

Matrices Related To the AHV Controlled with the Lateral Acceleration Characteristic Following Controller (LACF):

In this study, LACF strategy is proposed for the ATS system. In order to accomplish the lateral acceleration tracking, required states are identified as follows:

$$\boldsymbol{x_{LACF}} = [\boldsymbol{x} \quad \dot{\boldsymbol{x}} \quad \dot{v}_{\Delta} \quad \dots \quad \dot{v}_{l\Delta} \quad r_{\Delta} \quad \dots \quad r_{k\Delta}]^T \tag{C20}$$

The lateral acceleration following necessitates to obtain the derivatives of the original states. In the equation (C20), the first 2 terms stand for the original system states and theirs derivatives as additional states. The other terms indicates the time delayed states of the new system.

The differential equations given by (C21) and (C22) is used to derive the new state space system for the LACF strategy.

$$\ddot{v}(t - i\Delta) = \frac{1}{\Delta}[\dot{v}(t - (i-1)\Delta) - \dot{v}(t - i\Delta)] \tag{C21}$$

where $i = 1,2,3 \dots, l$

$$\dot{r}(t - i\Delta) = \frac{1}{\Delta}[r(t - (i-1)\Delta) - r(t - i\Delta)] \tag{C22}$$

where $i = 1,2,3 \dots, k$

The resultant form is written as follows:

$$\begin{Bmatrix} \dot{\boldsymbol{x}} \\ \ddot{\boldsymbol{x}} \\ \ddot{v}_{\Delta} \\ \vdots \\ \ddot{v}_{l\Delta} \\ \dot{r}_{\Delta} \\ \vdots \\ \dot{r}_{k\Delta} \end{Bmatrix} = \begin{bmatrix} [A]_{8x8} & [0]_{8x8} & [0]_{8xl} & [0]_{8xk} \\ [0]_{8x8} & [A]_{8x8} & [0]_{8xl} & [0]_{8xk} \\ [0]_{lx8} & [0]_{lx8} & [I]_{lxl} & [0]_{lxk} \\ [T]_{kx8} & [0]_{kx8} & [0]_{kxl} & [I_2]_{kxk} \end{bmatrix} \begin{Bmatrix} \boldsymbol{x} \\ \dot{\boldsymbol{x}} \\ \dot{v}_{\Delta} \\ \vdots \\ \dot{v}_{l\Delta} \\ r_{\Delta} \\ \vdots \\ r_{5\Delta} \end{Bmatrix} + \begin{bmatrix} [B]_{8x1} & [0]_{8x1} \\ [0]_{8x1} & [B]_{8x1} \\ [0]_{lx1} & [0]_{lx1} \\ [0]_{kx1} & [0]_{kx1} \end{bmatrix} \begin{Bmatrix} \delta_1 \\ \dot{\delta}_1 \end{Bmatrix}$$

$$+ \begin{bmatrix} [B_u]_{8x1} & [0]_{8x1} \\ [0]_{8x1} & [B_u]_{8x1} \\ [0]_{lx1} & [0]_{lx1} \\ [0]_{kx1} & [0]_{kx1} \end{bmatrix} \begin{Bmatrix} \delta_s \\ \dot{\delta}_s \end{Bmatrix} \tag{C23}$$

where

$$[T]_{kx8} = \begin{bmatrix} 0 & 0 & 1/\Delta & 0 & 0 & 0 & 0 & 0 \\ 0 & 0 & 0 & 0 & 0 & 0 & 0 & 0 \\ 0 & 0 & 0 & 0 & 0 & 0 & 0 & 0 \\ \vdots & \vdots & \vdots & \vdots & \vdots & \vdots & \vdots & \vdots \\ 0 & 0 & 0 & 0 & 0 & 0 & 0 & 0 \end{bmatrix}$$

$$[I]_{lxl} = \begin{bmatrix} 1/\Delta & -1/\Delta & 0 & 0 & 0 & 0 \\ 0 & 1/\Delta & -1/\Delta & 0 & 0 & 0 \\ 0 & 0 & 1/\Delta & -1/\Delta & 0 & 0 \\ \vdots & \ddots & \ddots & \ddots & \ddots & \vdots \\ 0 & 0 & 0 & 0 & 1/\Delta & -1/\Delta \end{bmatrix}$$

$$[I_2]_{kxk} = \begin{bmatrix} 0 & -1/\Delta & 0 & 0 & 0 & 0 \\ 0 & 1/\Delta & -1/\Delta & 0 & 0 & 0 \\ 0 & 0 & 1/\Delta & -1/\Delta & 0 & 0 \\ \vdots & \ddots & \ddots & \ddots & \ddots & \vdots \\ 0 & 0 & 0 & 0 & 1/\Delta & -1/\Delta \end{bmatrix}$$

In this case, there are two weighting factors associated with the quadratic performance index explained in Section 4.

APPENDIX D

WEIGHT FACTOR DETERMINATION

In this section, the weighting factors associated with each control strategy for all the test conditions are identified. For a quadratic performance index defined in the form of Equation D1, the Q and R matrices are the corresponding weighting factors of states and control variables of the system, respectively.

$$J = \int_0^\infty (x^T Q x + u^T R u)\, dt \qquad (D1)$$

The given quadratic performance index can be rewritten as follows:

$$J = \int_0^\infty \rho_1 [e(t)]^2 + \rho_2 [\delta_s(t)]^2\, dt \qquad (D2)$$

In that case, the cost function given by Equation D2 aims to minimize the defined error $e(t)$ with the use of the active steering control input $\delta_s(t)$. Also, corresponding weighting factors for the error and control input are identified as ρ_1 and ρ_2, respectively.

For the implementation of SR principle, Linear Quadratic Regulator technique is not valid for the control strategy. Thus, any weighting adjustment associated with the ATS strategy is not applicable in that case.

In case of ACS control strategy, the performance index given by Equation D1 is used for the minimization of equally important state variables of the system. As a result, the Q matrix associated with that control strategy is described as an identity matrix. For

each test conditions, following procedure is followed: The Q matrix is chosen as an identity matrix as mentioned above. Since there is only one virtual steerable axle, the weighting matrix R of the control input is a scalar quantity. Keeping the weighting of states as identity matrix, the relative importance of the control input is adjusted accordingly so that the best performance measures are obtained for each test maneuver.

For the remaining control strategies, the quadratic performance index in the form given by Equation D2 is applicable. The terms ρ_1 and ρ_2 are two different weighting factor in the cost function. At the beginning, the value of either weighting factor can be fixed. Afterwards, the other weighting factor may be adjusted by observing the behavior while its value is changing. Finally, the optimum weighting factors that provide the best performance measure at each test conditions are chosen. Note that different set of weight factors is associated with each standard test maneuvers. In addition, for the proposed control strategy, a similar trial-error procedure is used for the determination of the weighting factors.

On the other hand, there are some limitations for the use of some weighting factors set. In the study, the limitations are taken into consideration while determining the weighting factors associated with all control strategies:

- Any weight factor sets that lead to the response exceeding a maximum 4° slip angles at the axles should not be chosen. Therefore, the assumption of linearity in the cornering stiffness is satisfied.
- A weight factor set should provide the response having maximum 0.35g peak lateral acceleration at the vehicle units. Thus, the vehicle responses remain in the reasonable range of the linear vehicle model.